Energy Transfer Studies of Electron Donating Carbazole and Electron Accepting Perylene Dye Systems

Shaban Rajab Shaban

Submitted to the
Institute of Graduate Studies and Research
in partial fulfillment of the requirements for the Degree of

Master of Science
in
Chemistry

Eastern Mediterranean University
June 2013
Gazimağusa, North Cyprus

Approval of the Institute of Graduate Studies and Research

Prof. Dr. Elvan Yilmaz
Director

I certify that this thesis satisfies the requirements as a thesis for the degree of Master of Science in Chemistry.

Prof. Dr. Mustafa Halilsoy
Chair, Department of Chemistry

We certify that we have read this thesis and that in our opinion it is fully adequate in scope and quality as a thesis for the degree of Master of Science in Chemistry.

Prof. Dr. Huriye Icil
Supervisor

1. Prof. Dr. Huriye Icil

2. Assoc. Prof. Dr. Hamit Caner

3. Asst. Prof. Dr. Nur P. Aydınlık

ABSTRACT

Electron donating poly(2,7-carbazoles) are one of the most attractive materials emerged as *p*-type semiconductors for applications in photovoltaic devices in combination with relevant electron accepting systems. On the other hand, perylene dyes are known as versatile *n*-type building block materials for organic device architectures and supramolecular systems.

These polymeric- or small molecule-based organic materials are very important concerning controlled and improved light emission is therefore a key issue and blending of fluorescent dye materials with conjugated polymers could enhance transfer of energy (excitation) from host to guest.

In the present work, the electronic energy transfer between three different chromophoric materials of 2,7-carbazoles and perylene dyes were investigated. The carbazole compounds are considered as electron donors and perylene diimide is considered as electron accepting group. The energy transfer studies of three carbazole derivatives with perylene dye in three different kinds of varying polarity ($CHCl_3$, 4.81; CH_3CN, 37.5; CH_3OH, 32.6) reveal that most efficiency is achieved for the three of the carbazoles in $CHCl_3$. The critical transfer distances measured are in excellent agreement and in addition Stern-Volmer plots show efficient diffusion-controlled energy transfer in chloroform. Although there is no efficient nonradiative energy transfer in CH_3CN and CH_3OH, interesting charge transfer leading to electron transfer are evidenced from carbazole to perylene chromophore

Keywords: Energy Transfer, Stern-Volmer, Carbazole, Perylene

ÖZ

Elektron verici poli(2,7-karbazoller), fotovoltaik cihaz uygulamalarında ilgili elektron alıcı sistemlerle kombinasyon halinde kullanılan p-tipi yarı iletkenler olarak ortaya çıkan en ilgi çekici maddelerdendir. Diğer yandan, perilen boyalar, organik cihaz mimarileri ve supramoleküler sistemler için çok yönlü bir n-tipi yapı taşı olarak bilinmektedir.

Bu polimerik veya küçük molekül tabanlı organik maddeler gelişmiş ve kontrol edilebilir ışık emisyon özelliklerinden dolayı büyük önem kazanmaktadır. Bu nedenle, floresan boya malzemelerinin konjuge polimerlerle olan karışımları enerji transferinin artırılması açısından önemli bir konudur.

Bu çalışmada, perilen boyaları ile üç farklı kromoforik 2,7-karbazol malzemleri arasındaki elektronik enerji transferi incelenmiştir. Karbazol bileşikleri elektron verici, perilen diimid ise elekron alıcı grup olarak kabul edilmiştir. Üç karbazol türevinin perilen diimid ile değişen polaritedeki çözgenlerde ($CHCl_3$, 4.81; CH_3CN, 37.5; CH_3OH, 32.6) gerçekleştirilen enerji transfer çalışmalarında, üç karbazol türevi için de en etkili enerji transferi $CHCl_3$ çözücüsünde sağlanmıştır.

Ölçülen kritik transfer mesafeleri Stern-Volmer ilişkisine uygun olup, Stern-Volmer grafikleri kloroformda etkin difüzyon-kontrollü enerji transferi göstermektedir. CH_3CN ve CH_3OH çözgenlerinde etkin ışınımsız enerji transferi olmamasına rağmen, karbazolden perilen kromoforuna elektron transferine yol açan yük transferi gözlemlenmiştir.

Anahtar Kelimeler: Enerji Transferi, Stern-Volmer, Karbazol, Perilen

To My Family .....

ACKNOWLEDGMENTS

Bismillahi Rahmani Rahim

I want to thank deeply my supervisor Prof. Dr. Huriye Icil for her help and for giving me the opportunity to work in her group. I would like to mention that i have learned from her a lot of knowledge and experience during my master study not only in organic chemistry but in the general life as well as she give me that motivation and guide to do my work in the best way.

Iam grateful thanks to Jagadeesh Babu Bodapati for his helps. I am also thanks for every one in the research organic group and all my firends.

To my father…….. Rajab Shaban

To my mother ……. Zemrod Ahmed

To my Fiancee ……. Nargz Ahmed

To my brothers and sisters, grandmother, uncles, aunts, cousins and all my relatives.

TABLE OF CONTENTS

LIST OF TABLES

LIST OF FIGURES

LIST OF SCHEMES

LIST OF SYMBOLS / ABBREVIATIONS

$\overset{o}{A}$	Armstrong
A	Acceptor molecules
A*	Excited acceptor
ATP	Adenosine triphosphate
AU	Arbitary unit
c	Concentration
CHL	Chloroform
CT	Charge transfer
D	Donor molecules
D*	Excited donor
EDA	Electron donor/acceptor
ET	Energy transfer
Ev	Electron volt
F	Fluorescence
FRET	Förster resonance energy transfer
ISC	Iintersystem crossing
IC	Internal conversion
Hv	Irradiation
K_f	Fluorescence rate constant
1	Path length
LEDs	light emitting diodes
M	Molar concentration
max	Maximum

OLEDs	Organic light-emitting diodes
Φ_f	Fluorescence quantum yield
PH	Phosphorescence
PDI	Perylene diimide
PET	photoinduced electron transfer
RET	Resonance energy transfer
S	state
T	Tirplet state
u	Unknown
UV-vis	Ultraviolet visible light absorption
vs.	Versus
λ	Wavelength
λ_{max}	Maximum wavelength

Chapter 1

INTRODUCTION

1.1 Energy Transfer – An Overview

Energy dwindling is one of the current important issues faced by human and the consequent global warming and extenuating carbon emission were the cruel terawatt challenges. The top precedence of most developed countries is securing clean energy. (Wen D.et al. 2009). It is a known fact that energy conversion and transportation occur readily in atomic or molecular levels and plenty of hopes are concentrated on nanoscience and nanotechnology. Nanotechnology is one of the most effective and efficient path ways that can play a major role in revitalizing the energy-based industries. Thus, laboratory efficiencies of energy conversion based on nanomaterials could encourage development of renewable energy industries.

Radiative absorption of the material is the primary aspect after which the electron and energy transfer mechanisms take place according to the type of material. Synthetic based nano-sized materials are more active and effective for transporting and converting the energy. In fact, the transfer of energy from one material to another and/or energy conversion from one type to another is a mimic of natural photosynthesis. The natural photosynthesis and related energy transfer mechanism is shown in (Figure 1.1).

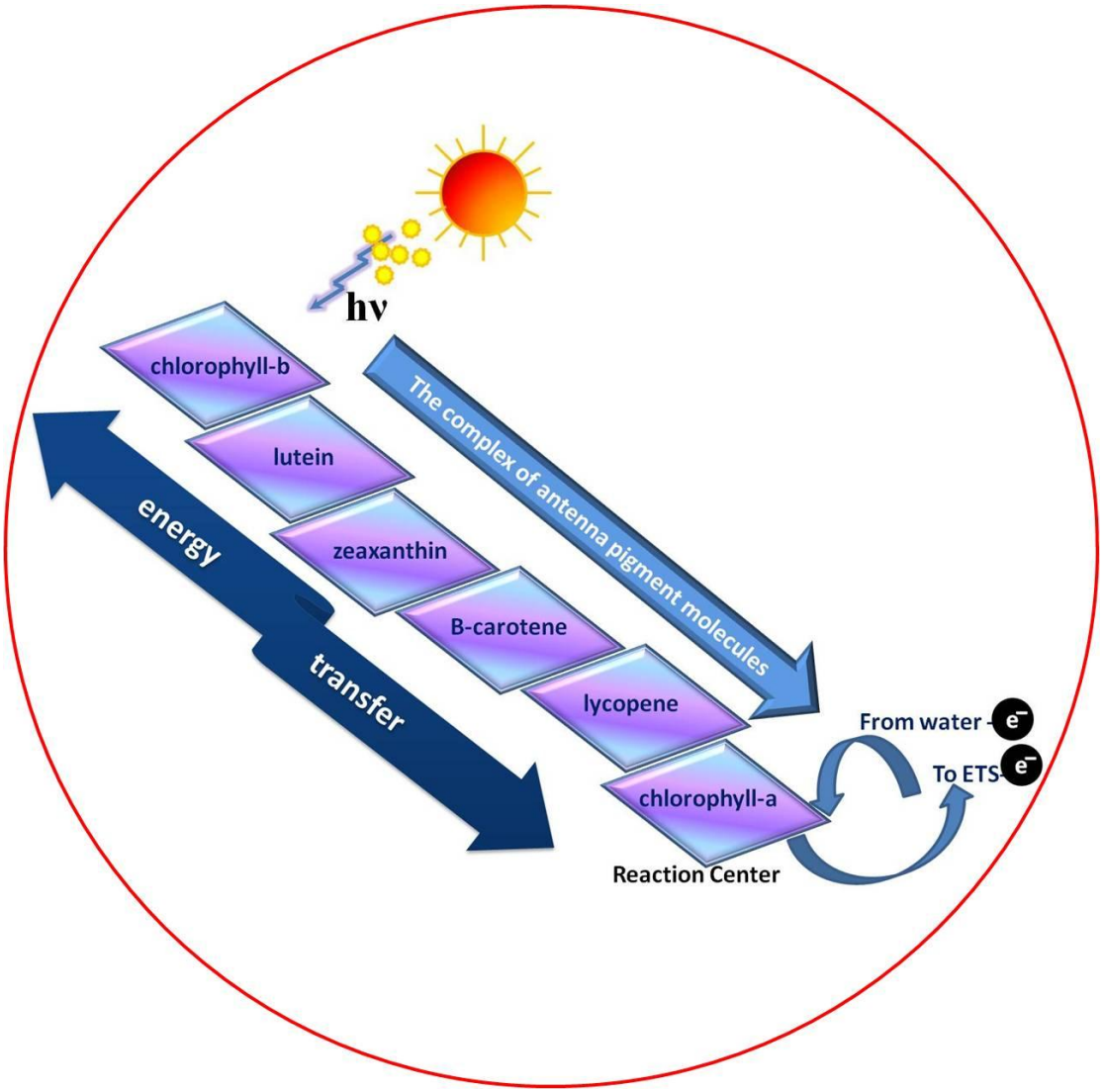

Figure 1.1. Energy Transfer Mechanism in Photosynthesis

In photosynthesis, there are several antenna pigment molecules such as β-carotene and chlorophyll-b as shown in Figure 1.1. These pigment molecules transfer the energy that is radiatively absorbed from sunlight (in terms of photons). The ultimate purpose is to carry the energy to chlorophyll-a which is the reaction center that drive the primary object of photosynthesis.

1.2 Energy Transfer and Donor-Acceptor (D/A) Materials

Based on the idea, several synthetic pigment molecules are synthesized that can transfer the energy. Conjugated aromatic dyes with electron donating and electron accepting functional groups are the familiar materials which are applied in energy transfer mechanisms. The structures are well suitable also for photoinduced electron transfer (PET) mechanisms. These two physical phenomena describe many reactions that occur between photochemical and biological systems. The electron- and energy-transfer processes are therefore applicable in constructing renewable energy systems and biological sensing systems (Jia et al. 2012 and Zhao et al. 2011).

The theory of energy transfer based on the synthetic electron donating and accepting materials was proposed by Förster. The concept of excitation energy transfer is therefore described as Förster resonance energy transfer (FRET). FRET is actually very sensitive to nanoscale range-proximities and hence the distance between donor molecules (D) and acceptor molecules (A) matters the efficiency of energy transfer. On the other hand, Dexter mechanism also explains the critical distance between the D and A molecules and the process of energy transfer.

Depending on the FRET and Dexter theories, proper selection of various chromophoric materials and fluorophores could give potential optoelectronic and medicinal applications. Although the rate of energy transfer depends on several key factors, the prime point is selection of D/A materials. Many theories such as molecular orbital theory were developed to address the interactions of donor-acceptor systems. Structure-property relations of these materials are needed to explore the applicability in relevant fields. Therefore, several materials are

synthesized and applied for efficient energy transfer to explore the utility in a technological way.

The objective of this work is to study the FRET and possible other energy transfer mechanisms between electron donating carbazole materials and electron accepting perylene chromophoric molecules (Figure 1.2).

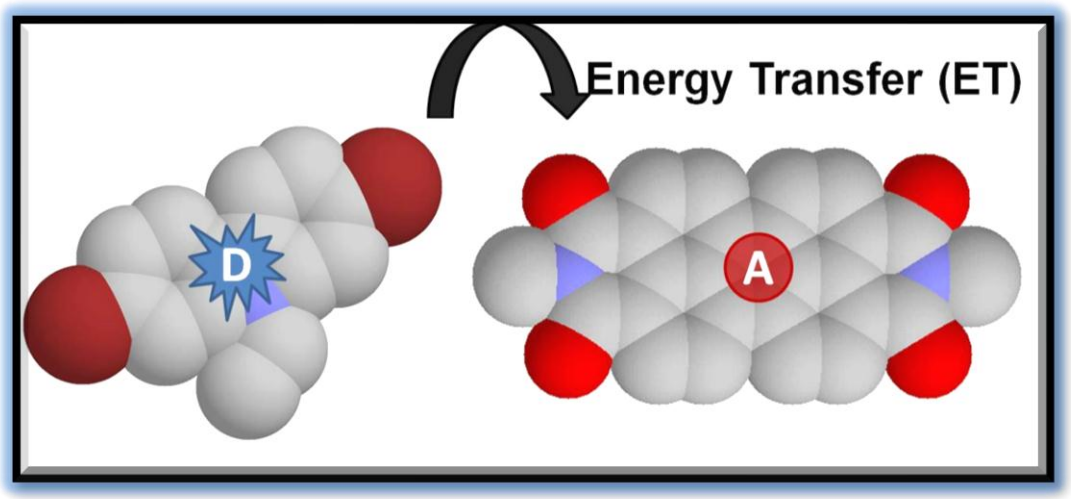

Figure 1.2. General Energy Transfer Between Carbazole–Donor and Perylene Dye–Acceptor Compounds

We have studied the mechanisms in detail via fluorescence measurements as both the donor and acceptor materials are fluorescent and hence fluorescence resonance energy transfer could be more efficient. Comparatively, the absorption capacities were studied for both materials. The critical transfer distances were calculated to explain the efficiency of energy transfer and Stern-Volmer kinetics are discussed.

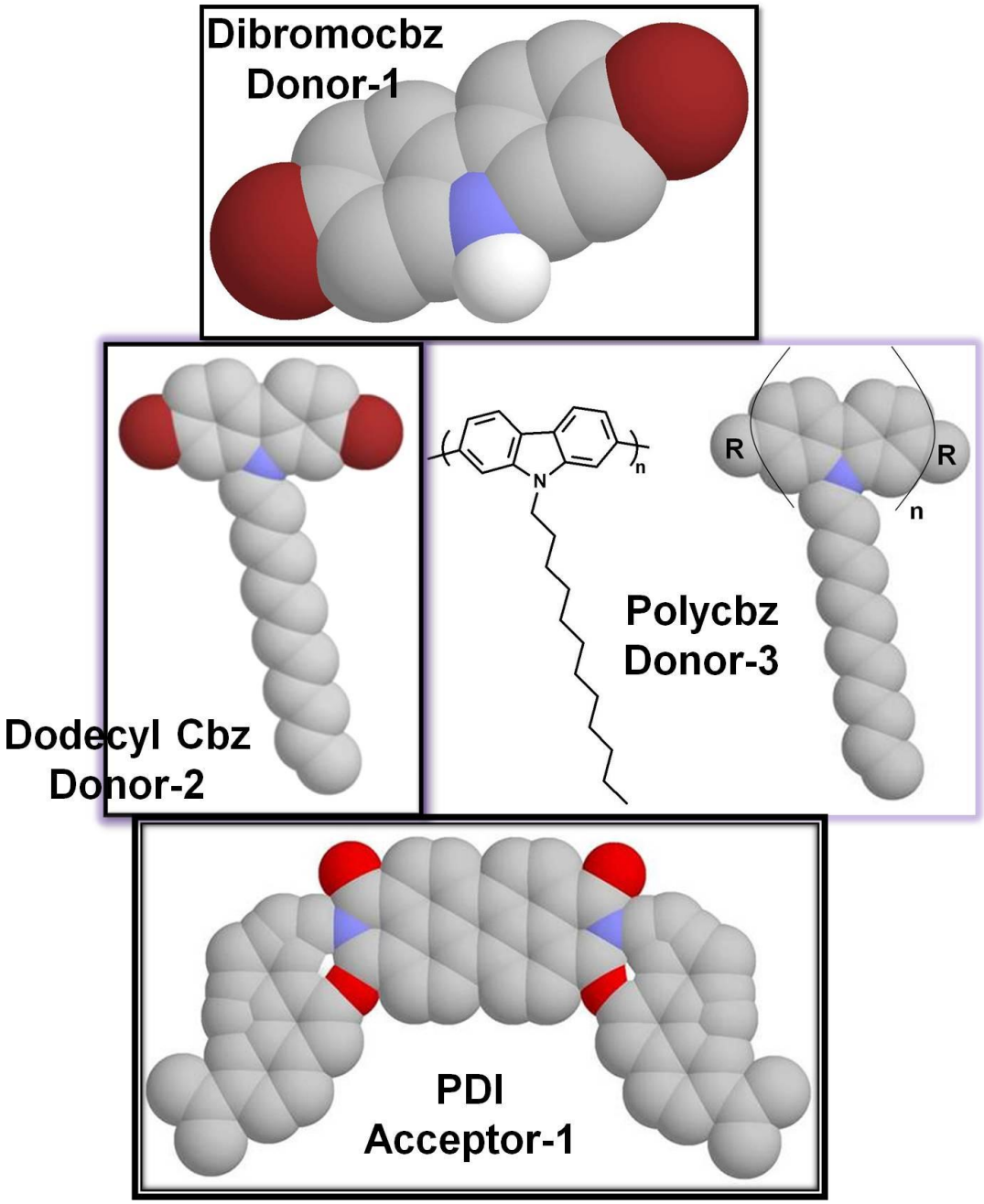

Figure 1.3. The Compounds Studied in Energy Transfer

Chapter 2

THEORETICAL

2.1 The Basics of Excited State From Jablonski Diagram

Singlet excited and triplet excited states are two distinct classes of excited state with different physical and chemical properties. Excited state characteristics of these singlet and triplet states are very interesting and are very much influenced by many variables like temperature, solvent polarity, pH, etc. As it is well known that the electron spin angular momentum causes the singlet and triplet states distinct. When photons of right frequency hit the molecules, excited states are generally produced by absorption of light. It leads to a state of the similar multiplicity, which is triplet to triplet or singlet to singlet. As all ground states are singlets, mostly singlet to singlet excitations are formed.

Excited singlet states have a significant higher energy than the excited triplet states. If the excited state electron has a spin opposite to that of its fellow spin, so the state is a singlet excited state; however, if the spin of the excited electron is similar to that of its fellow spin, the excited state is a triplet excited state. The singlet and triplet states are extended in the order of rising energy and numbered in the similar order as S0, S1, S2, …,Sn and T1, T2… ,Tn.

By Jablonski diagram can explain the some processes that occurs in the excited states, the Jablonski diagram is shown in (figure 2.1) , and the processes that occurs

can divided in to two types, first radiative processes: like a fluorescence(F) (spin allowed) and phosphorescence(PH) (spin forbidden), second non-raditive processes, like an intersystem crossing(ISC) (spin-forbidden) and internal conversion(IC) (spin-allowed) (Figure2.1).

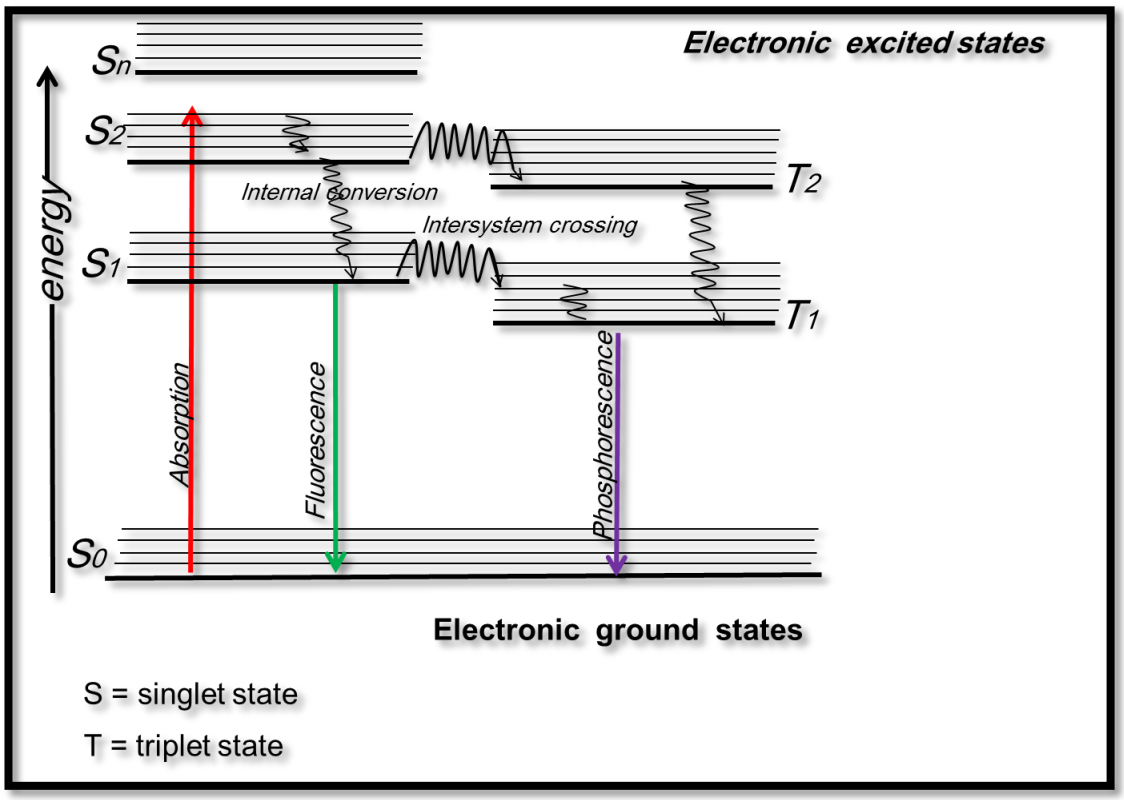

Figure 2.1. The Simple Jablonski Diagram

2.2 Electron Donor and Acceptor Systems

In organic photochemistry, electron transfer between electron donor/acceptor (EDA) systems occur through highly polar (ionic) electronic excited state charge-transfer (CT) mechanism, although both interacting molecules e.g. an electron acceptor (A) and an electron donor (D), are neutral species. Electron donor/acceptor systems have important attentions in view of their potential applications in sensors, solar cells, electrochromic devices, field effect transistors, and light emitting diodes (LEDs) (Jia et al. 2012 and Deperasinska et al. 1998).

Electron donor-acceptor complex is the stable complex that results in the ground state when the interaction between acceptor and donor is strong, whereas, when the interaction between D and A is very weak, the excited charge transfer (CT) state can still be formed as a consequence of an electron transfer between excited type donor–D* or acceptor–A* and its EDA complement in the ground state (each A or D, respectively) (Gao et al. 2011).

2.2.1 Energy Transfer in Donor Acceptor Systems

Energy transfer (ET) between molecular entities is ongoing interest in the evolution of molecular founded photonic systems, including photovoltaics, sensor technologies and molecular electronics. The efficiency in both energy- and electron- transfers in photosynthesis mechanisms of bacteria and plant are mainly achieved via optimum spatial arrangements in supramolecular systems and matching of energy profiles of D/A systems. In order to achieve such a control in the synthetic/artificial systems is a challenging task as naturals are held together with tight self-organized molecular assemblies of membranes and proteins.

In synthetic donor acceptor systems the efficient energy transfer can be achieved by two different ways: through a bonding-interactions mechanism or through a space mechanism. Depending on the through-space energy transfer mechanisms (for example, Förster/Dexter energy transfer mechanisms) between D/A chromphore units, the efficiency is variable and mainly depends on the factor of overlap of fluorescence spectrum of donor–D and absorption of acceptor–A and also on their spatial existence.

Synthetically, the energy overlaps can be achieved and tuned via tailoring of materials by introducing suitable substituents to the chromophores and fluorophores. This provides various electronic properties of D/A chromophores. Yet, the control/tuning of spatial distributions and orientations between the D/A units is difficult to achieve (Jankowska et al. 2008). Generally, there are two known approaches for controlling the spatial arrangements: the non-covalent and covalent arrangements of D/A units. Both approaches have their own advantages and disadvantages and were successful in achieving efficient energy transfer and in understanding of physics of the mechanisms such as FRET (Hurenkamp et al. 2008 and Albinsson et al. 2007).

2.2.2 Electron Transfer

Electron transfer occurs when an electron (e−) shifts from an atom/a molecule to another atom/molecule. Electron transfer symbolizes one of the simplest chemical reactions. Electron transfer is involved everywhere in the systems related to physics, biology, organic, and inorganic chemistry. Currently, interpretation and control of electron transfer reactions is one of the broadest and most dynamic subjects of physical chemistry.

In the nature, electron transfer happens in relation with the transduction of energy. In the photosynthesis mechanism, charge imbalance is achieved through the transfer of electron which finally causes pumping of proton to create adenosine triphosphate (ATP) (Barbara et al. 1996 and Hoffmann N. 2008).

In chemistry, corrosion is a familiar phenomenon occurs due to the surface electron transfer between metallic iron and oxygen. On the other hand, in organic chemistry, some bond making and breaking processes occur through electron transfer mechanism (shown in Figure 2. 2, formation of a benzyl halide radical).

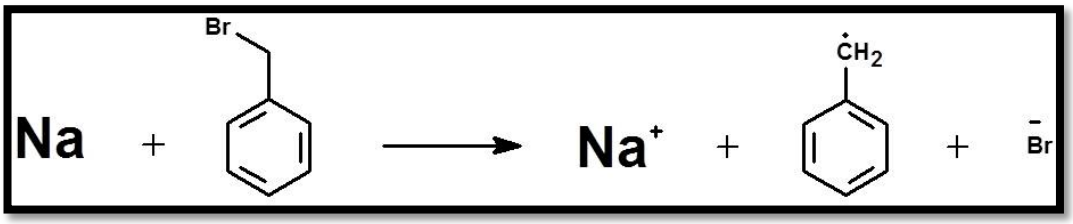

Figure 2.2. Electron Transfer Mechanism – Formation of a Benzyl Halide Radical

Electron transfer can be classified into many types and it is determined by the state of the two choromophores and their connectivity:

Inner-sphere electron transfer

In inner-sphere electron transfer mechanism (Figure 2.3), the two chromophores (An electron donor and acceptor) are covalently linked together. This link can be permanent or temporary, in the former one, the electron transfer occuring is called intramolecular electron transfer and in the later one, the electron transfer occuring is termed as intermolecular electron transfer.

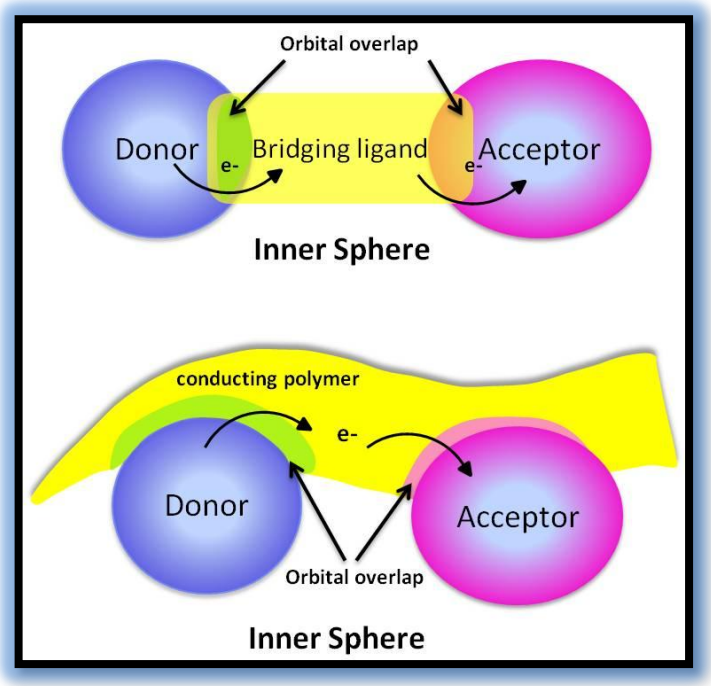

Figure 2.3. The General Representation of Inner-sphere Electron Transfer Mechanism

Outer-sphere electron transfer

In outer-sphere electron transfer reactions (Figure 2.4), the chrmophoric/redox redox centers that participate in electron transfer mechanism are not linked by any bond. Though, the electron transfer occurs via 'hopping' of electrons through the space from the reducing center/donor of a chromophore to the acceptor. Reactions involving outer sphere electron transfer can happen in between the same chemical species or in between dissimilar chemical species having different oxidation states. So, most electron transfer reactions occur by outer sphere electron mechanism.

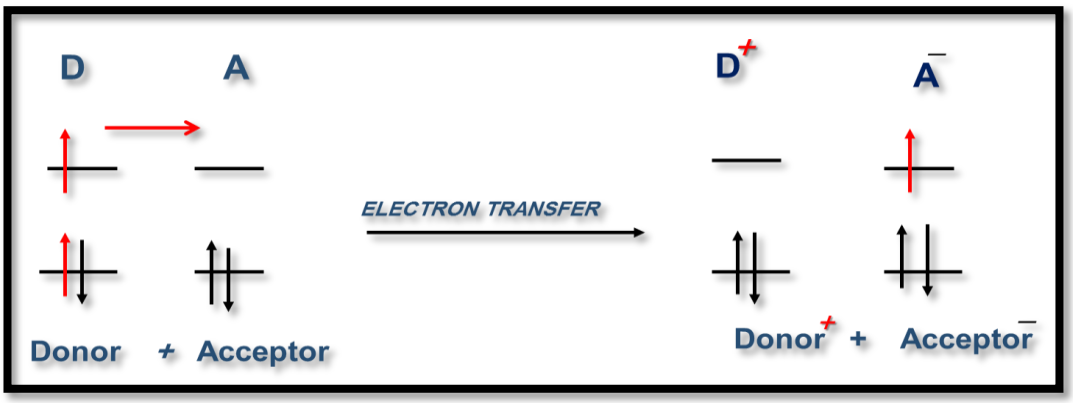

Figure 2.4. Outer-sphere Electron Transfer

2.3 Types of Energy Transfer

An excited state formed can move from one site to another through an organic semiconductor by the transfer of its energy non-radiatively. Generally, this energy transfer is related to one-step mechanism where the excited donor molecule (D*) is deactivated while the acceptor molecule (A) in ground state becomes excited during a coupling interaction.

$$D^* + A \xrightarrow{\text{coupling interaction}} D + A^*$$

Energy transfer can occur by either Dexter (exchange) or Forster (coulombic) mechanisms or by direct generation of singlet and triplet excitons on the guest molecules. In electron exchange, a bordering molecule contributes an electron to the HOMO level of the donor molecule, whilst the electron in the LUMO gets transport to the excited state of the accepter. By the emission of fluorescence light the accepter can return to the lower energetic ground state (Kohler et al. 2009, Hurenkamp et al 2008 and Wrobel et al. 2011).

2.3.1 Forster Energy Transfer

The Forster energy transfer is a dipole-dipole coupling process. It occurs when the energy of the fluorescent donor molecule in the excited state is non-radiatively transfers its energy to an unexcited acceptor molecule. The scheme of FRET models is presented in Fig.2.5.

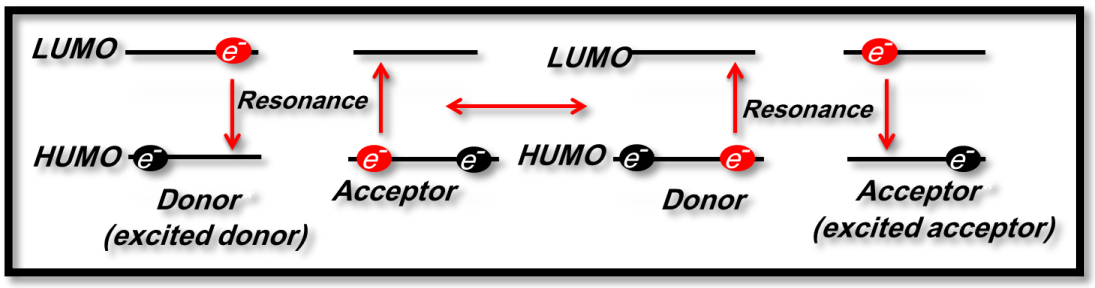

Figure 2.5. The Coulombic Energy Transfer Mechanism

In Forster's theory, the dipole–dipole term is important where the Coulomb interaction between donor-D and acceptor-A is approximated by the dipole term. Transfer happens between suitable electron donor and acceptor where the oscillations-induced electronic coherence on the donor D are in good resonance with the electronic band gap energies of acceptor A. The transition dipole interaction decides the strength interaction, which based on the magnitude of the D and A transition matrix elements, separation of the dipoles and their alignment.

2.3.2 Dexter Energy Transfer (Electron Exchange)

Dexter electron transfer is an excited electron state transport from donor molecule to an acceptor molecule by quenching mechanism. This process needs a wave function overlap among the acceptor and donor, which means it can only happen at short-range distances; usually of the order 15-20 Å. The excited state can be exchanged in two separate charge exchange steps, or in a single step. The scheme of Dexter models is presented in (Fig.2.6).

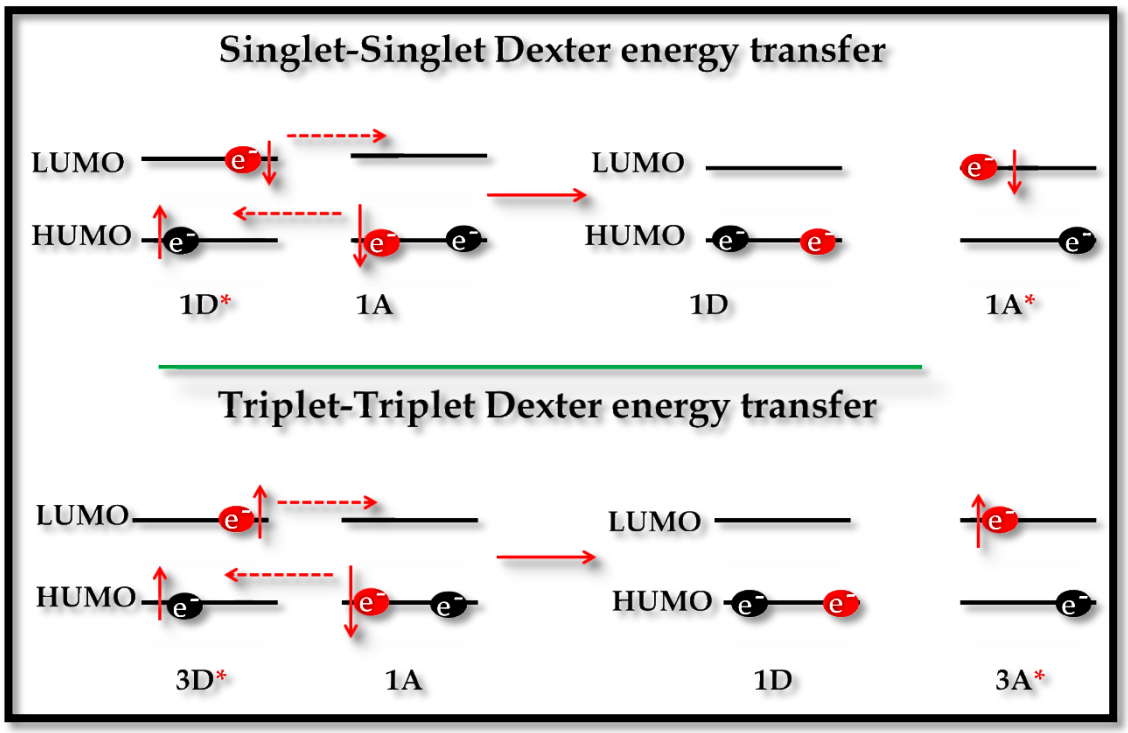

Figure 2.6. The Electron-Exchange (Dexter) Energy Transfer Mechanism

In the strong coupling interaction (when energy of interaction between donor and acceptor is greater than the display of the transitions) according to the exchange mechanism the process of energy transfer is classified by Dexter, which requires overlapping of wave functions of donor and acceptor. The excitation is oscillates back and delocalize over donor and acceptor and forth between them (Wrobel et al. 2011 and Jun Lu et al. 2012).

Another noticing point is of donor impact on the excitation of chromophoric acceptor molecules in the visible light and electron transport from HOMO of donor-D to HOMO of acceptor-A which occur in the excited state. The electronic process thus causes quenching of fluorescence emission of donor-D when comparing to the standard molecule. The efficiency of the processes of photoinduced electron and energy transfers from donor-D to acceptor-A moieties were usually investigated by

spectroscopic methods such as UV–vis absorption and photoluminescence and voltammetric techniques such as cyclic voltammetry (Fatma B. et al 2011).

2.4 Applications of Electronic Energy Transfer

Many reactions in photochemistry and radiation, physics and biology depend on the transfer of electronic energy transfer. The applications and observation of resonance energy transfer (RET) stretch well further than the present day technology of harvesting light. The energy transfer mechanism has a significant function in luminescence detectors and in the operation of organic light-emitting diodes (OLEDs), in transition metal doped-crystalline solid materials and glasses, in laser frequency conversions. In the fields of computation and optical communications and in several logic gate devices and optical switching (based on the similar principle) include mechanism of electronic energy transfer. This recent discovery of electron spin being able to transfer along with the energy brings many potential applications in many fields.

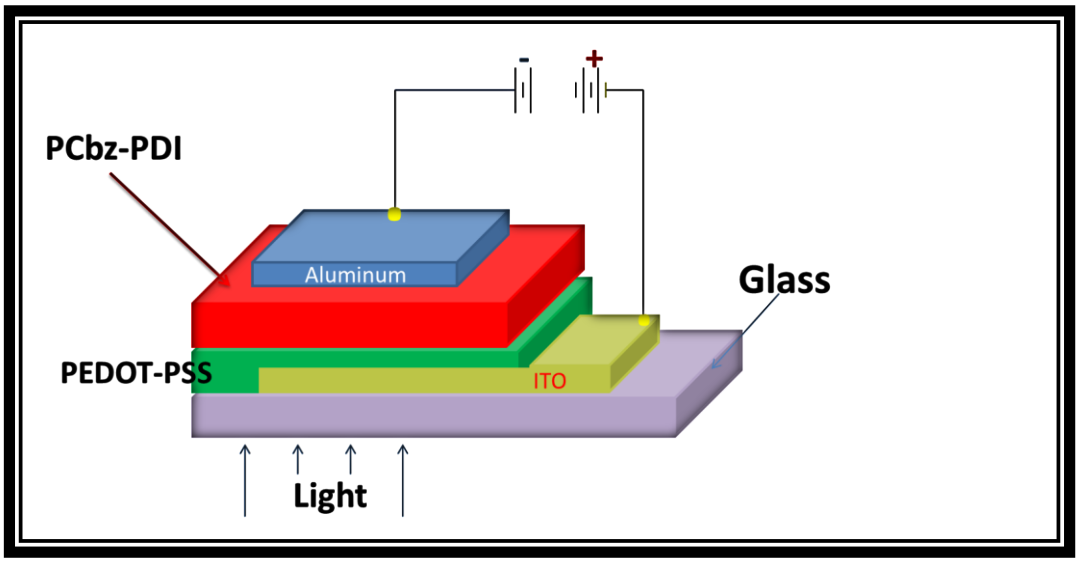

Figure 2.7. Application of Energy Transfer: (polyCbz-PDI Used as a Active Layer in Photovoltaic Device Strecture)

The energy transfer process can be noticeably modified via interaction with a stationary/static electric field. In the field of molecular biology, the characterization of dynamical processes and the determination of protein structures are strengthened by studies of the transport of energy between materials or chromophores. Further

applications of ultrasensitive molecular photography are again depend on the same basic principle. In the other applications like photodynamic therapy, the energy transfer systems are used to act as sensitizers, and as analyte-specific sensors. Also, the quantum mechanics and electromagnetism are arising from the nanoscale interaction due to the rich ground that provides by electronic energy transfer.

Chapter 3

EXPERIMENTAL

3.1 Materials

Spectroscopic grade solvents were used directly for spectroscopic analyzes without any purification and all other solvents employed in the study were distilled by common purification techniques.

3.2 Instruments

UV-vis Absorption Spectra

The absorption of electromagnetic radiation data of the compounds were studied via UV-vis absorption spectra of solutions which were obtained by using a Varian Cary-100 spectrophotometer.

Emission Spectra

The Emission and fluorescence profiles of the compounds were studied via emission spectra measurements at excitations wavelengths of 318 (for 2,7-dibromo-substituted-carbazole and 2,7-dibromo-substituted-N-dodecylcarbazole) and 295.5 (for polycarbazole), respectively by using Varian Cary Eclipse spectrophotometer.

3.3 Synthesis of 2,7-Dibromo-N-dodecylcarbazole

(Zubair, R. M., MS Thesis 2013, submitted)

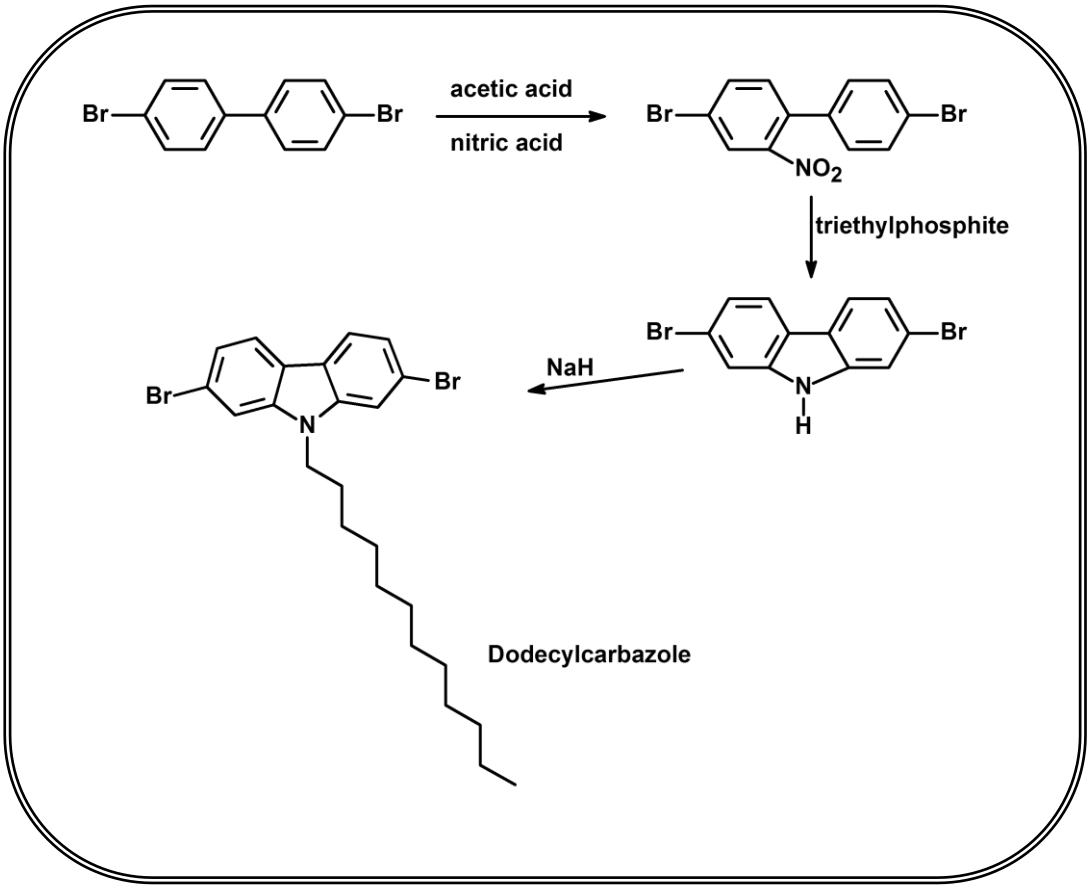

Scheme 3.1. Synthesis of 2,7-dibromo-N-dodecylcarbazole, dodecylcbz (Zubair, R. M., MS Thesis 2013, submitted)

The synthesis of 2,7-dibromo-N-dodecylcarbazole was synthesized and characterized according to the reported proceudres from the thesis of Zubair, 2013.

3.4 Synthesis of Poly(N-dodecylcarbazole)-2,7-diyl

(Hassan, P. J., MS Thesis 2013, submitted)

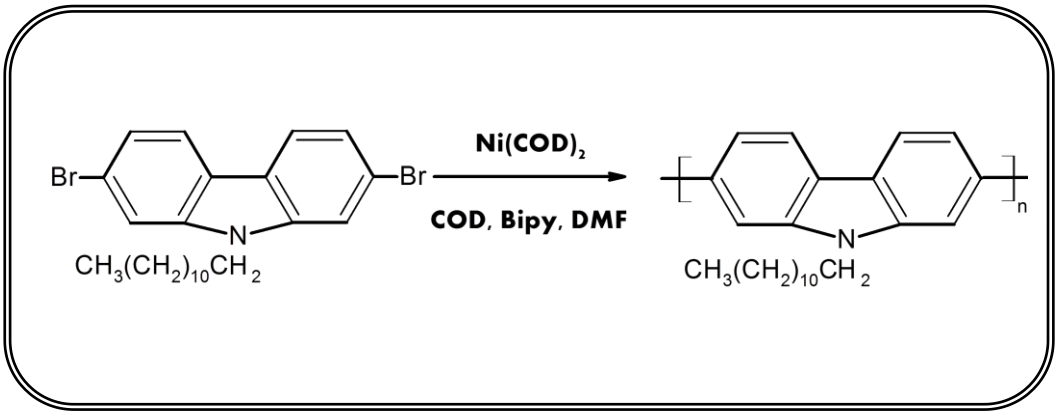

Scheme 3.2. Synthesis of Poly(N-dodecylcarbazole)-2,7-Diyl, Polycbz (Hassan, P. J., MS Thesis 2013, submitted)

The synthesis of polycarbazole was synthesized and characterized as described in the thesis of Hassan, 2013.

3.5 Synthesis of N,N – Di-(-1-Dehydroabietyl) Perylene -3,4,9,10-Bis(Dicarboximide)

(Icil et al. 1998)

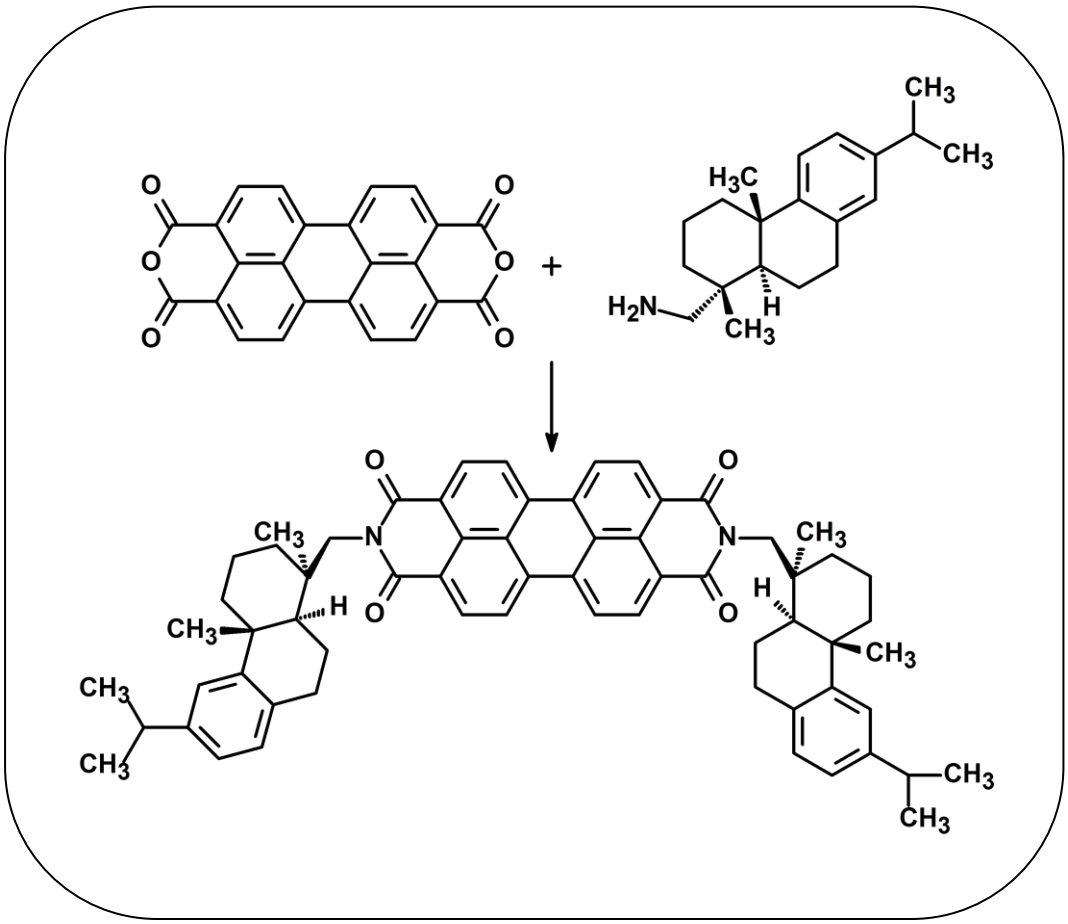

Scheme 3.3. Synthesis of N,N – Di-(-1-Dehydroabietyl) Perylene -3,4,9,10-Bis(dicarboximide) (Icil et al. 1998)

The synthesis of dehydroabietyl PDI was carried out according to the reported procedure of Icil and et al.

3.6 General Representation of Energy Transfer Mechansim Between Donor and Acceptor Molecules

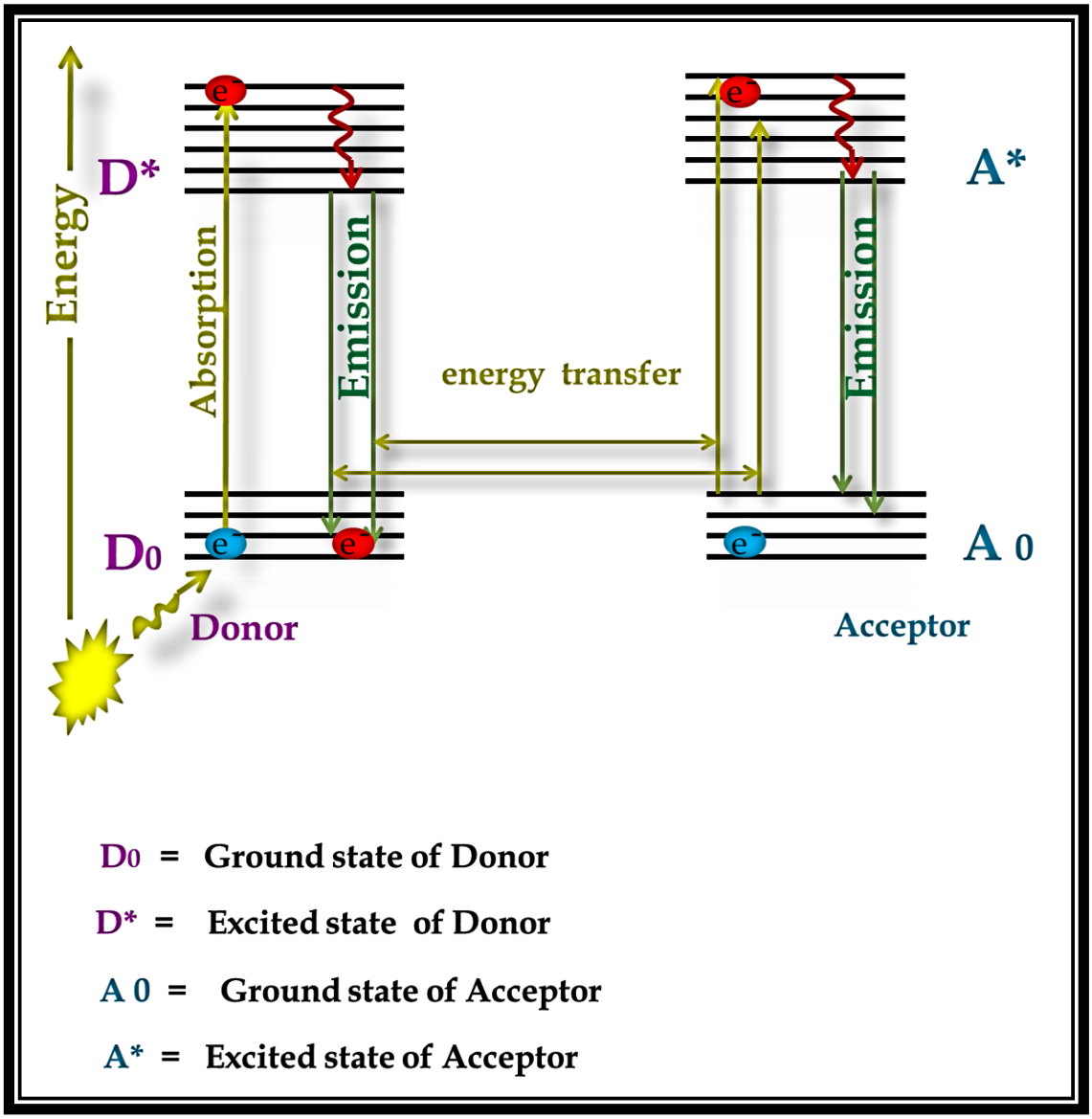

Figure 3.1. General Schematic Representation of Energy Transfer Mechanism

Chapter 4

DATA AND CALCULATIONS

4.1 Fluorescent Quantum Yield

The fluorescent quantum yield (Φ_f) of electron donating carbazole derivatives (2,7-dibromo-9H-carbazole, 2,7-dibromo-N-dodecylcarbazole, and poly(N-dodecylcarbazole)-2,7-diyl) were considered as 0.5 according to the literature values. This was the optimum value (in the usual range of 0.2 – 0.7) presented for carbazole compounds.

4.2 Maximum Absorption Co-effcients (ε_{max})

According to the Beer-Lamberts law, the linear relationship between absorbance and concentrtion can give the maximum absorption coefficient as shown in the equation below.

$$\varepsilon_{max} = \frac{A}{cl}$$

Where,

ε_{max} : Maximum extinction co-efficient in L mol^{-1} cm^{-1} at

A : Absorbance

c : Concentration (mol L $^{-1}$)

l : Path length (cm)

Calculation of Maximum Absorption Coefficients of Dehydro – PDI

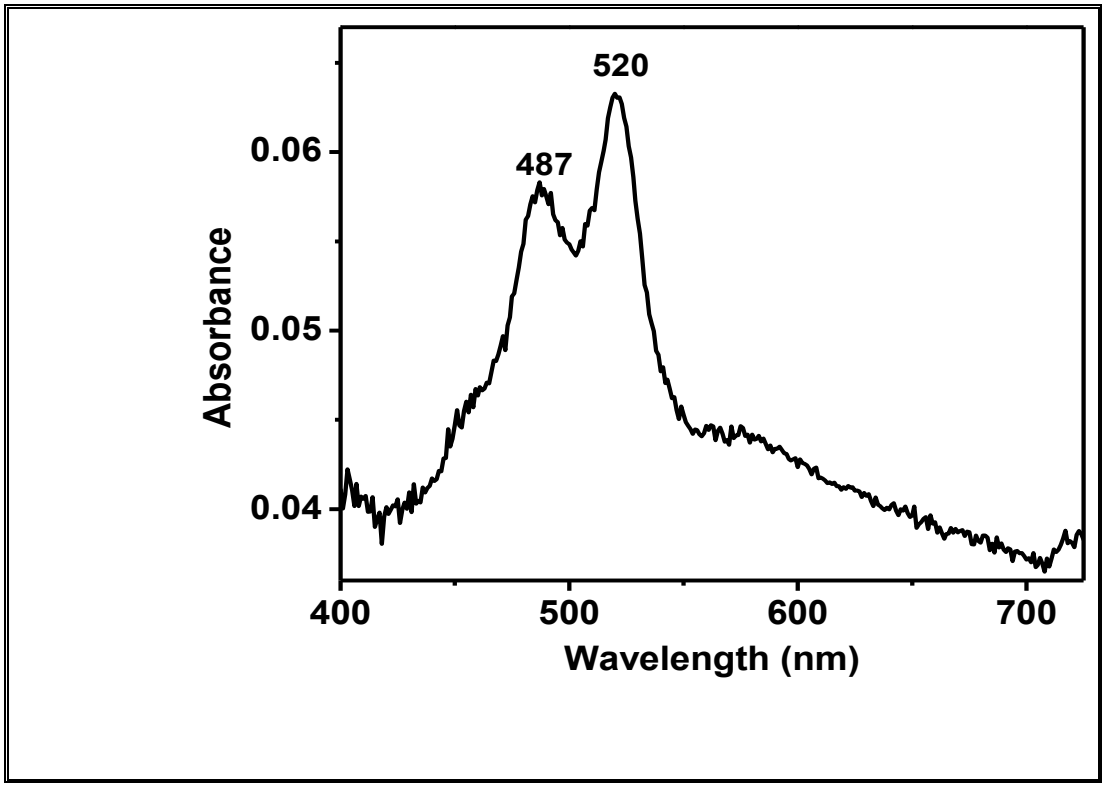

Figure 4.1. Absorption Spectrum of Dehydro-PDI in Methanol at 1 x 10^{-5} M Concentration

By the absorption spectrum of Dehydro-PDI (Figure 4.1),

The absorption (A) = 0.06328 at the λ_{max} = 520 nm

c= 1 x 10^{-5}M

l = 1 cm

$$\varepsilon_{max} = \frac{0.06328}{1 \text{ x } 10^{-5} \text{ x } 1}$$

ε_{max} = 6328 L. mol^{-1} . cm^{-1}

Similarly, the molor absorption of the compound-PDI in other solvents were calculated by the same method and the values are listed below (Table 4.1).

Table 4.1. Molar absorptivity data of Dehydro-PDI in Methanol, $CHCl_3$ and acetonitrile

Solvent	Con. (M)	Absorbance	λ_{max}(nm)	ε_{max}($Lmol^{-1}$ cm^{-1})
$CHCl_3$*			526	93200
Methanol	1 x 10^{-5}	0.06328	520	6328
CH_3CN	1 x 10^{-6}	0.05	520	50000

*(Icil H. et al. 1998)

4.3 Full Width-Half Maximum (FW-HM) of the Selected Absorption ($\Delta\overline{\nu}_{1/2}$)

The full width-half maximum absorption is generlly described as half of the full absorption of the compound (bending at half of maximum intensity).

$$\Delta\,\overline{\nu}_{1/2} = \overline{\nu}_{I} - \overline{\nu}_{II}$$

Where,

$\overline{\nu}_{I}$, $\overline{\nu}_{II}$: The frequencies from the absorption spectrum in cm^{-1}

The FW-HM of the Selected Absoption of Carbazole :

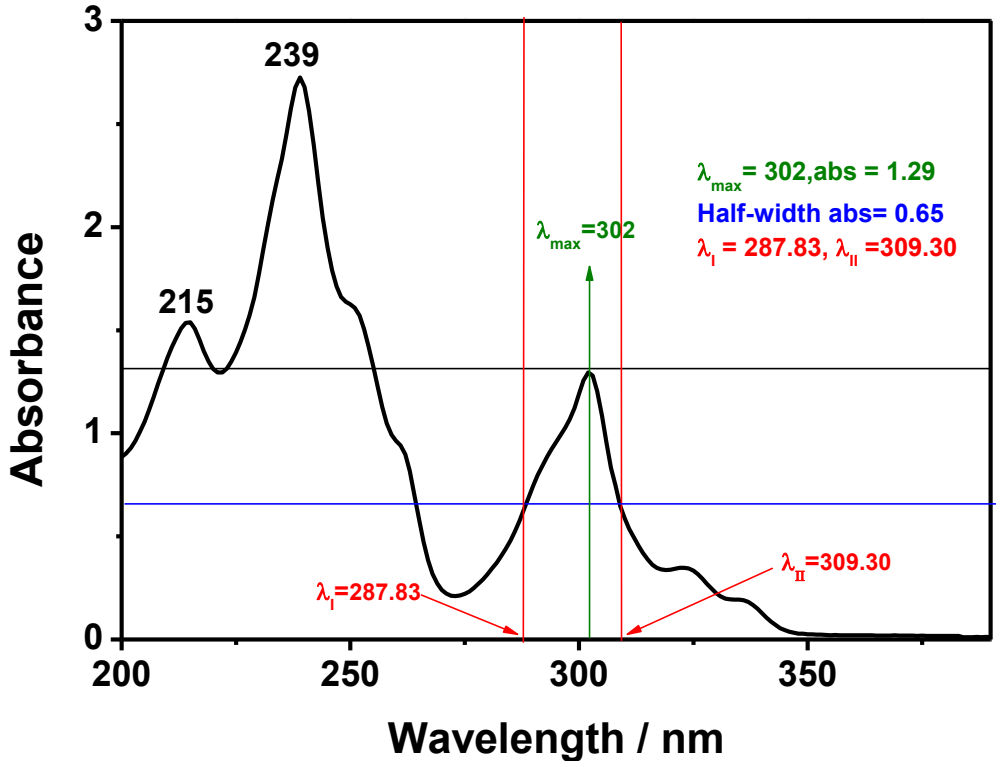

Figure 4.2. Absorption Spectrum of 2,7-dibromocarbazole in CH_3CN

From the Figure 4.2

λ_I = 287.83 nm

λ_I = 287.83 nm x$\frac{10^{-9}\text{m}}{1\text{nm}}$ x$\frac{1\text{cm}}{10^{-2}\text{m}}$ = 2.8783 x 10^{-5} cm

$\bar{\nu}_I = \frac{1}{2.8783\ x\ 10^{-5}\ cm}$ = 34742.73 cm^{-1}

λ_{II} = 309. 30 nm

λ_{II} = 309.30 nm x$\frac{10^{-9}\text{m}}{1\text{nm}}$ x$\frac{1\text{cm}}{10^{-2}\text{m}}$ = 3.0930 x 10^{-5} cm

$\bar{\nu}_{II} = \frac{1}{3.0930\ x\ 10^{-5}\ cm}$ = 32331.07 cm^{-1}

$\Delta\,\overline{\nu}_{1/2} = \overline{\nu}_I - \overline{\nu}_{II}$

$\Delta\,\overline{\nu}_{1/2}$= 34742.73 cm^{-1} – 32331.07 cm^{-1}

$\Delta\,\overline{\nu}_{1/2}$ = 2411.66 cm^{-1}

By the similar method of above, the half-widths were calculated and presented in the tables below.

Table 4.2. FWHM of the Selected Absorption of Carbazole Compound

Solvent	ε_{max}($Lmol^{-1}$ cm^{-1})	λ_I (nm)	λ_{II} (nm)	$\Delta\,\overline{\nu}_{1/2}$($cm^{-1}$)
$CHCl_3$	24360	289.14	313.13	2649.71
Acetonitrile	7680	287.83	309.30	2411.66
Methanol	10166	274.45	310.44	4224.16

Table 4.3. FWHM of the Selected Absorption of Dodecylcbz Compound

Solvent	ε_{max}(Lmol^{-1} cm^{-1})	λ_I (nm)	λ_{II} (nm)	$\Delta\,\overline{\nu}_{1/2}$(cm^{-1})
$CHCl_3$	2080	291.05	313.65	2475.68
Acetonitrile	9540	287.22	311.22	2684.90
Methanol	2020	287.83	310.97	2585.29

Table 4.4. FWHM of the Selected Absorption of Polycarbazole* Compound

Solvent	ε_{max}(Lmol^{-1} cm^{-1})	λ_I (nm)	λ_{II} (nm)	$\Delta\,\overline{\nu}_{1/2}$(cm^{-1})
$CHCl_3$	74.42	303.78	313.52	1022.66
Acetonitrile	70.22	299.74	311.88	1298.63
Methanol	75.68	300.67	310.71	1074.70

*The ε_{max} and τ_0 values of polymer are calculated per monomer unit mass.

4.4 Natural/Theoretical Radiative Lifetimes (τ_0)

The formula below shows as that the natural radiative lifetime related to an excited molecule without radiationless transitions.

$$\tau_0 = \frac{3.5\ x\ 10^8}{\overline{\nu}^2_{max}\ x\ \varepsilon_{max}\ x\ \Delta\ \overline{\nu}_{1/2}}$$

Where,

τ_0 : Natural Radiative Lifetime

$\bar{\nu}_{max}$: Mean frequency of the maximum absoption band in cm^{-1}

ε_{max} : The maximum absorption coefficient in L mol^{-1} cm^{-1} at maximum absorption wavelength, λ_{max}

$\Delta\ \overline{\nu}_{1/2}$: Half-width of the selected absorption in units of cm^{-1}

Natural/Theoretical radiative lifetime of Carbazole in chloroform:

From Figure 4.2 , λ_{max}= 303 nm

λ_{max} = 303nm x$\frac{10^{-9}}{1nm}\ x\ \frac{1cm}{10^{-2}m}$ = 3.03 x 10^{-5} cm

$\bar{\nu}_{max} = \frac{1}{3.03\ x\ 10^{-5}\ cm}$ = 33003.30 cm^{-1}

$\overline{\nu}^2_{max}$ = (33003.30 cm^{-1})^2 = 10.8 x 10^8 cm^{-2}

ε_{max} = 24000 L. mol^{-1} .cm^{-1} (Frome Figure 4.2)

$$\tau_0 = \frac{3.5 \times 10^8}{\bar{\nu}_{max}^2 \times \varepsilon_{max} \times \Delta\bar{\nu}_{1/2}}$$

$$\tau_0 = \frac{3.5 \times 10^8}{(33003.30)2 \times 24000 \times 2649.71}$$

τ_0 = 0.51 x 10^{-8} s

τ_0 = 5.01 ns

By the similar method of calculation, $\boldsymbol{\tau_0}$ of the compounds in the choloroform are presented in the table below.

Table 4.5. Theoretical Radiative Lifetimes of Carbazole, Dodecylarbazole and Polycarbazole in Chloroform

Solvent	τ_0 of carbazole	τ_0 of dodecylcbz	τ_0 of polycbz*
chlroform	5.0	10.7	403.2
acetonitrile	5.1	28.8	230.2
methanol	10	48.5	3000

*The ε_{max} and $\tau_0$values of polymer are calculated per monomer unit mass.

4.5 Natural Fluorescence Life Times(τ_f)

The theoretical flourescence related to the theoretical rate time of the molecule remains in the excited state before emitting a photon(fluorescence)

$$\tau_f = \tau_0 \, x \, \Phi_f$$

Where,

τ_f : Fluorescence lifetime

τ_0 : Theoretical radiative lifetime

Φ_f : Fluorescence quantum yield

Theoretical Fluorescence Life times

$\tau_f = \tau_0 \, x \, \Phi_f$

Natural Fluorescence Life times of carbazole:

τ_0 = 50.9 ns

Φ_f = 0.5

$\tau_f = \tau_0 \, x \, \Phi_f$

$\tau_f = 5.0 \, x \, 0.5 = 2.5$

Table 4.6. Natural fluorescence life times data of carbazole derivatives

Compound	τ_0	Φ_f	τ_f
Cbz	5.0	0.5	2.5
R-cbz	10.7	0.5	5.35
Polycbz*	403.2	0.5	201.6

*The ε_{max} and $\tau_0$values of polymer are calculated per monomer unit mass.

4.7 Calculation of Critical Transfer Distances

By the Forster equation can be calculated Critical Transfer Distances (R_0^6) :

$$R_0^6 = \frac{9000(ln10)K^{2\Phi}{}_D}{128\pi^5 n^4 N} \int_0^\infty \frac{F_D(\mathrm{v})\varepsilon_A(\mathrm{v})}{\mathrm{v}^4} d\mathrm{v}$$

Where,

Φ_D : is the emission quantum yield of the donor in the absence of the acceptor

K : is the orientation factor(K^2=0,67 for randomly distributed olecules)

N : is Avagadros number

n : is the refactive index of the solvent

$F_D(\mathrm{v})$: overlap integral for the fluorescence spectrum of the donor normalized to unity($F_D(\mathrm{v})d\mathrm{v}=$)

$\boldsymbol{\varepsilon}_A(\mathrm{v})$: is the molar extinction co-efficion of acceptor at the wavenumber (v)

From the normalized emission spectrum of the donor, polycarbazole (Figure 4.3), the normalized area in chloroform $F_D(\lambda) = 82.31$

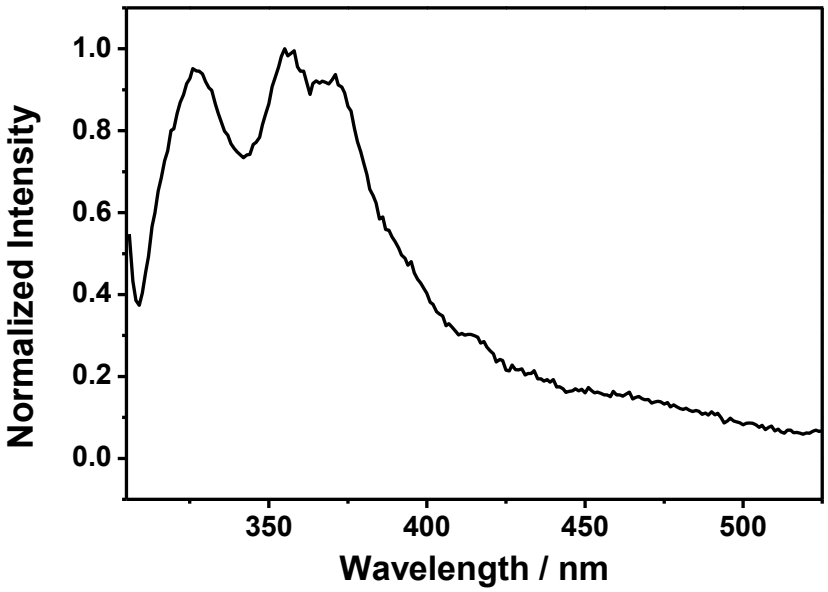

Figure 4.3. Normalized emission spectrum of the donor, polycarbazole (c = 5×10^{-3} M/monomer unit) in the absence of acceptor, Dehydro-PDI in chloroform

The absorption spectrum of acceptor, Dehydro-PDI in chloroform is shown below (Figure 4.4). The reported $\boldsymbol{\varepsilon}_{max}$ of 93200 is used for the calculation.

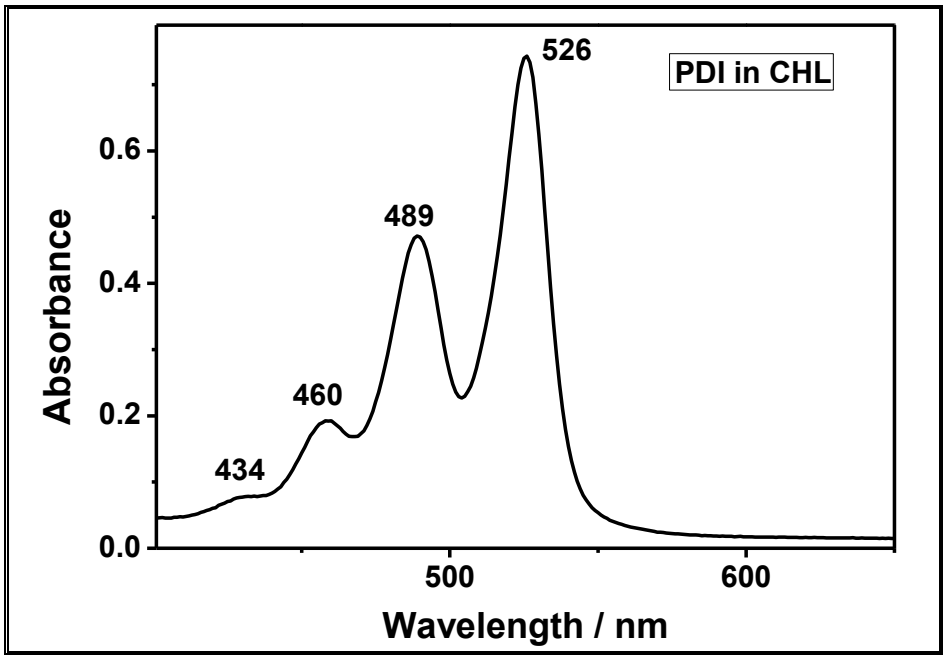

Figure 4.4. Absorption spectrum of Dehydro-PDI at c = 1×10^{-5} M in chloroform

⇨ $J = \int_0^\infty F_D(\lambda)\, \varepsilon_A(\lambda)\, \lambda^4\, d\lambda$

⇨ $J = 82.31 \times 93200 \times (526)^4$

⇨ $J = 5.87\times10^{17}$

⇨ $R_0^6 = \frac{8.785 \times 10^{-5}\, \kappa^2\, \Phi_D\, J}{n^4}$

⇨ $R_0^6 = 8.785\times10^{-5} \times 0.67 \times 0.5 \times 5.87\times10^{17}/(1.4429)^4$

⇨ $R_0^6 = 4 \times10^{12}$

⇨ $R_0 = 126$ Å

Table 4.7. Critical Ttransfer Distances Data of Carbazole Derivatives with Dehydro-PDI in Different Solvents

Solvent	R_0 of carbazole	R_0 of dodecylcbz	R_0 of polycbz*
chlroform	112 Å	120 Å	126 Å
acetonitrile	108 Å	107 Å	118 Å
methanol	78 Å	75 Å	85 Å

*The polymer concentrations are calculated per monomer unit mass.

4.8 Calculation of Rate Constants for Bimolecular Fluorescence Quenching (k_q)

The Rate constants for bimolecular fluorecence quenching values were calculated by Stern-Volmer plots.

$$\frac{I_0}{I} = 1 + k_q \,.\, \tau_0[Q]$$

Where,

$\frac{I_0}{I}$: Relative fluorescence intensity of donor

I_0 : Fluorescence intensity of donor without acceptor

I : Fluorescence intensities of donor quenched with acceptor

k_q : Rate Constant for Bimolecular Fluorescence Quenching

τ_0 : Natural radiative lifetime of donor in the absence of quencher

From the Figure 4.34 the emission intensities of polycarbazole were calculated in the absence (I_0) and presence (I) of Dehydro-PDI quencher (at different concentrations) and plotted the values of donor *vs.* quencher concentration.

The plot was shown in Figure 4.35 and the data obtained from the plot was shown in the diagram.

Slope of the plot from the data of linear regression = $k_q\tau_0$ = 312600

$$\Rightarrow \; k_q = \frac{27.74}{5.22\times10^{-9}\text{s}} \left(312600/403.2\times10^{-9}\right) = 7.77\times10^{11}\ \text{M}^{-1}\ \text{s}^{-1}$$

$k_q = 7.77\times10^{11}\ \text{M}^{-1}\ \text{s}^{-1}$

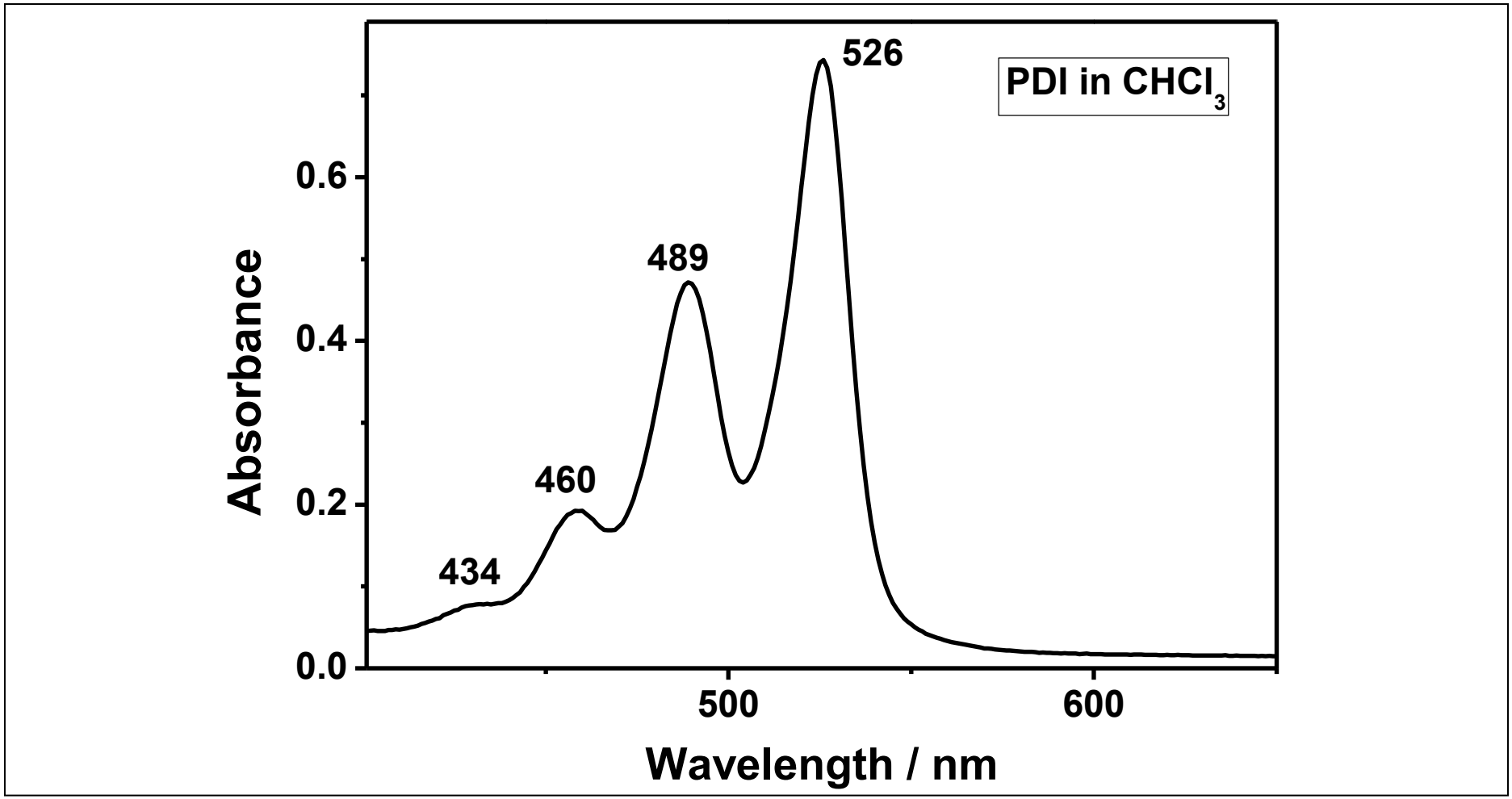

Figure 4.5. UV-vis Absorption Spectrum of 1 x 10^{-5} M PDI in $CHCl_3$

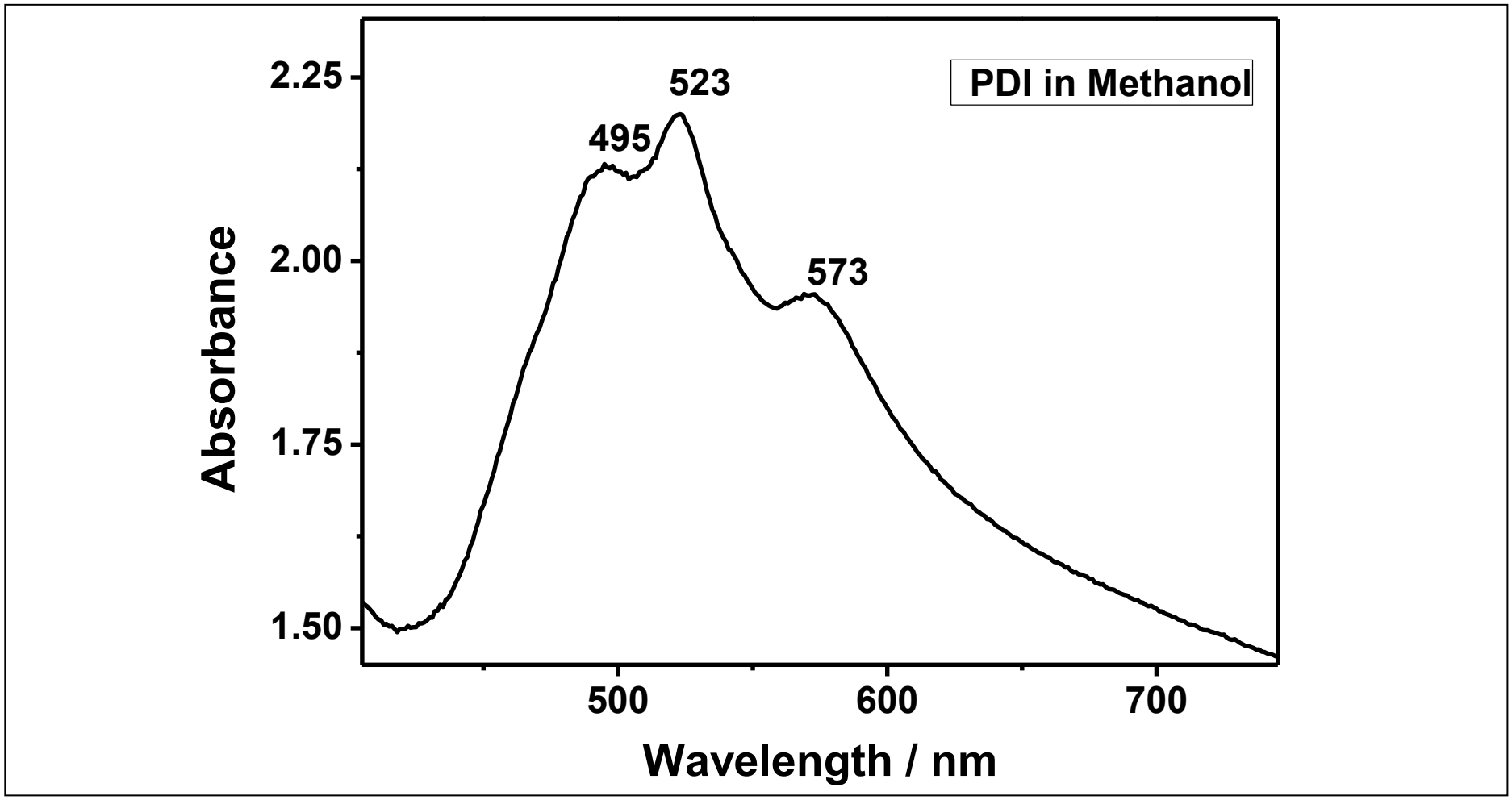

Figure 4.6. UV –vis absorption spectrum of 5 x 10^{-5} M PDI in Methanol

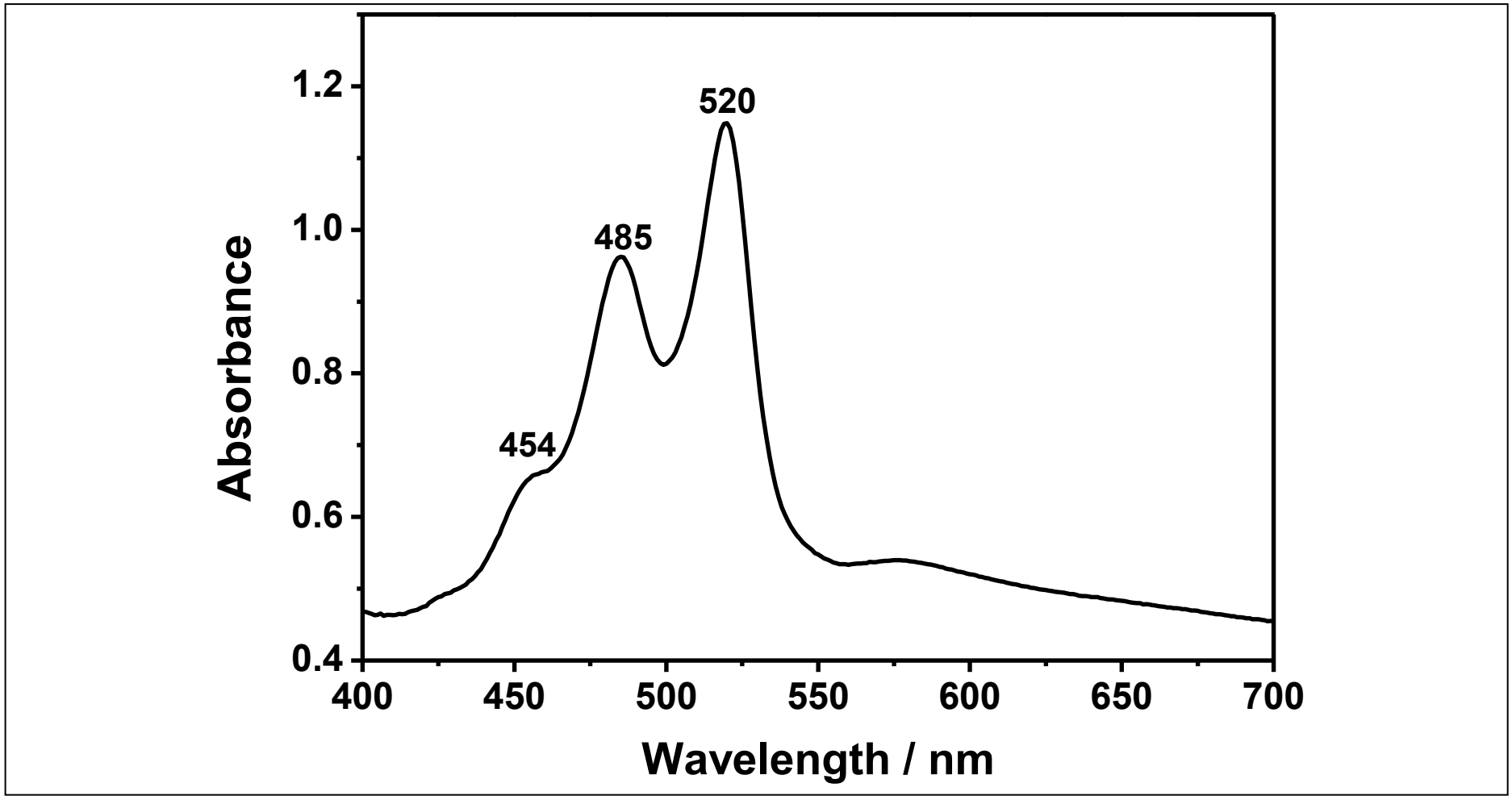

Figure 4.7. UV –vis Absorption Spectrum of 1 x 10^{-6} M PDI in CH_3CN

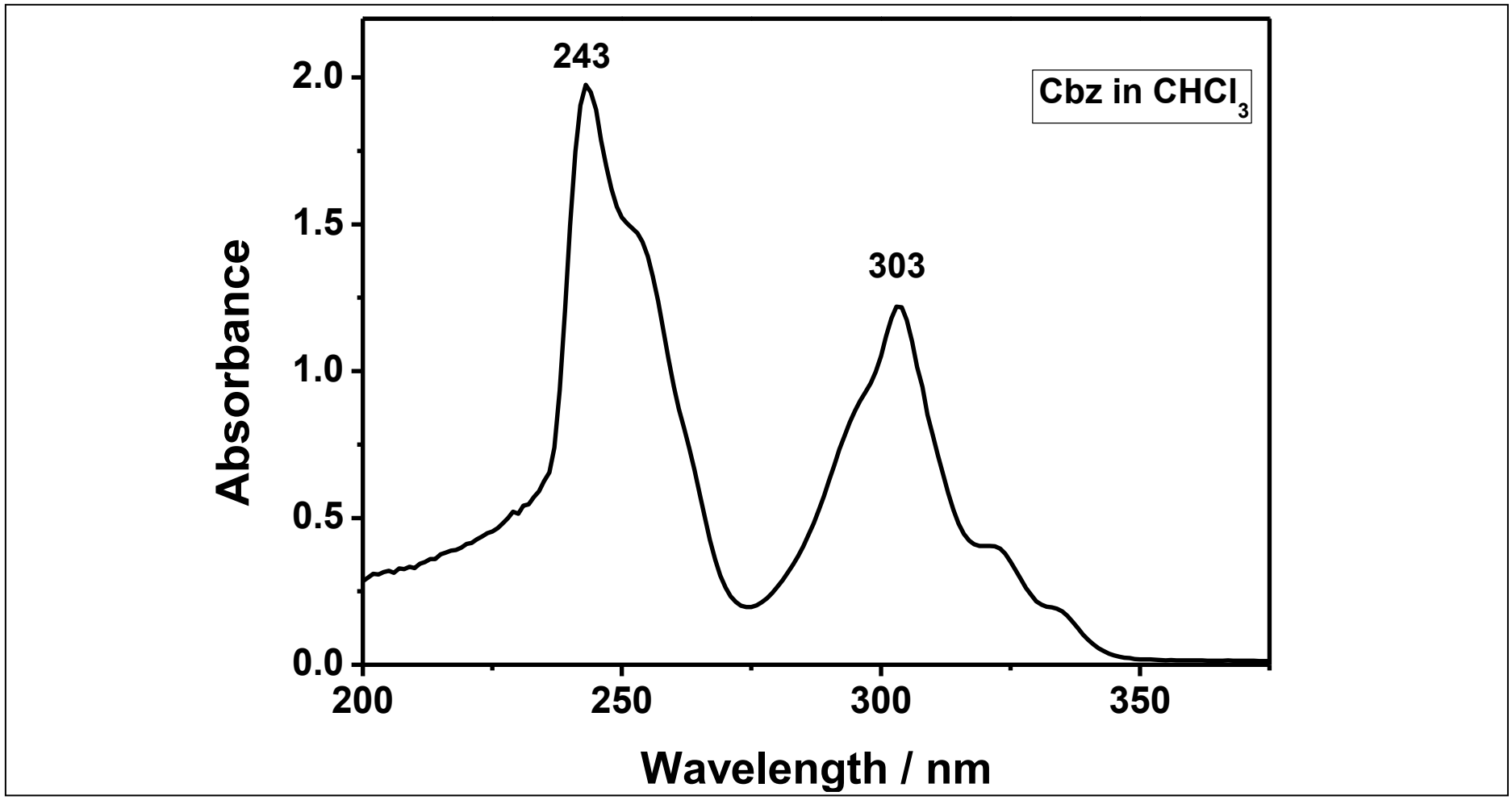

Figure 4.8. UV-vis Absorption Spectrum of Carbazole in Chloroform

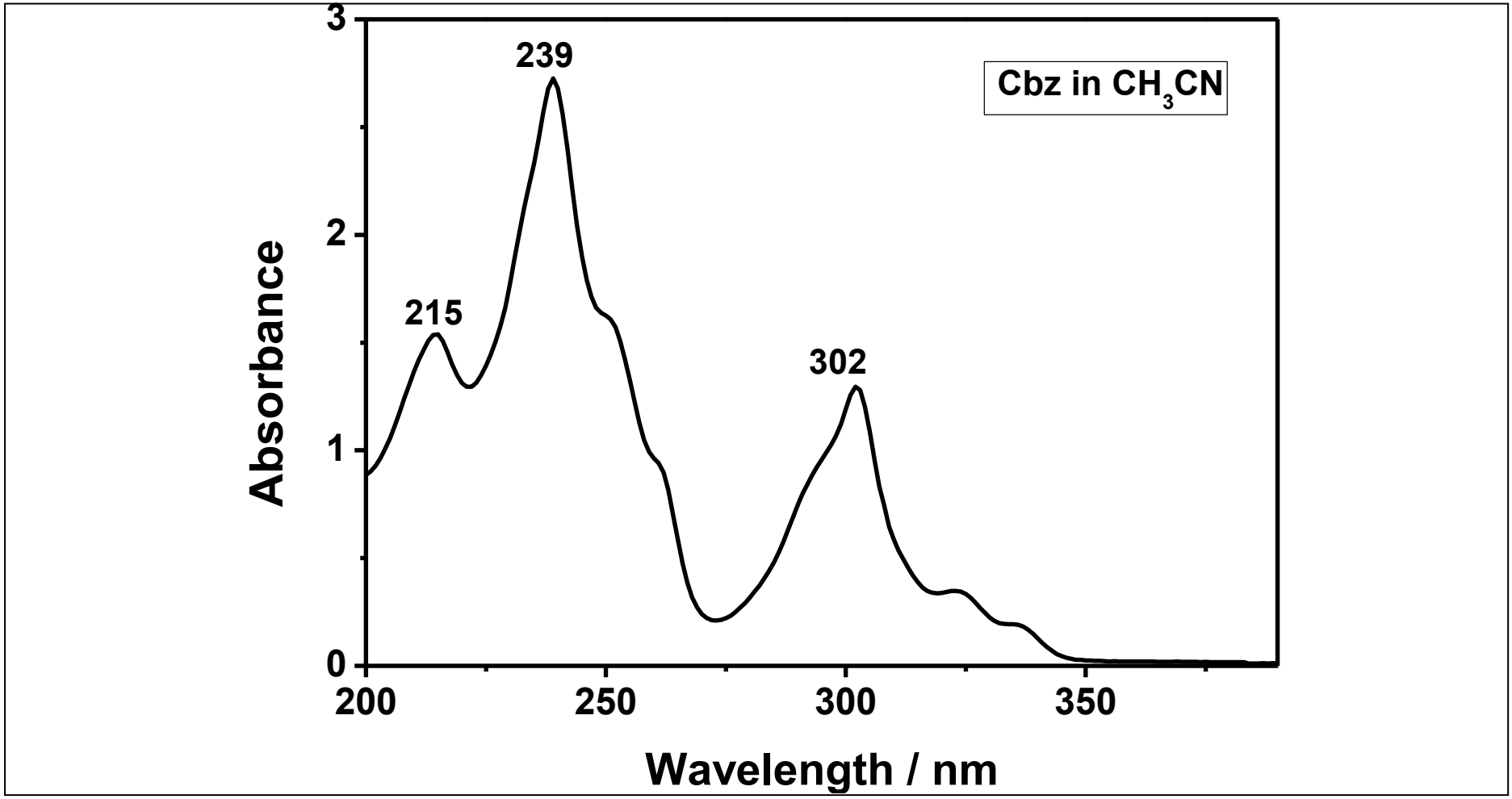

Figure 4.9. UV-vis Absorption Spectrum of 5 x 10^{-5} M Carbazole in CH_3CN

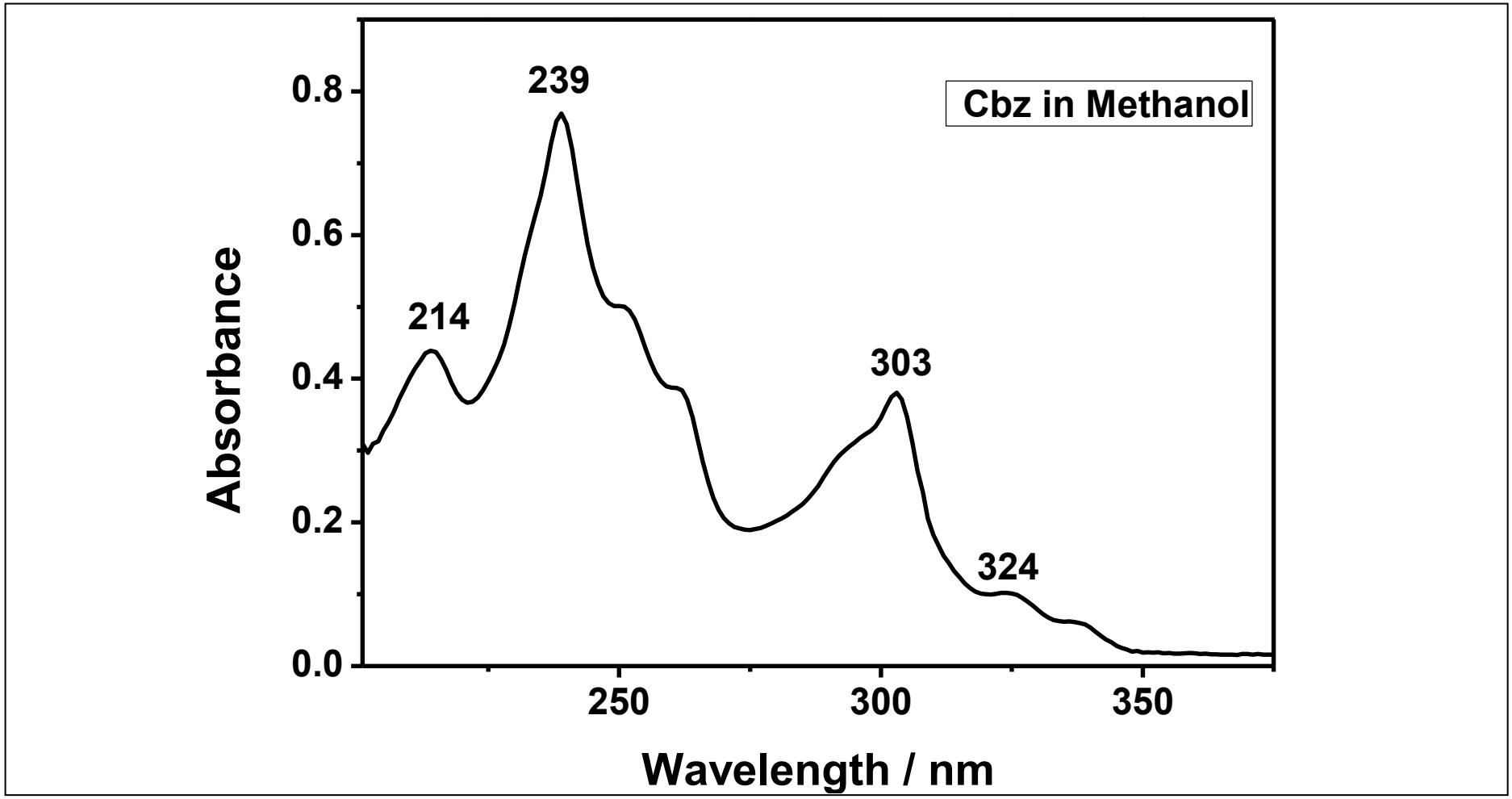

Figure 4.10. UV-vis Absorption Spectrum of 5 x 10^{-5} M Carbazole in Methanol

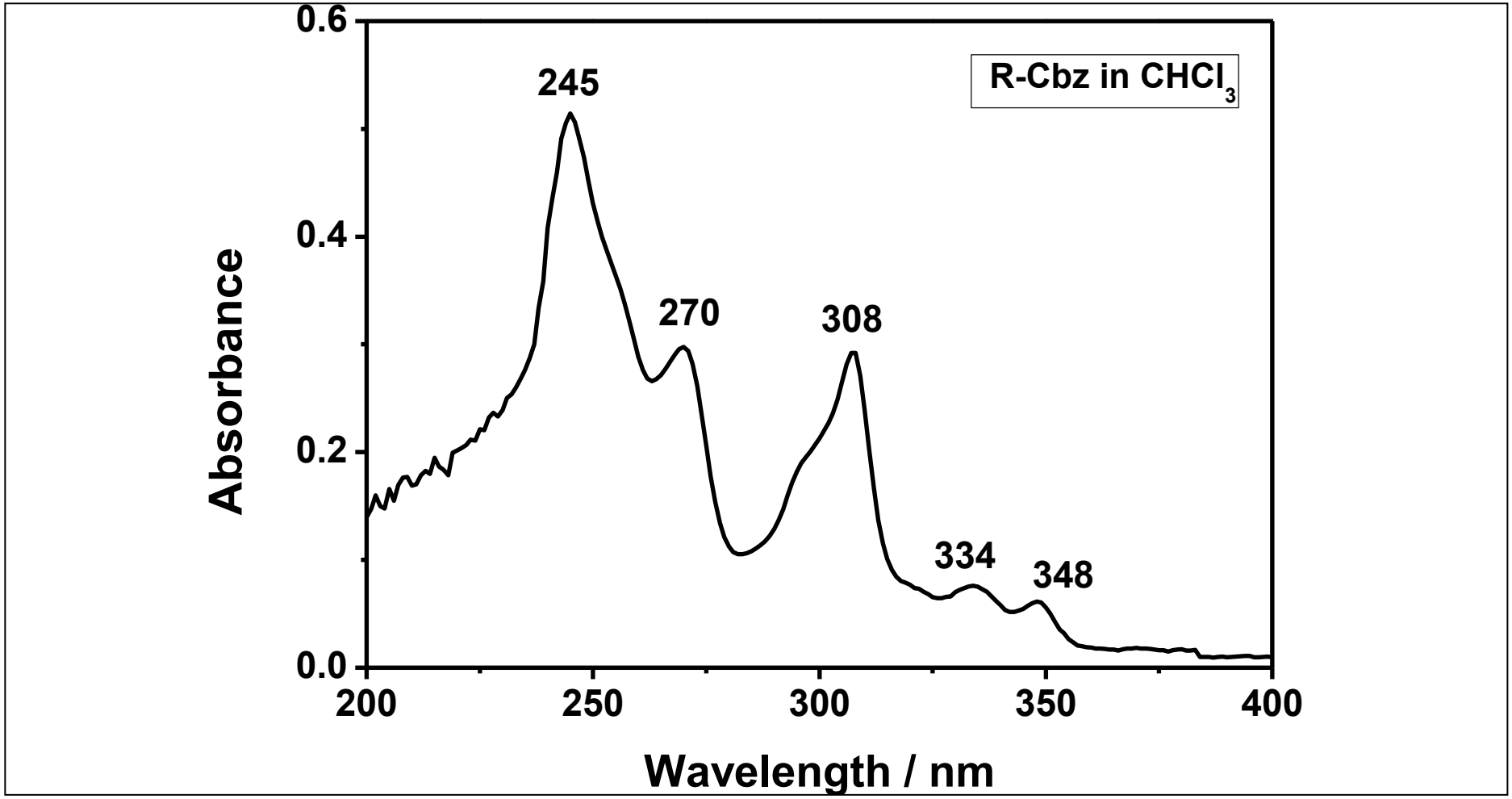

Figure 4.11. UV –vis Absorption Spectrum of 5 x 10^{-5} M Dodecylcbz in Chloroform

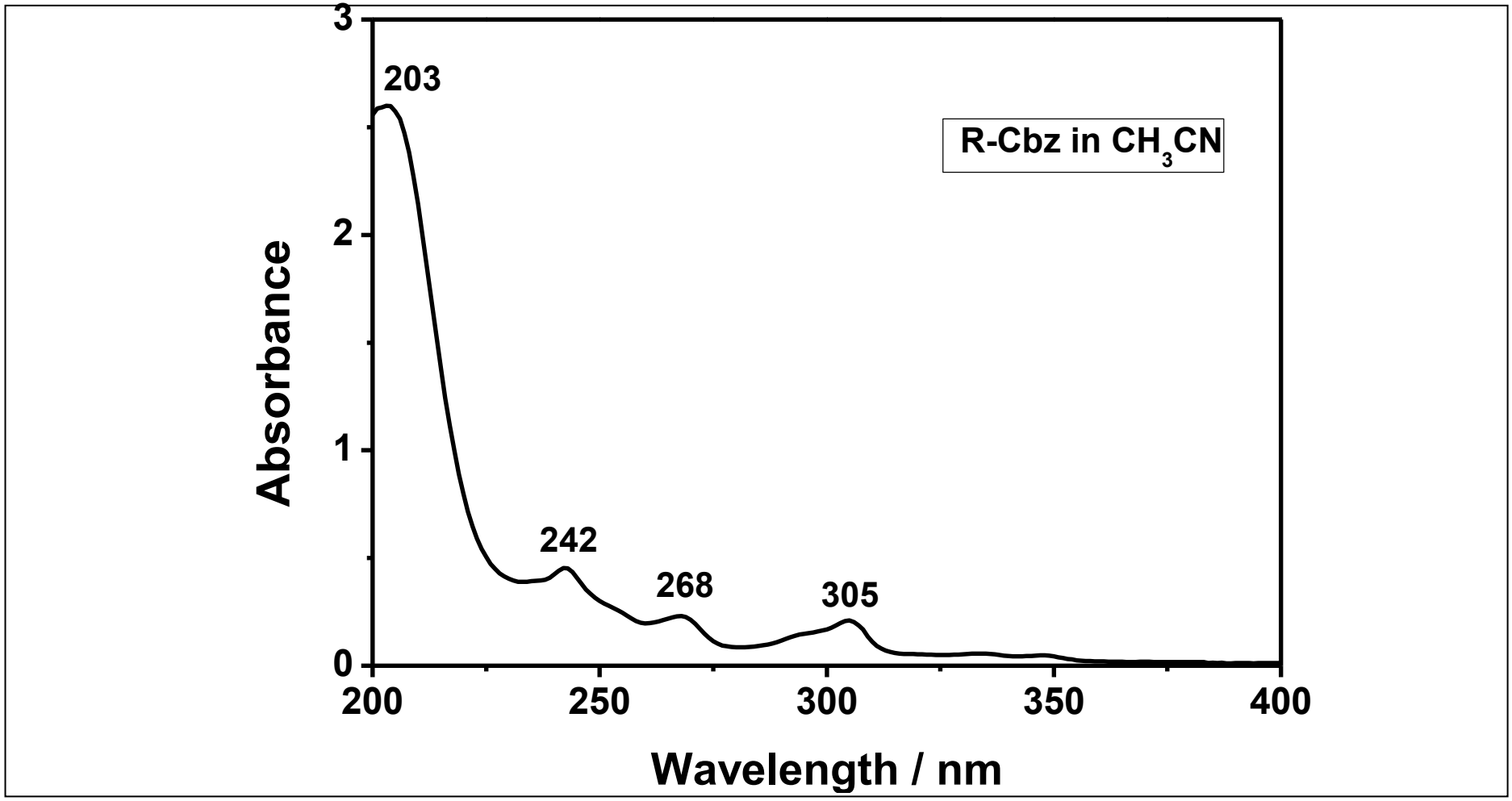

Figure 4.12. UV-vis Absorption Spectrum of 5 x 10^{-5} M Dodecylcarbazole in CH_3CN

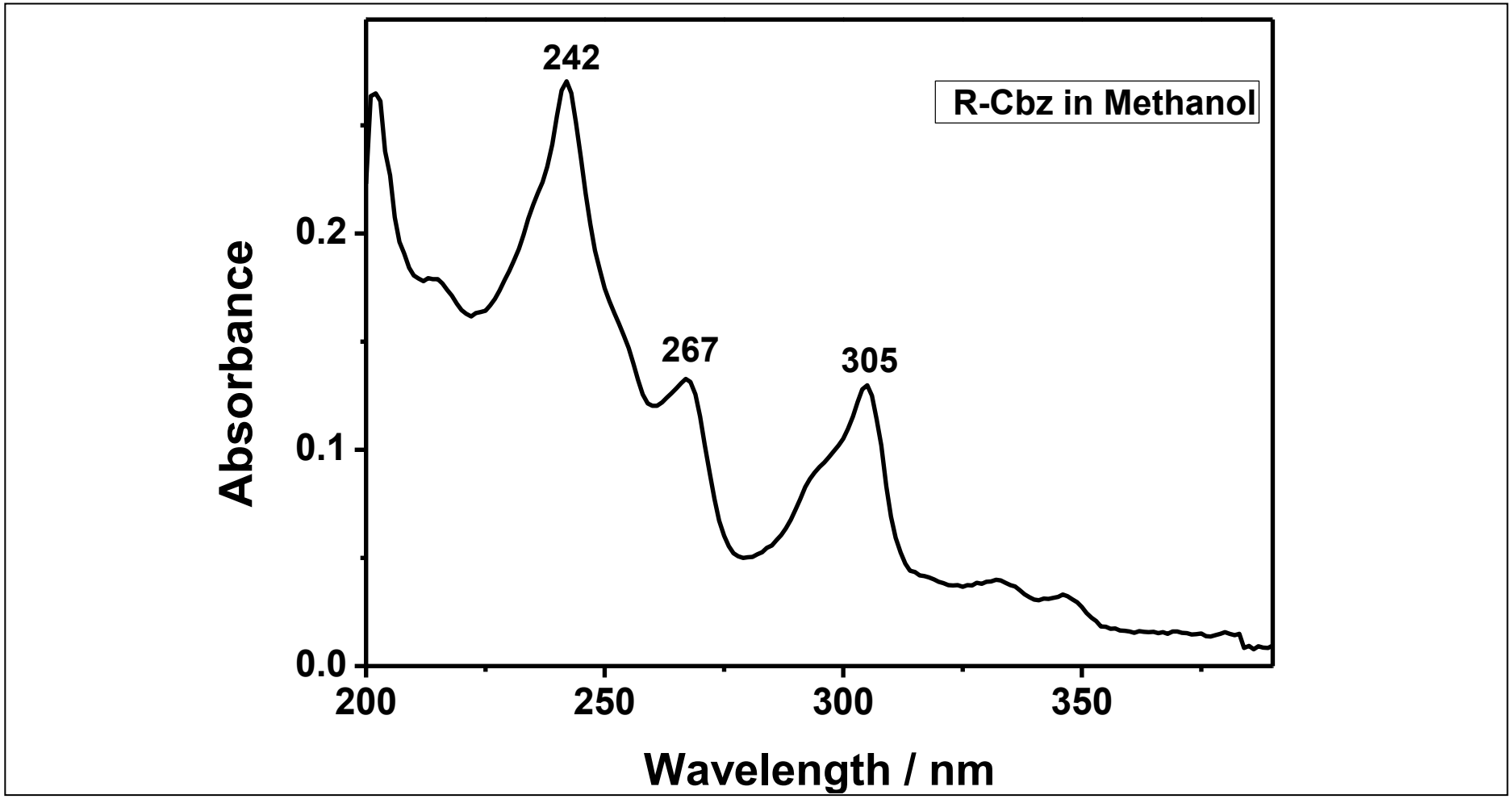

Figure 4.13. UV -vis Absorption Spectrum of 5 x 10^{-5} M Dodecylcarbazole in Methanol

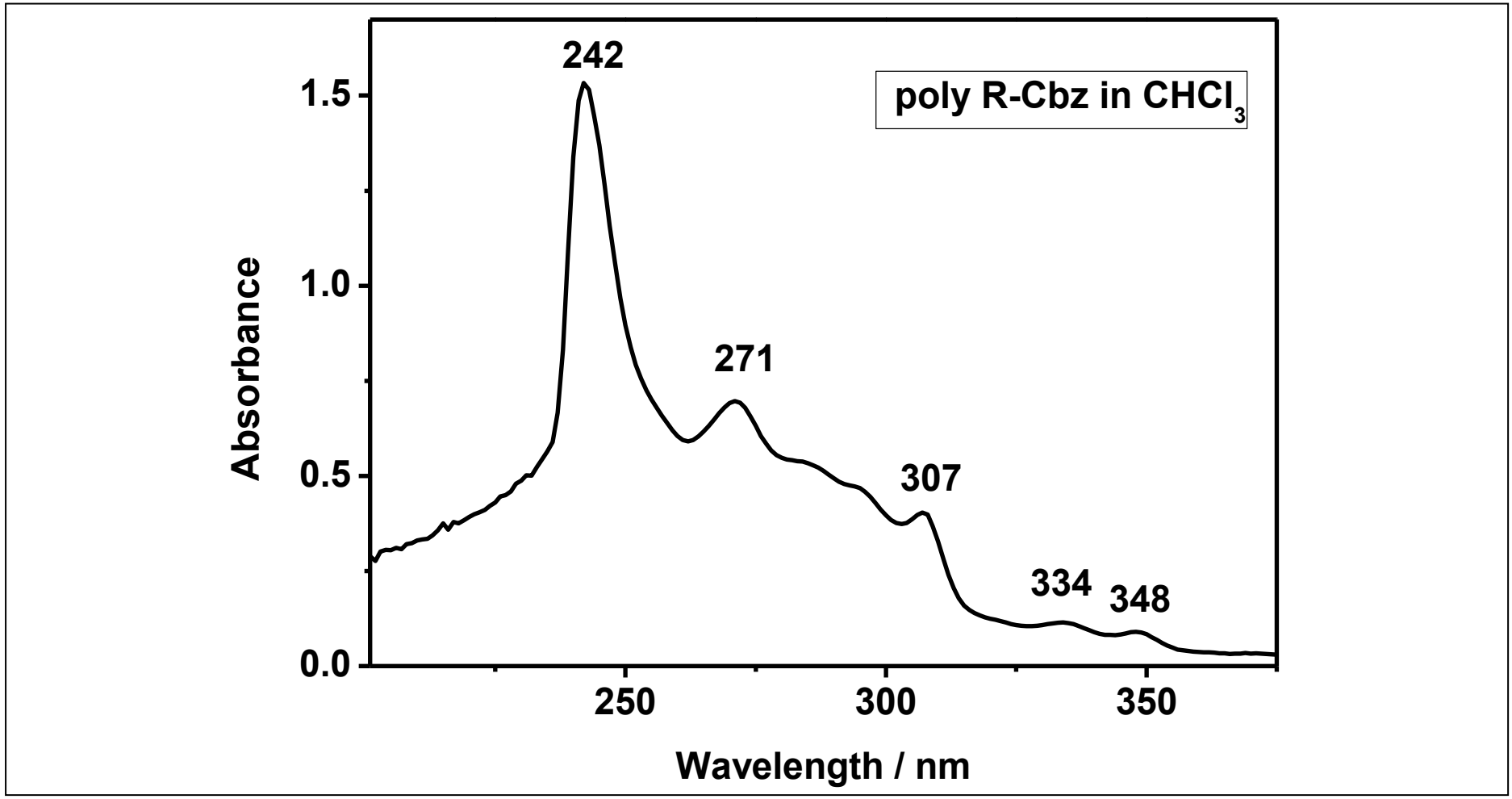

Figure 4.14. UV -vis Absorption Spectrum of 5 x 10^{-3}M Polycbz in Chloroform

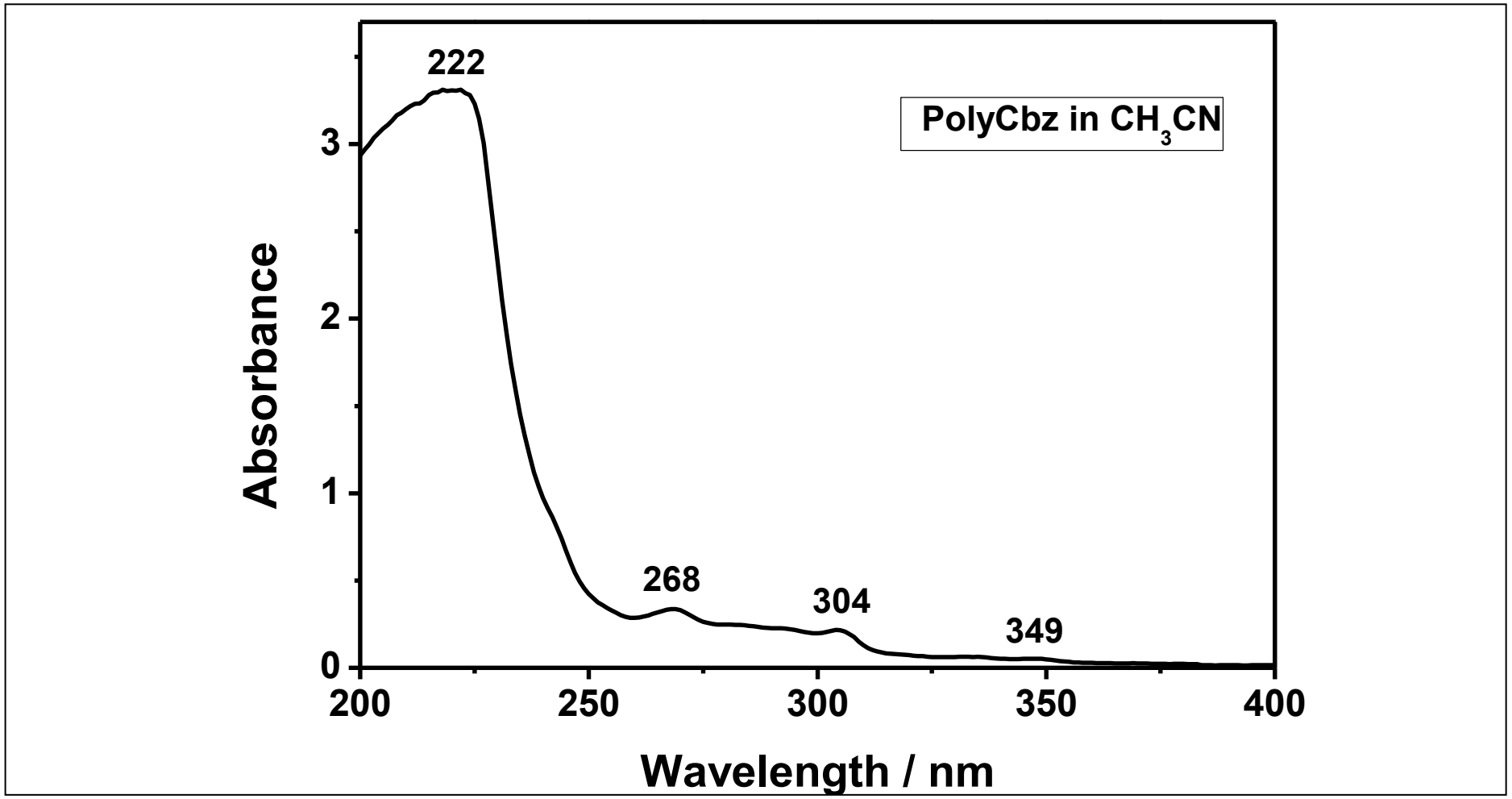

Figure 4.15. UV -vis Absorption Spectrum of 5 x 10^{-3} M Polycarbazole in CH_3CN

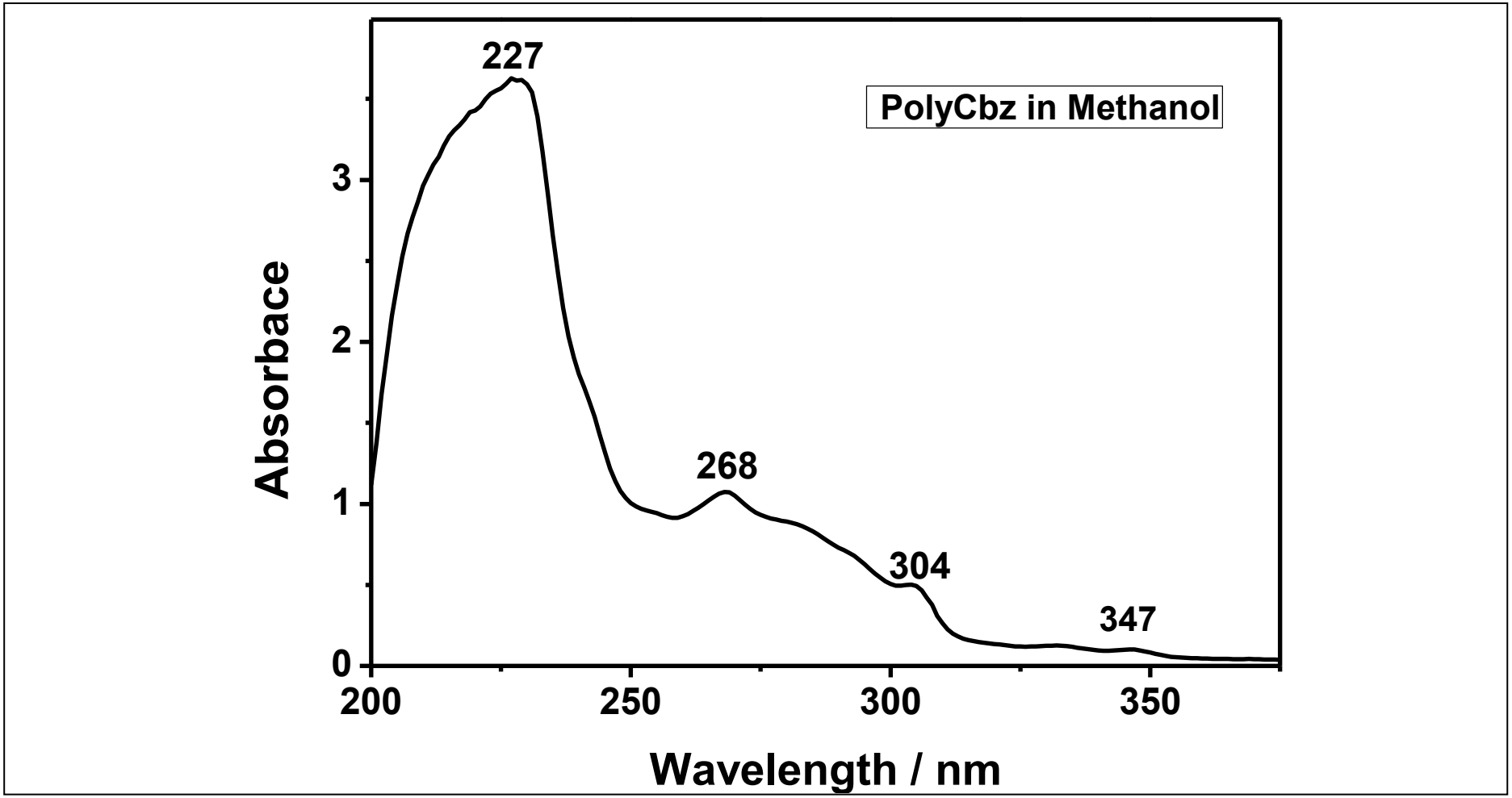

Figure 4.16. UV -vis Absorption Spectrum of 5 x 10^{-3} M Polycarbazole in Methanol

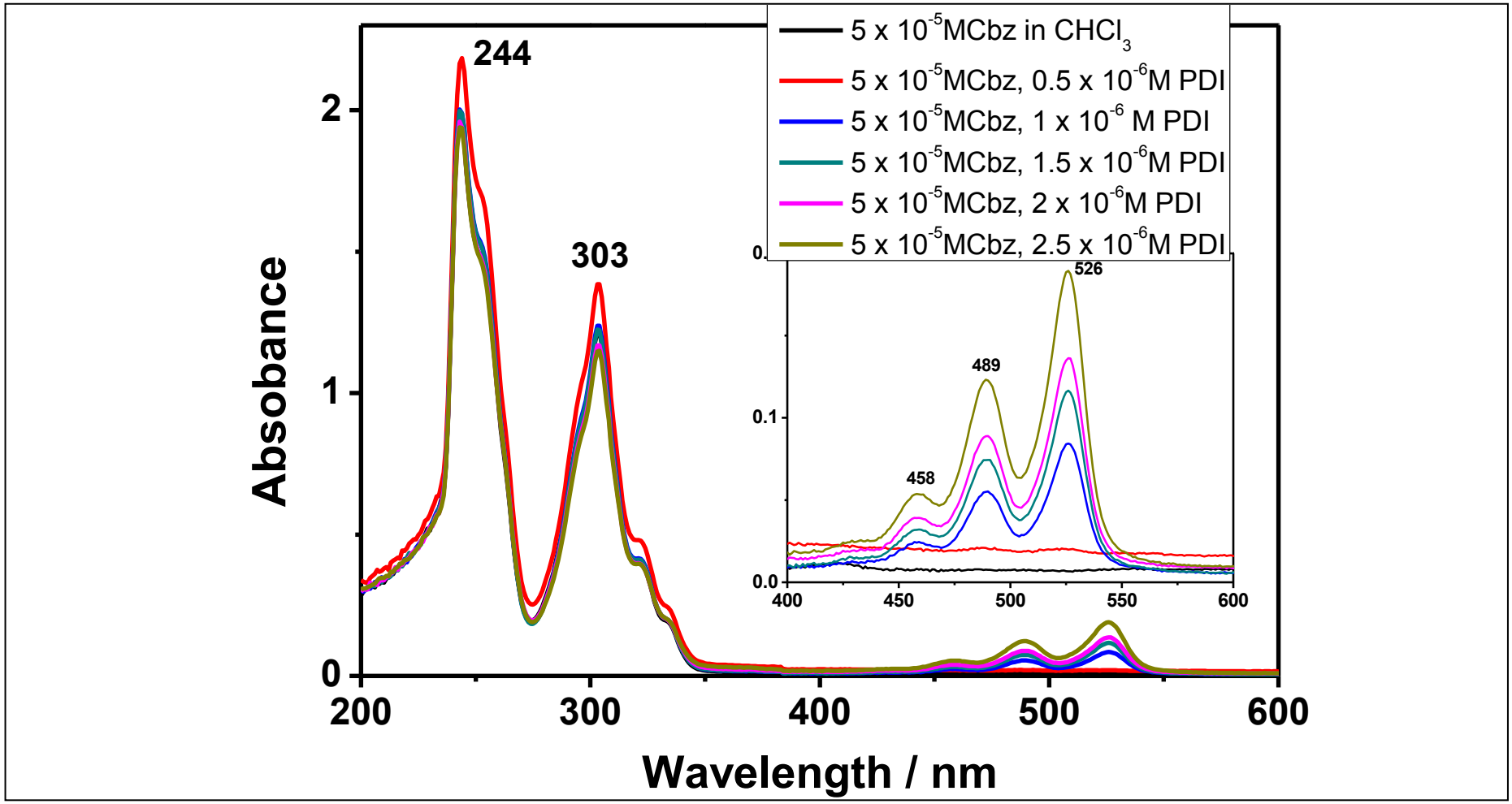

Figure 4.17. UV –vis Absorption Spectra of 5 x 10^{-5}M Cbz with Different Concentrations of PDI in Chloroform

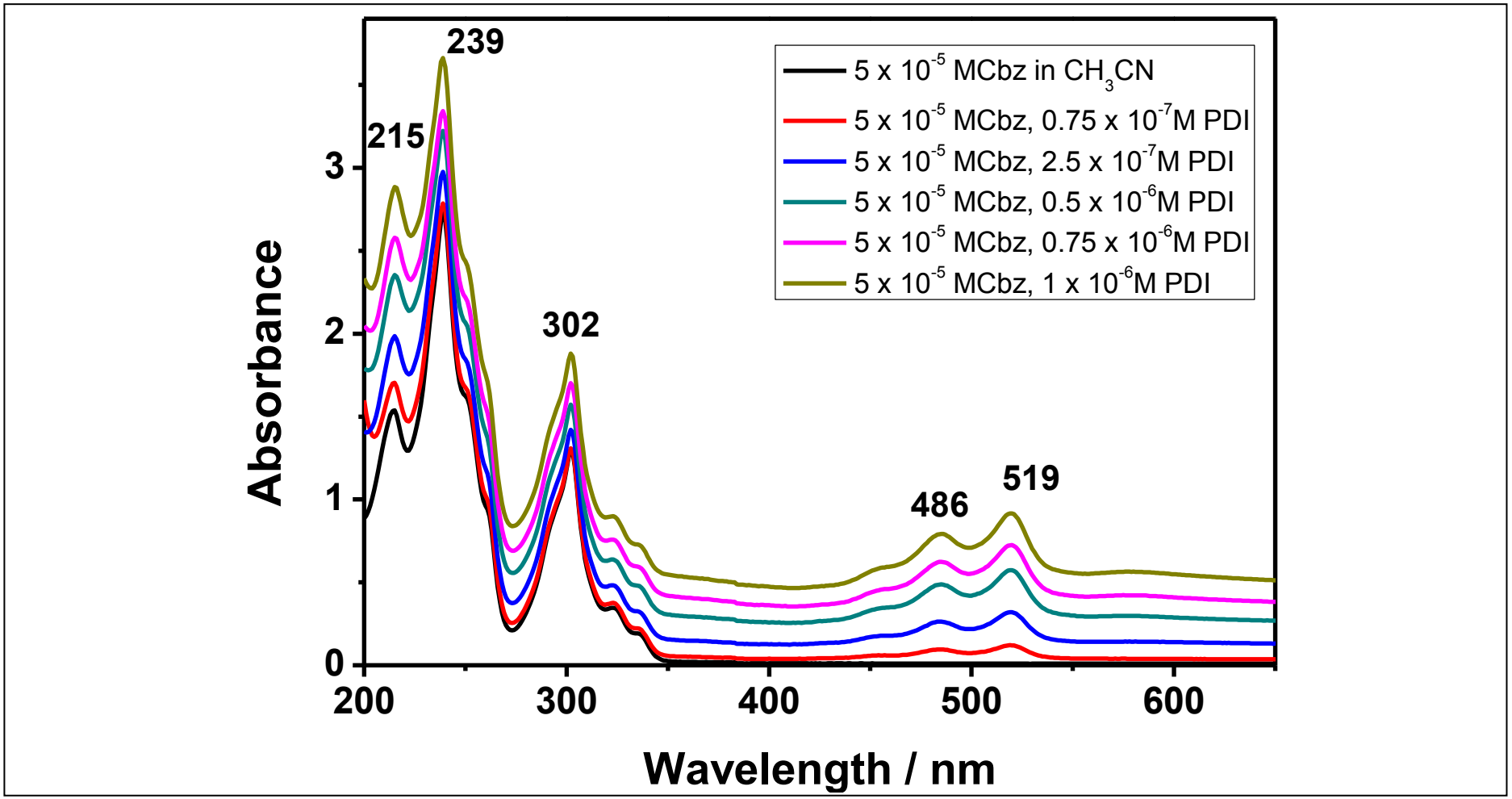

Figure 4.18. UV –vis Absorption Spectra of 5 x 10^{-5}M Cbz with Different Concentrations of PDI in CH_3CN

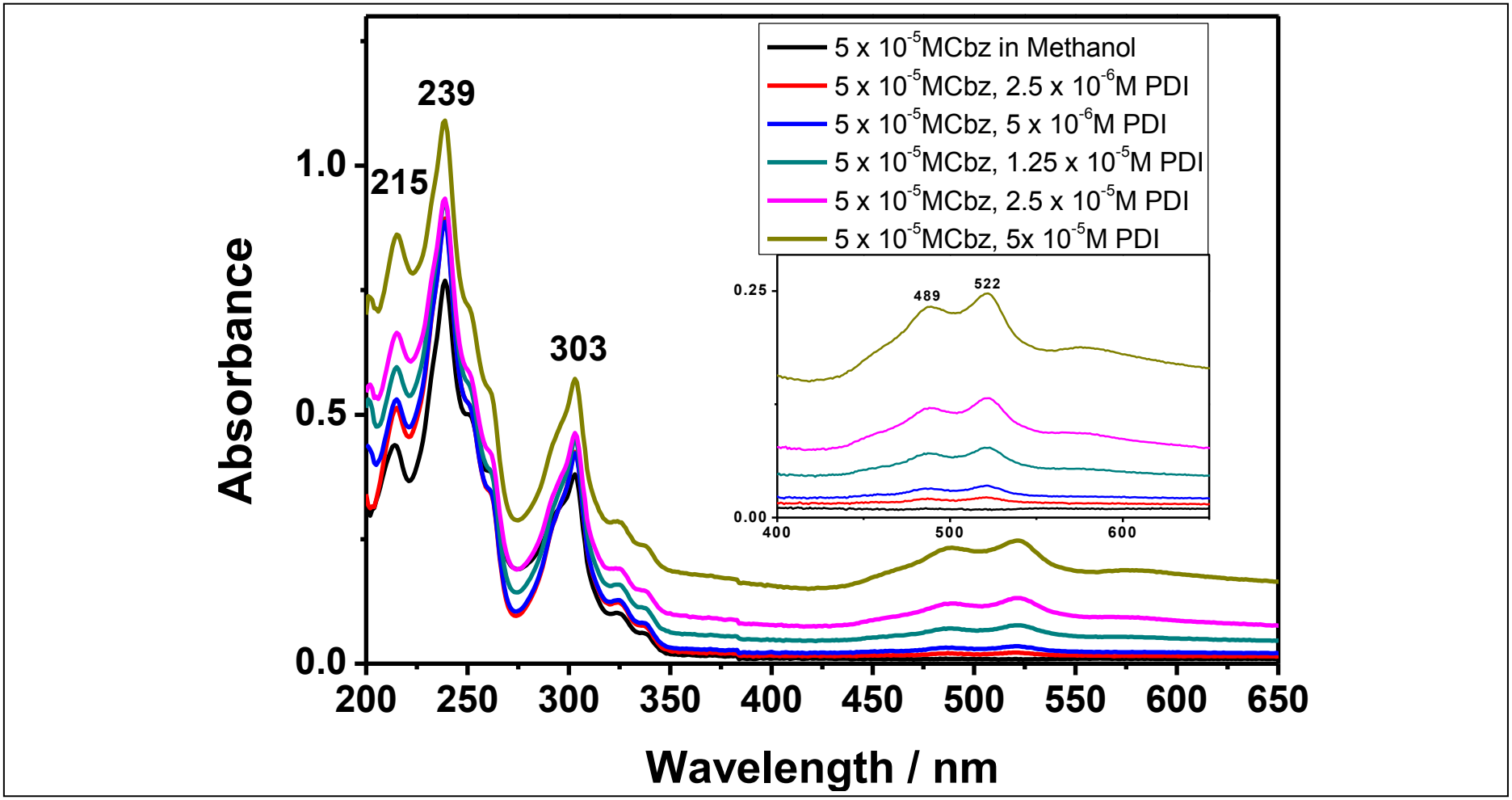

Figure 4.19. UV –vis Absorption Spectra of 5 x 10^{-5}M Cbz with Different Concentrations of PDI in Methanol

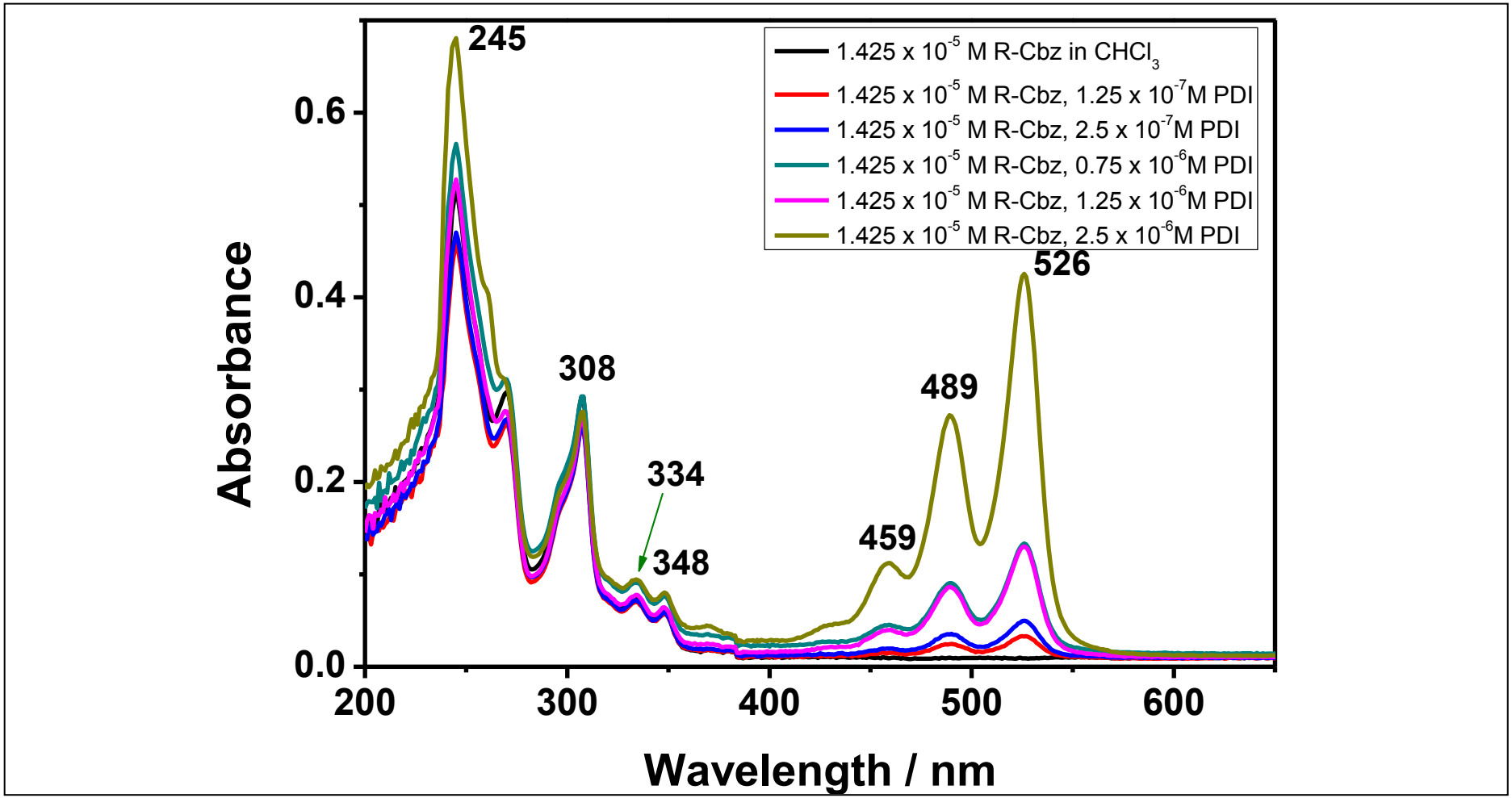

Figure 4.20. UV –vis Absorption Spectra of 1.425 x 10^{-4}M Dodecylcarbazole with Different Concentrations of PDI in Chloroform

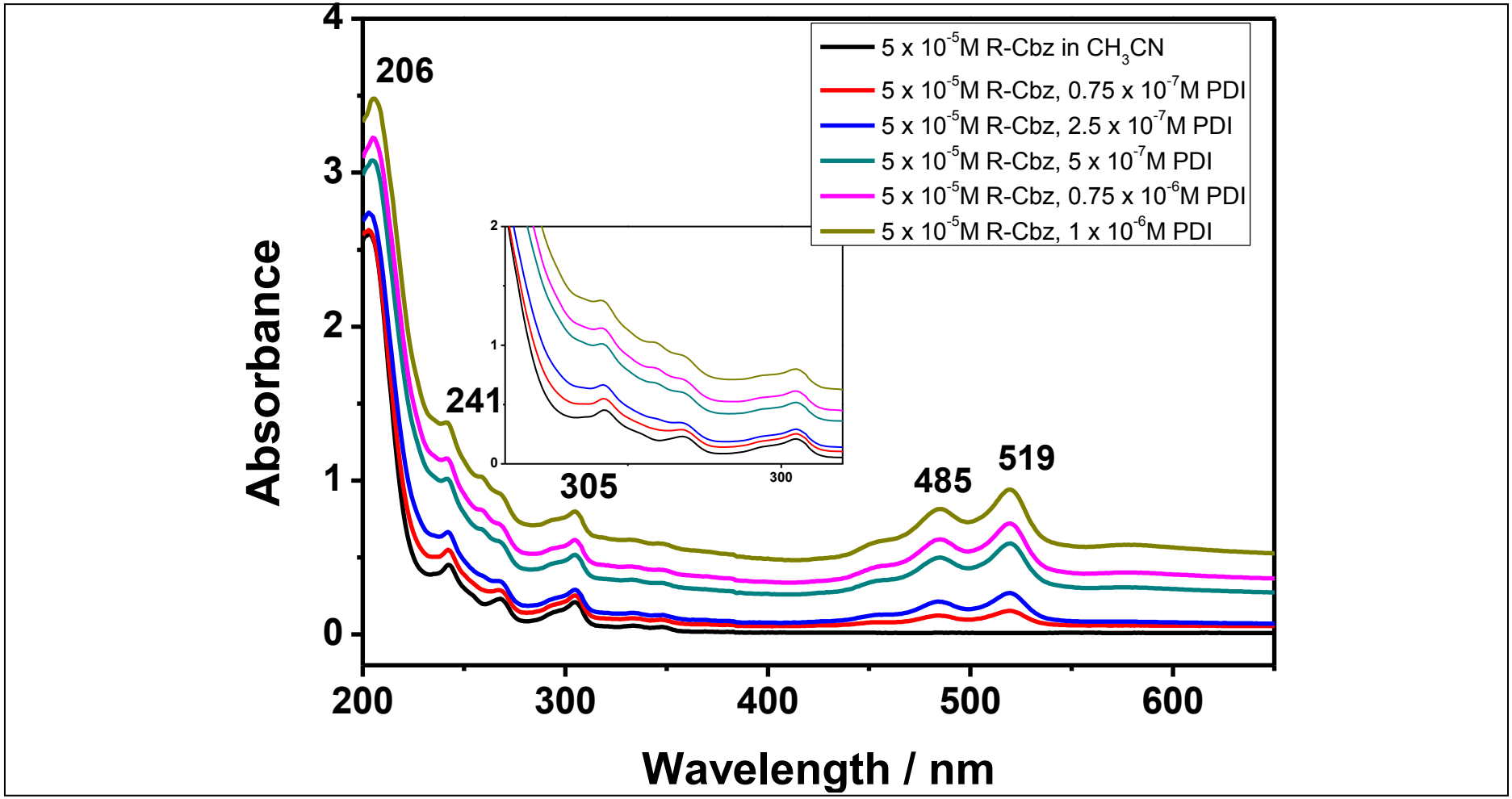

Figure 4.21. UV –vis Absorption Spectra of 5 x 10^{-5}M Dodecylcarbazole with Different Concentrations of PDI in CH_3CN

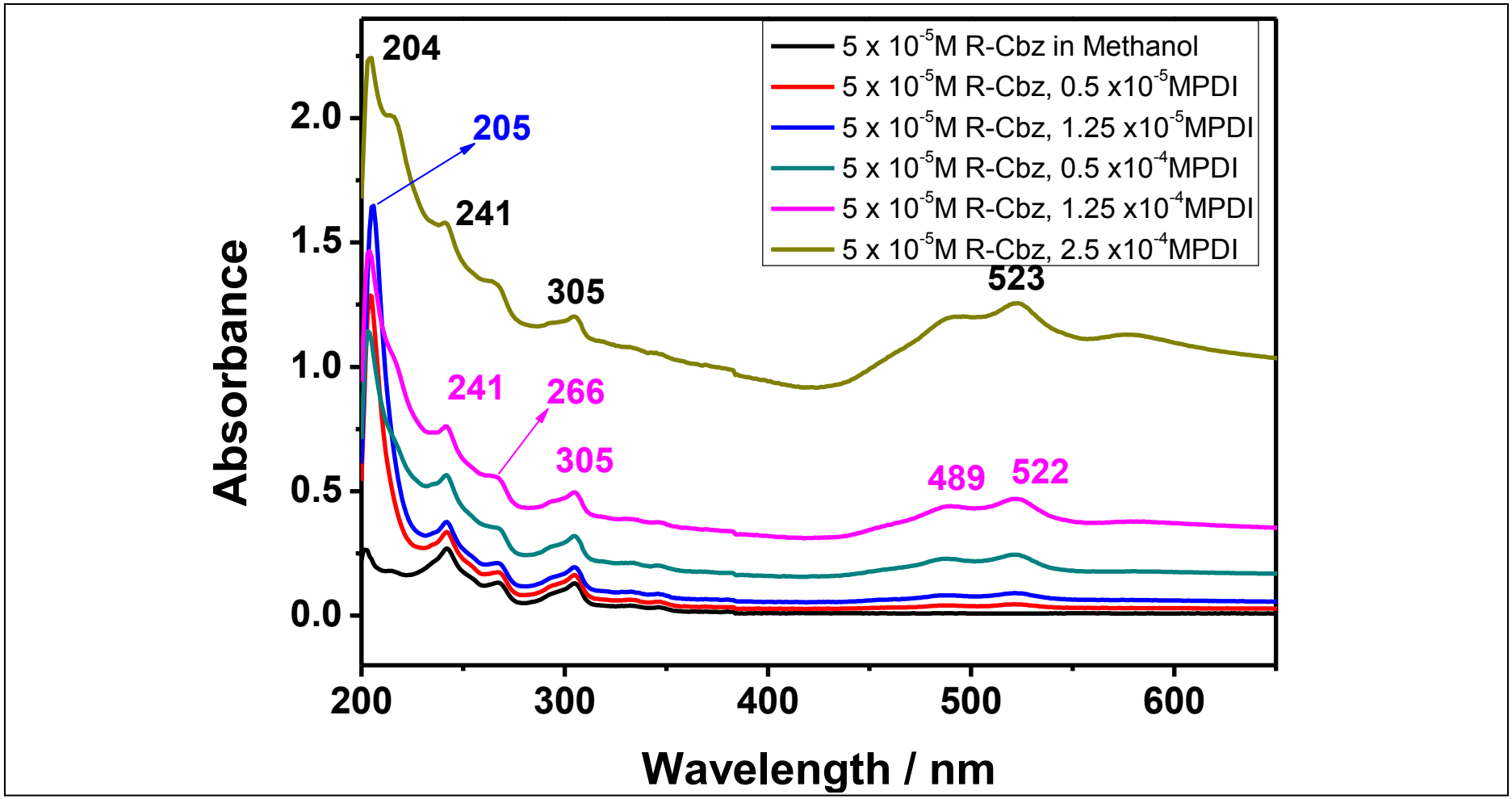

Figure 4.22. UV –vis Absorption Spectra of 5 x 10^{-5}M Dodecylcarbazole with Different Concentrations of PDI in Methanol

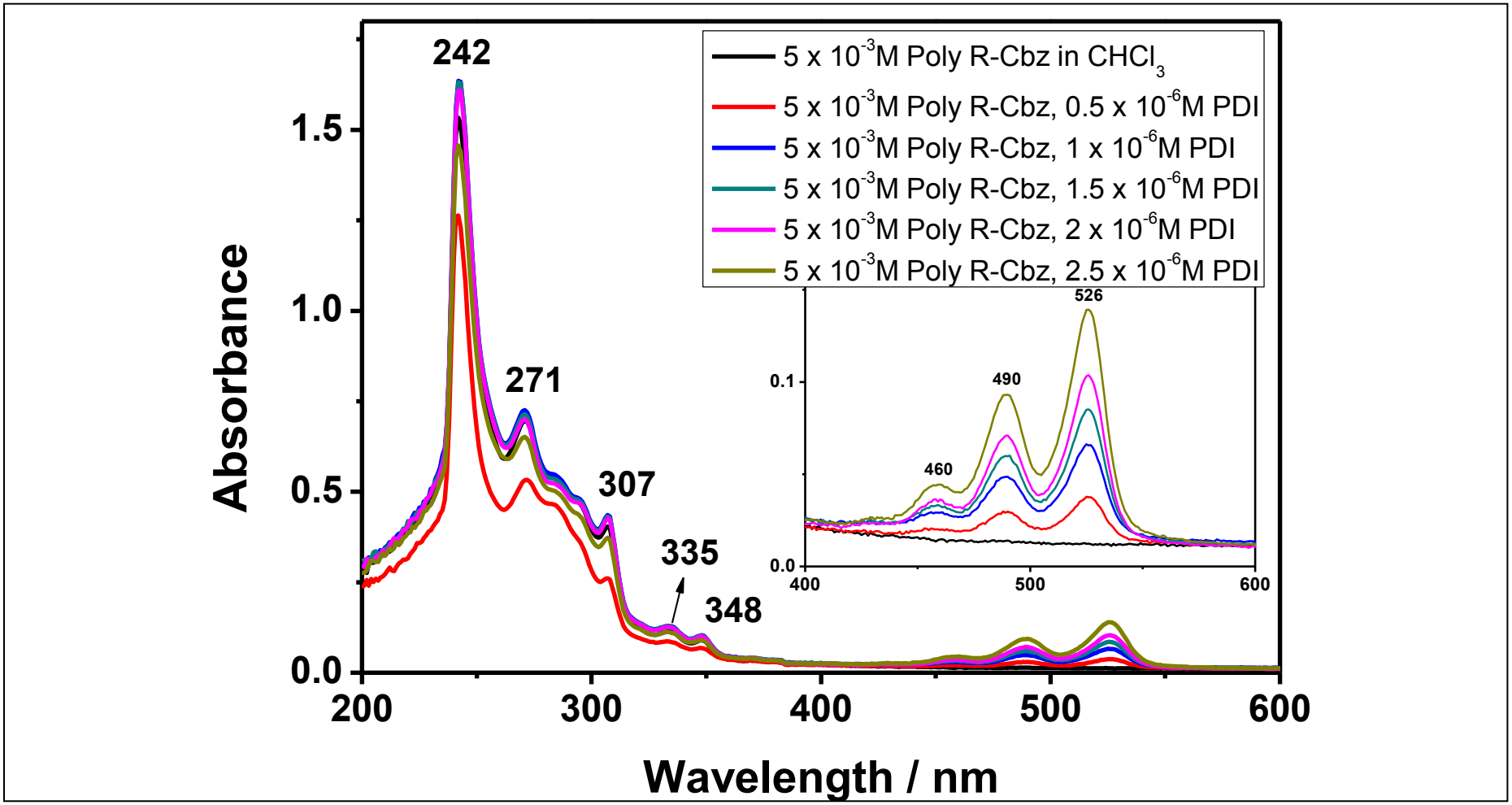

Figure 4.23. UV –vis Absorption Spectra of 5 x 10^{-3}M Polycarbazole with Different Concentrations of PDI in Chloroform

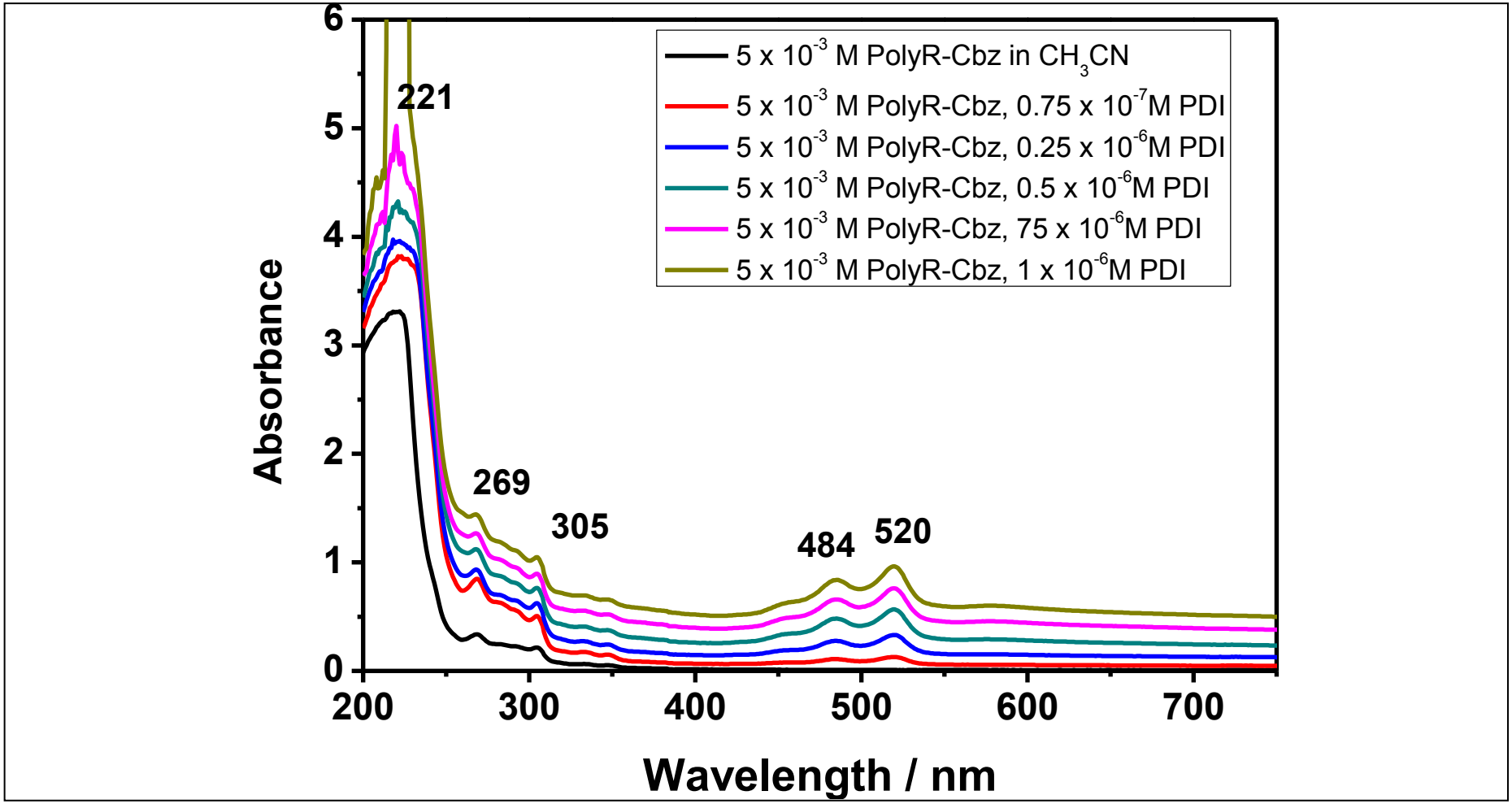

Figure 4.24. UV –vis Absorption Spectra of 5 x 10^{-3}M Polycarbazole with Different Concentrations of PDI in CH_3CN

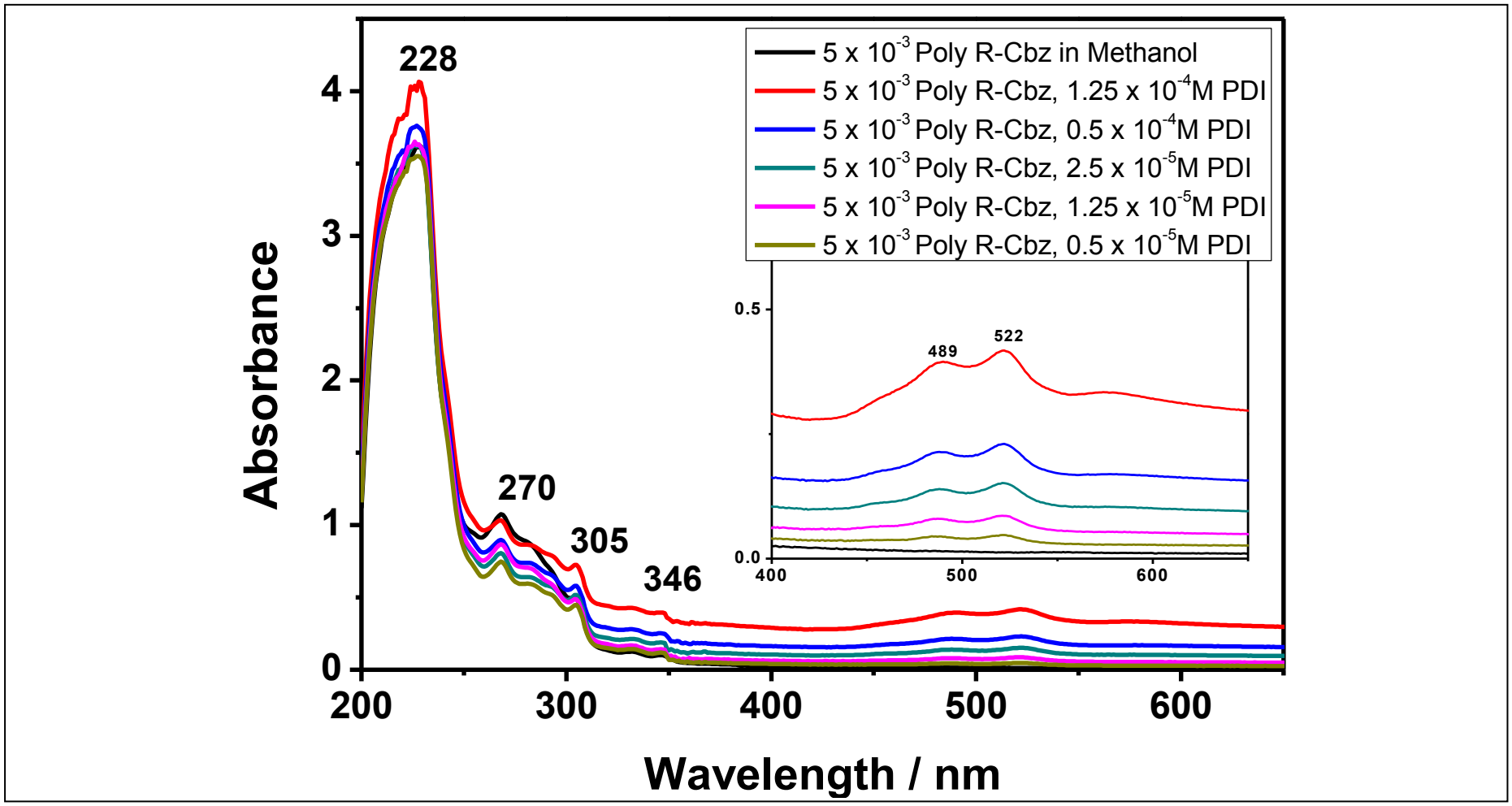

Figure 4.25. UV –vis Absorption Spectra of 5x 10^{-3}M Polycarbazole with Different Concentration PDI in Methanol

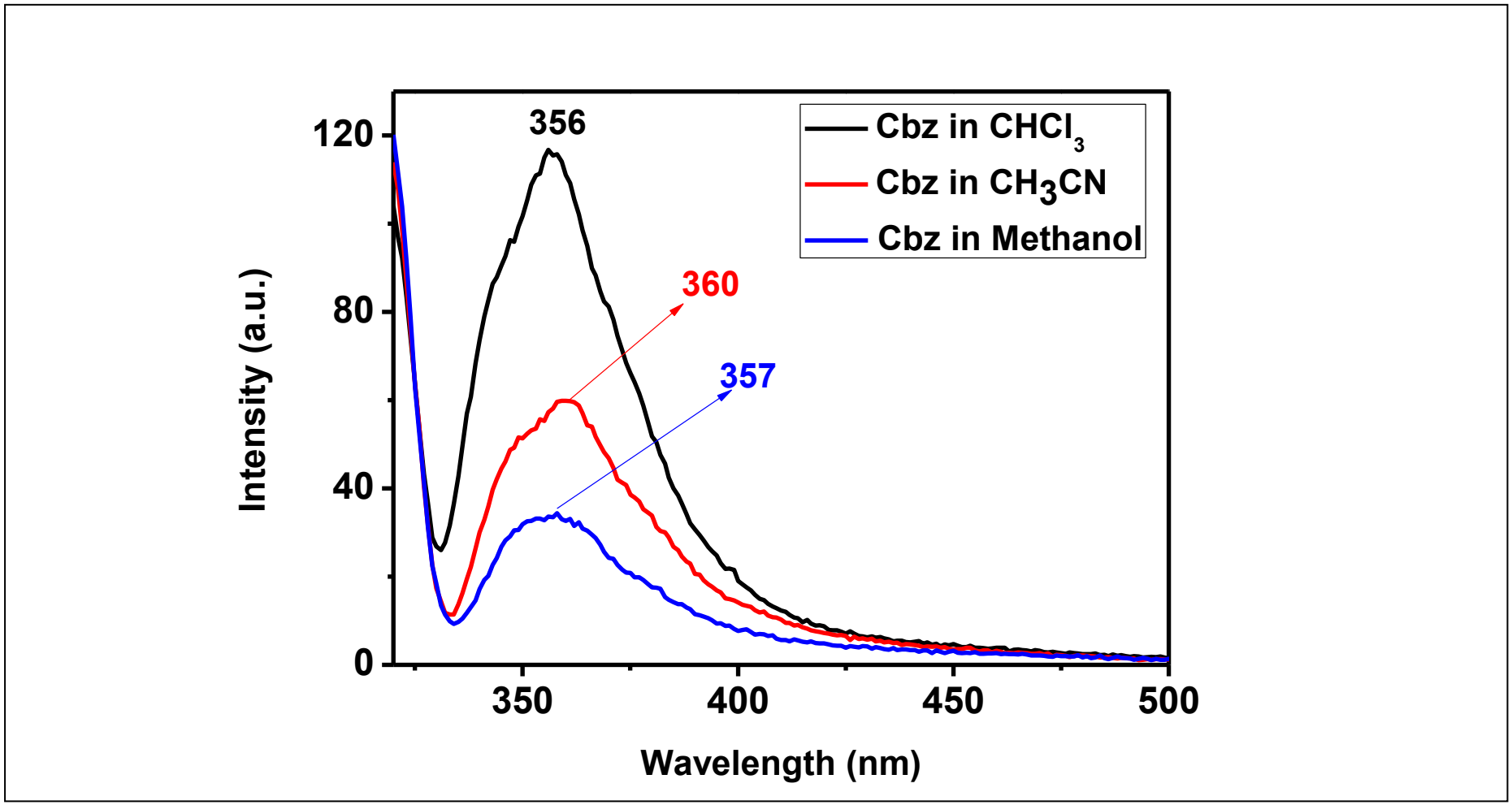

Figure 4.26. Emission (λ_{exc} = 318nm) Spectrum of 5 x 10^{-5} M Cbz in $CHCl_3$, CH_3CN and Methanol

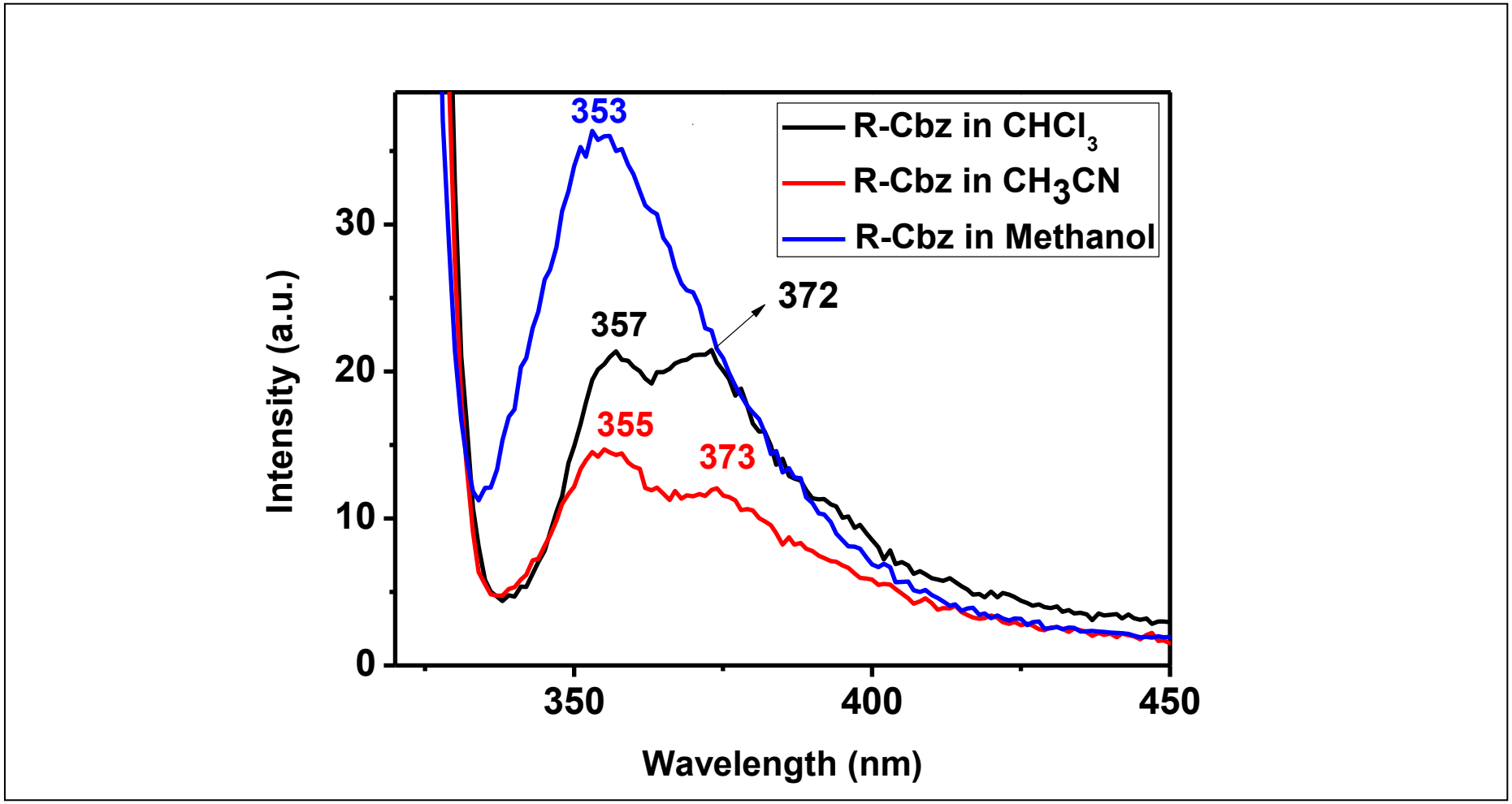

Figure 4.27. Emission (λ_{exc} = 318nm) Spectrum of 5 x 10^{-5} M Dodecylcarbazole in $CHCl_3$, CH_3CN and Methanol

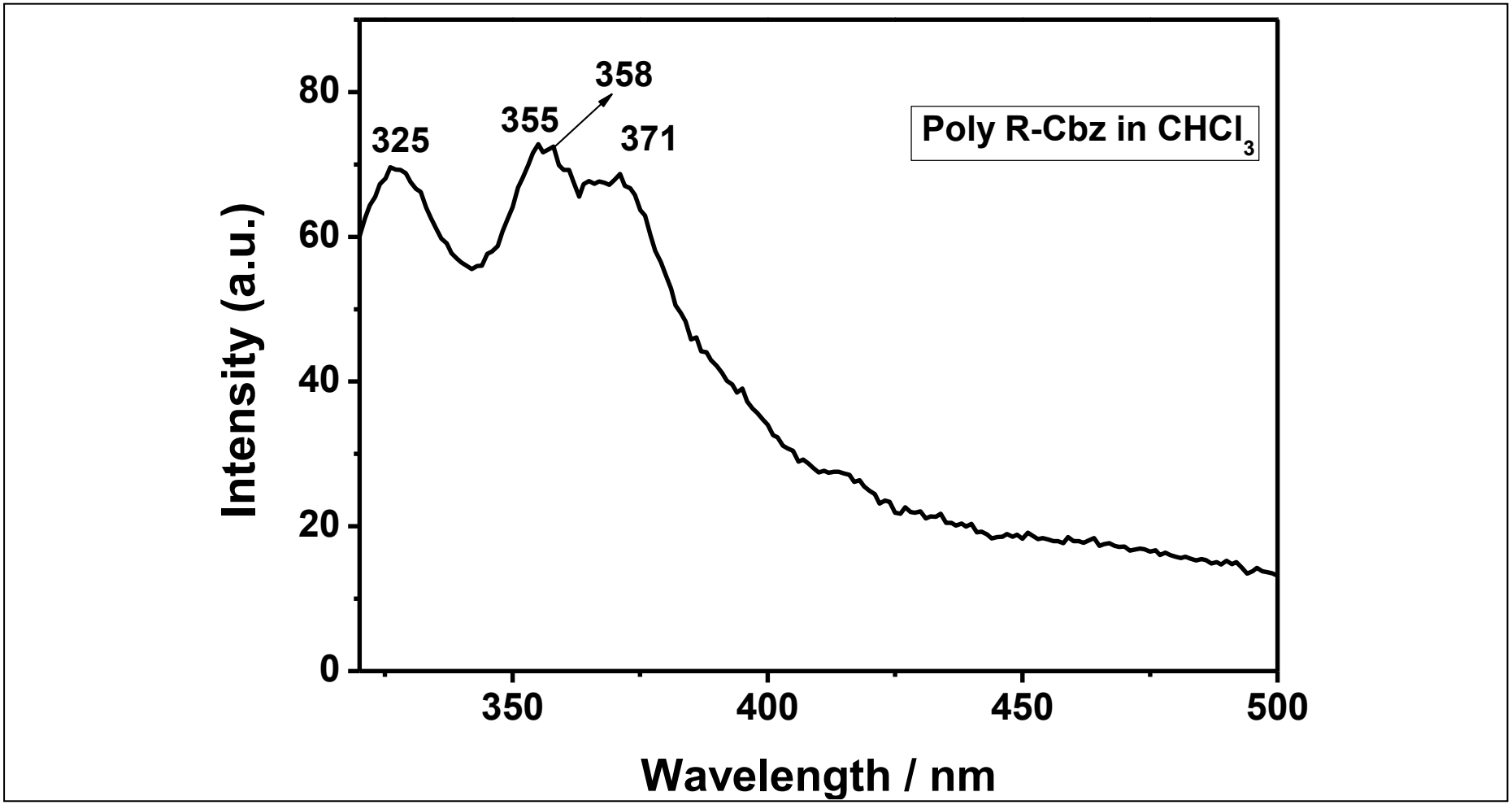

Figure 4.28. Emission (λ_{exc} = 295.5 nm) Spectrum of 5 x 10^{-3}M Polycarbazole in $CHCl_3$

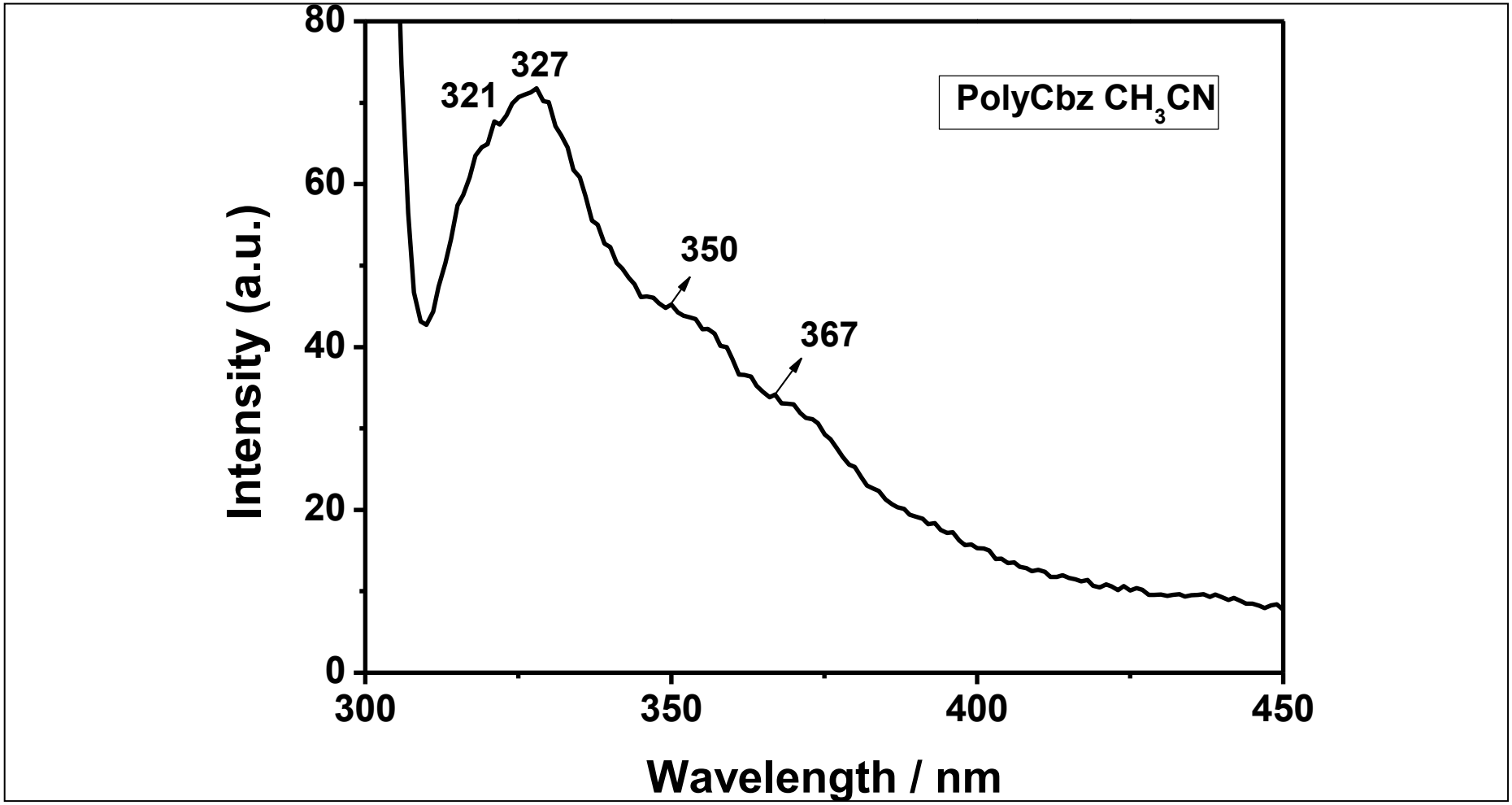

Figure 4.29. Emission (λ_{exc} = 295.5 nm) Spectrum of 5 x 10^{-3}M Polycarbazole in CH_3CN

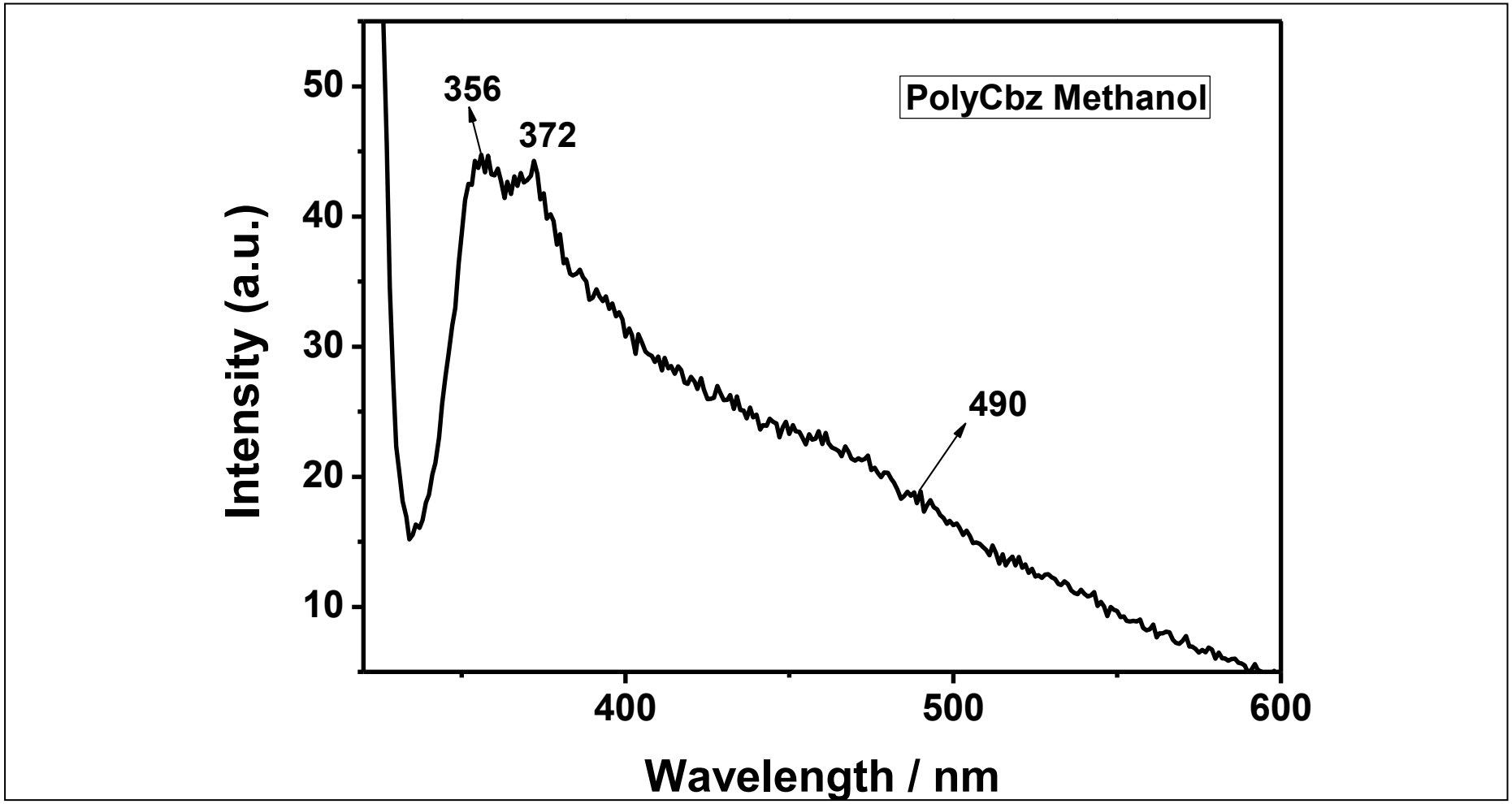

Figure 4.30. Emission (λ_{exc} = 295.5 nm) Spectrum of 5 x 10^{-3}M Polycarbazole in Methanol

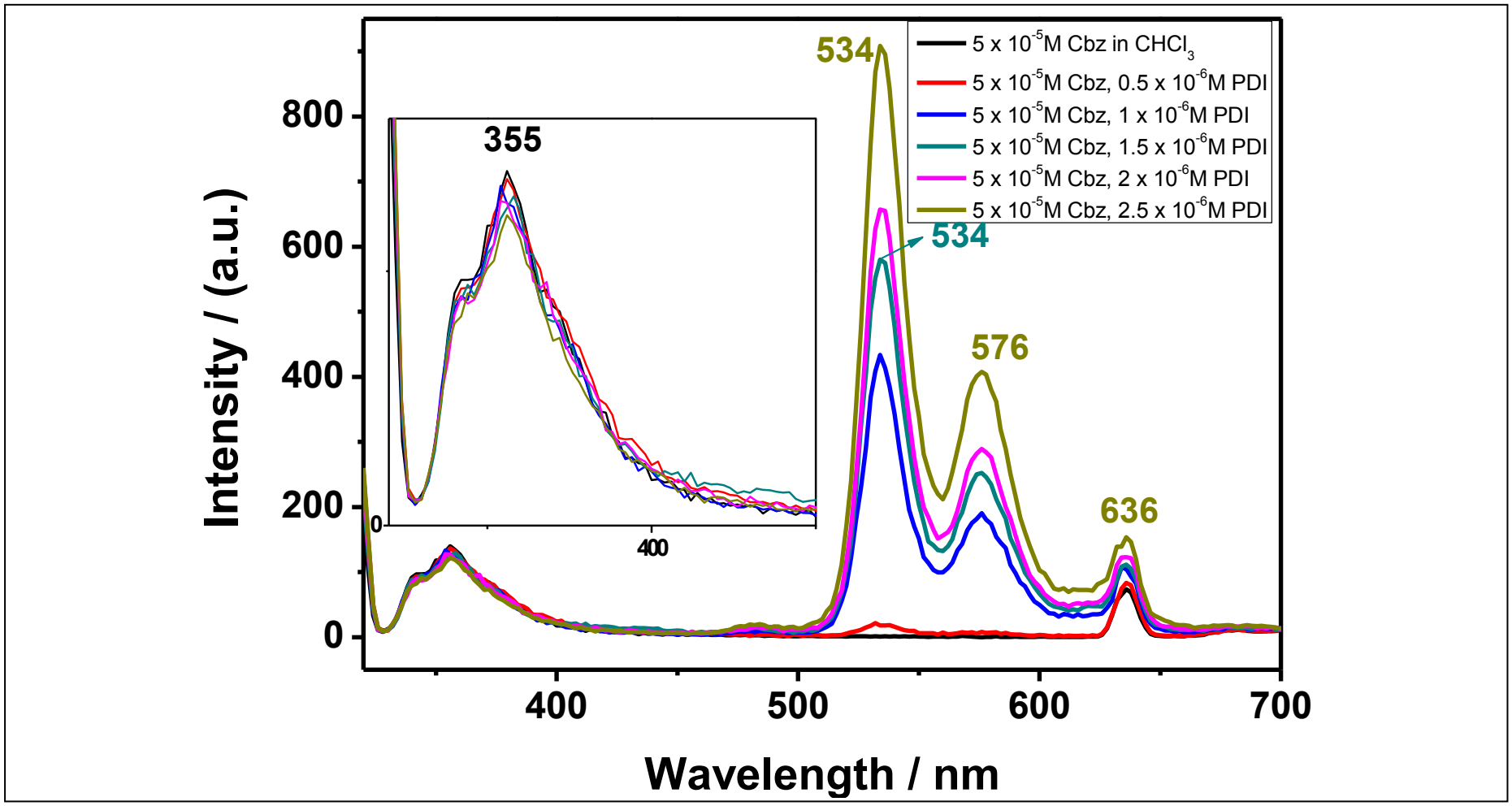

Figure 4.31. Emission (λ_{exc} = 318nm) Spectrum of 5x 10-5 M Cbz with Different Concentrations of PDI in $CHCl_3$

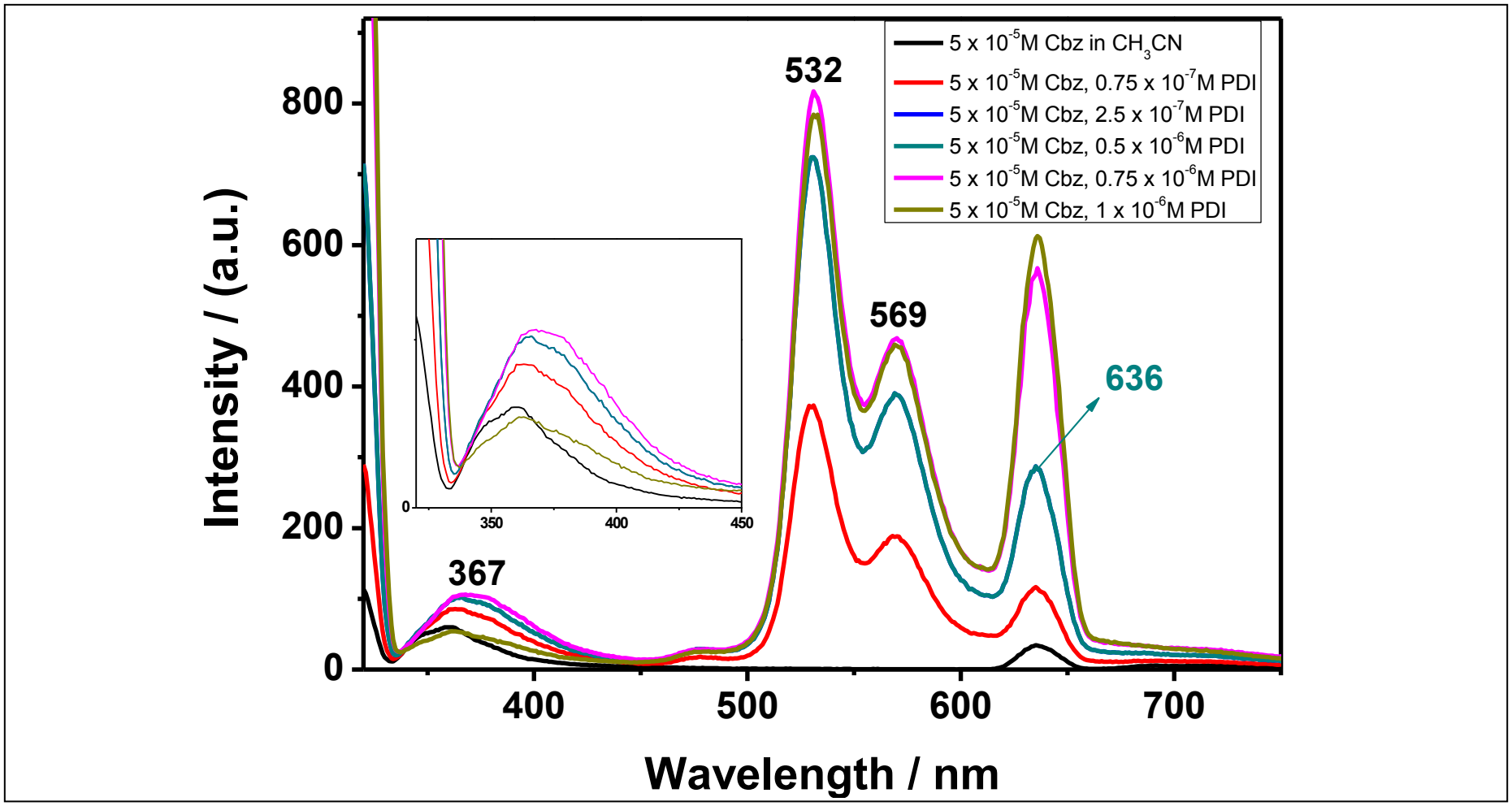

Figure 4.32. Emission (λ_{exc} = 318nm) Spectrum of 5x 10^{-5}M Cbz with Different Concentrations of PDI in CH_3CN

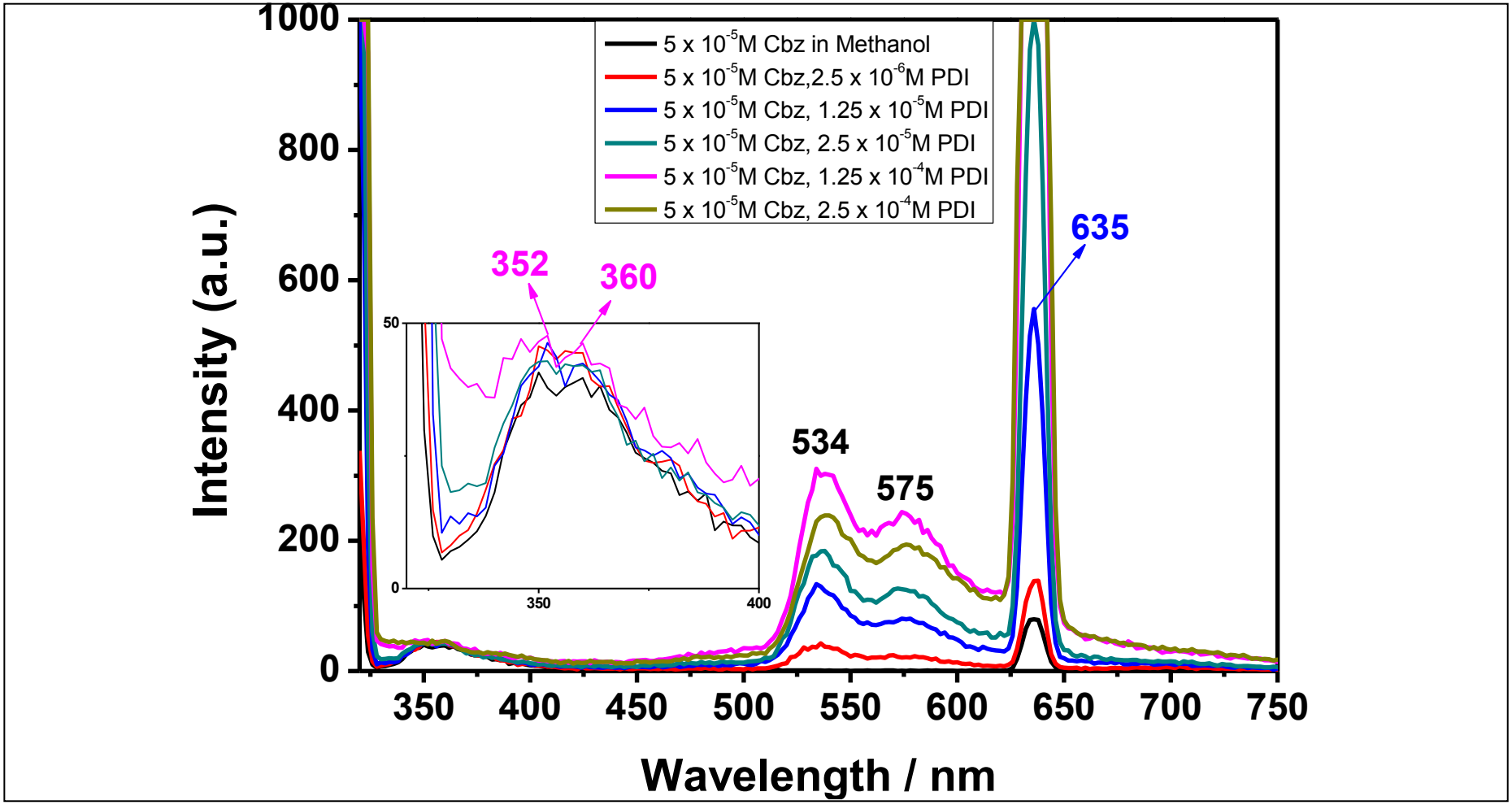

Figure 4.33. Emission (λ_{exc} = 318nm) Spectrum of 5x 10^{-5} Cbz with Different Concentrations of PDI in Methanol

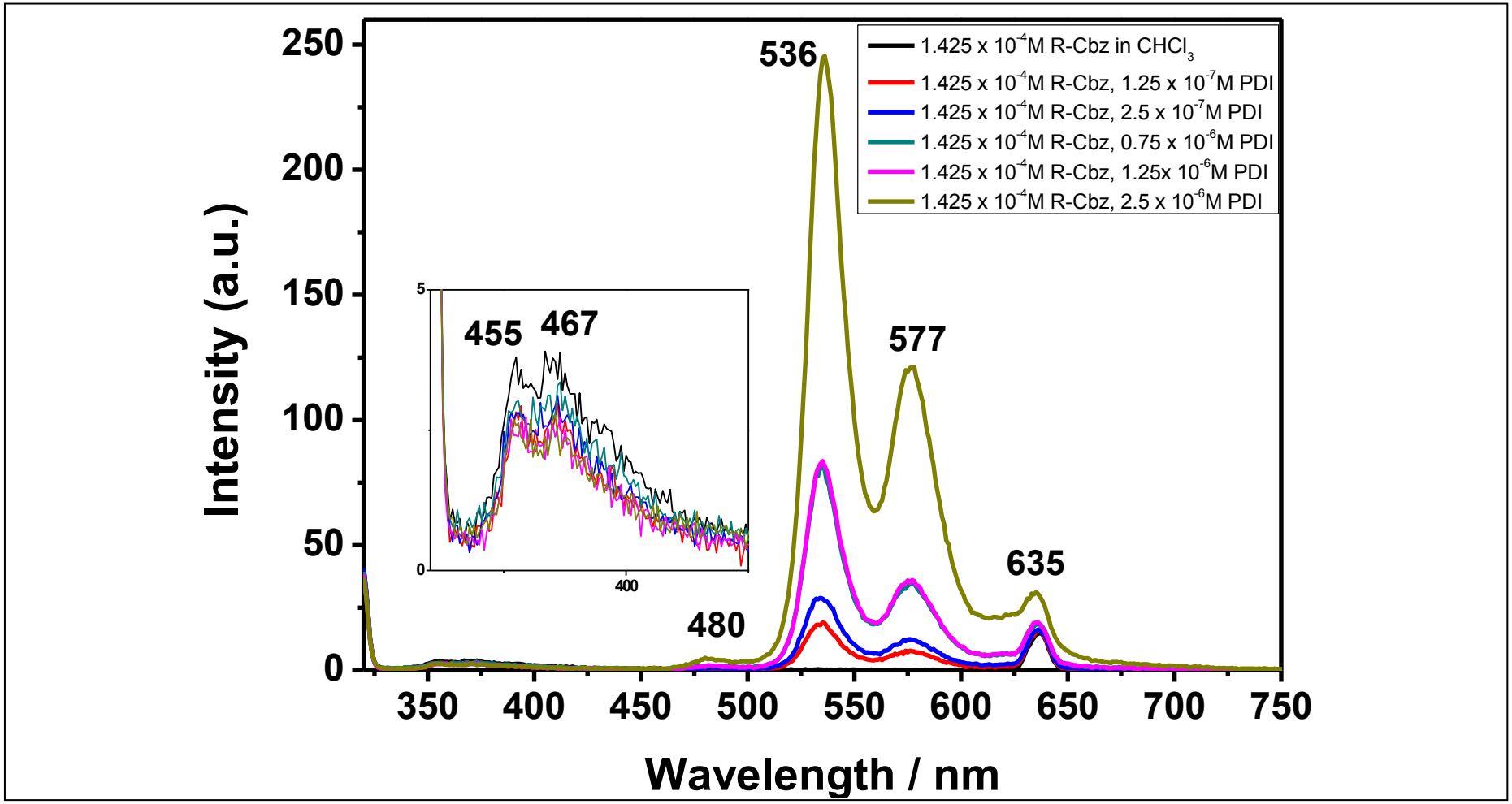

Figure 4.34. Emission (λ_{exc} = 318nm) Spectrum of 1.425x 10^{-4} M Dodecylcbz with Different Concentrations of PDI in $CHCl_3$

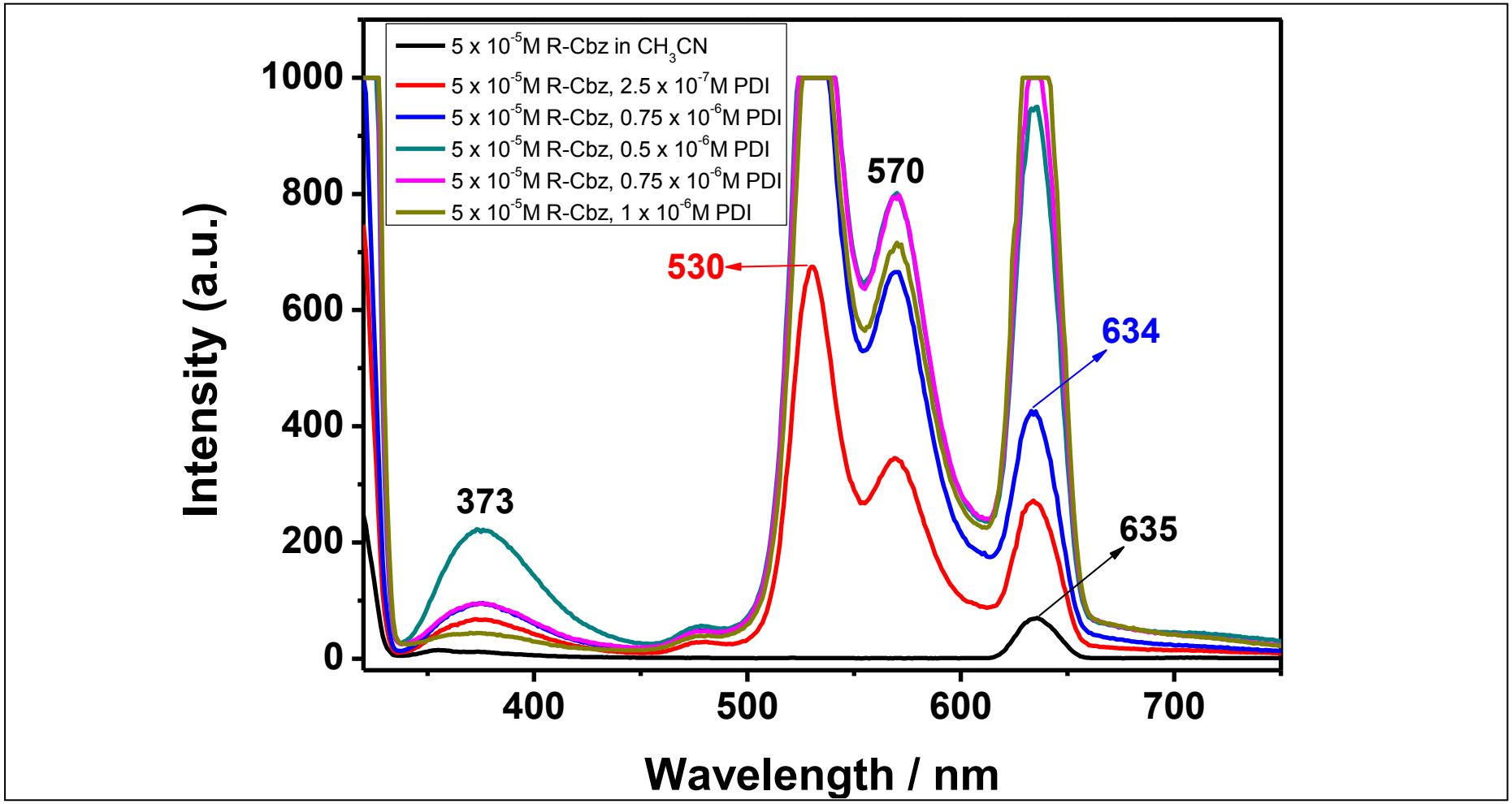

Figure 4.35. Emission (λ_{exc} = 318nm) Spectrum of 5x 10^{-5}M Dodecylcbz with Different Concentrations of PDI in CH_3CN

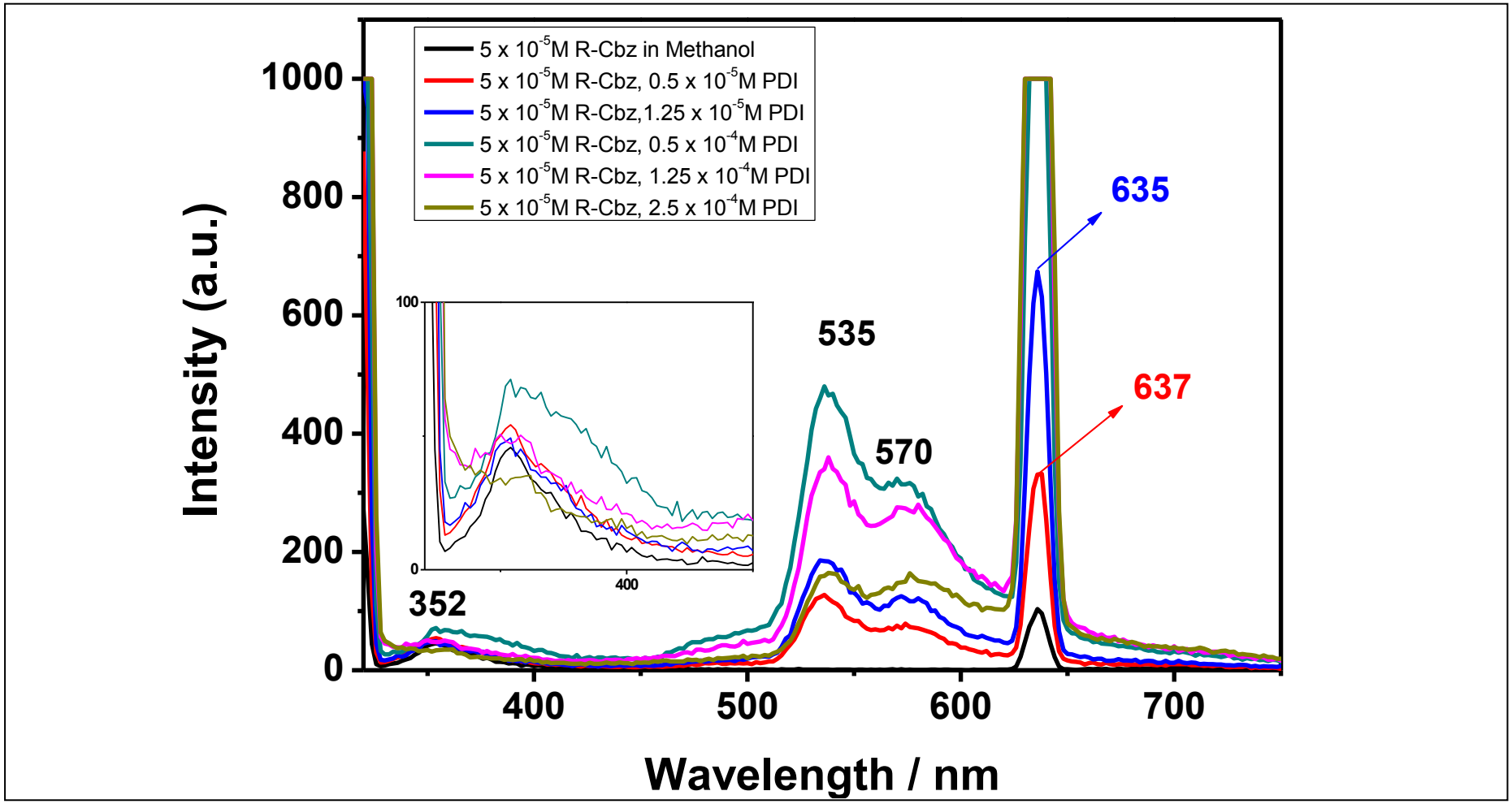

Figure 4.36. Emission (λ_{exc} = 318nm) Spectrum of 5 x 10-5M Dodecylcbz with Different Concentrations of PDI in Methanol

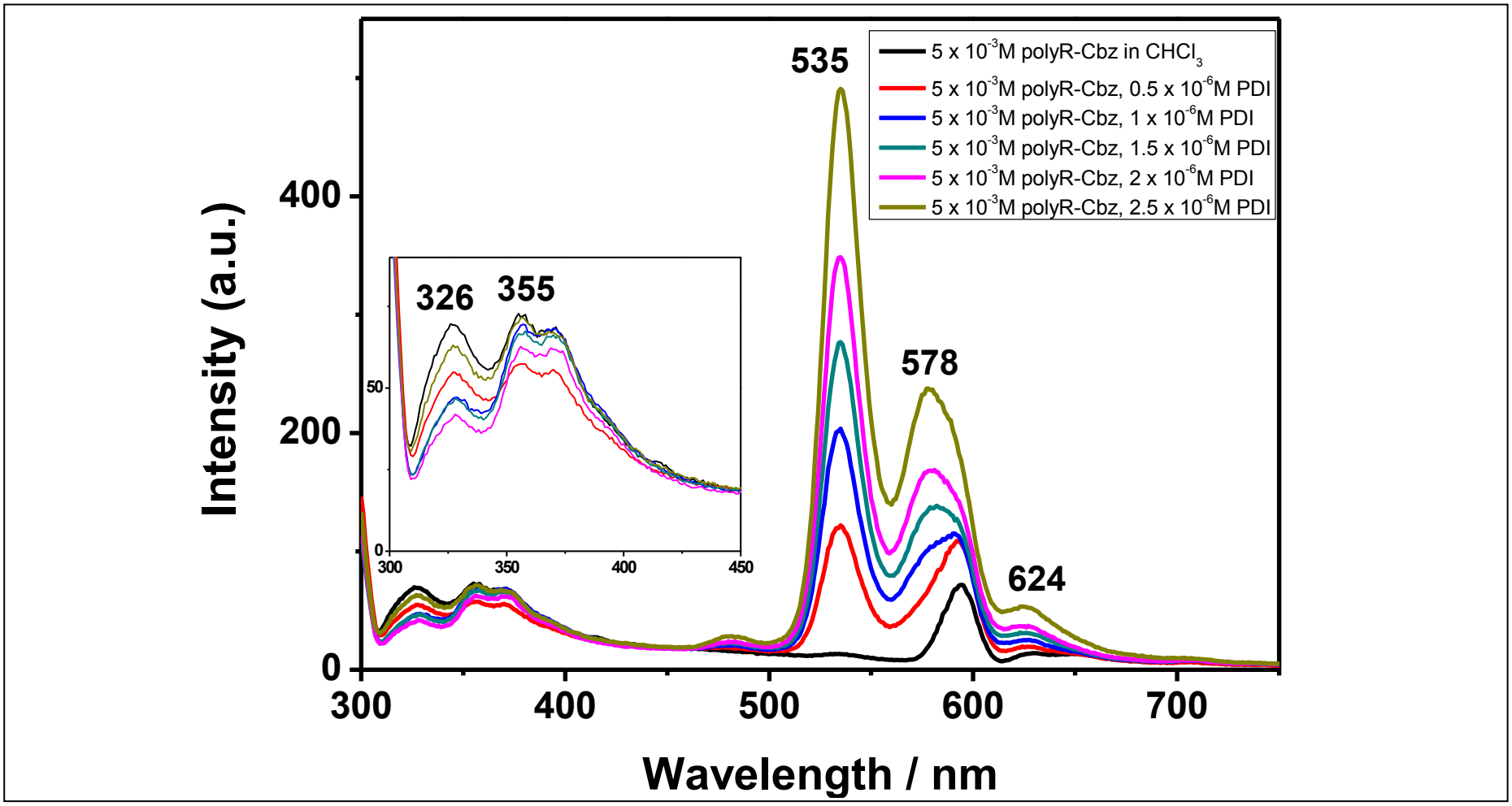

Figure 4.37. Emission (λ_{exc} = 295.5 nm) Spectrum of 5x 10^{-3}M Polycbz with Different Concentrations of PDI in $CHCl_3$

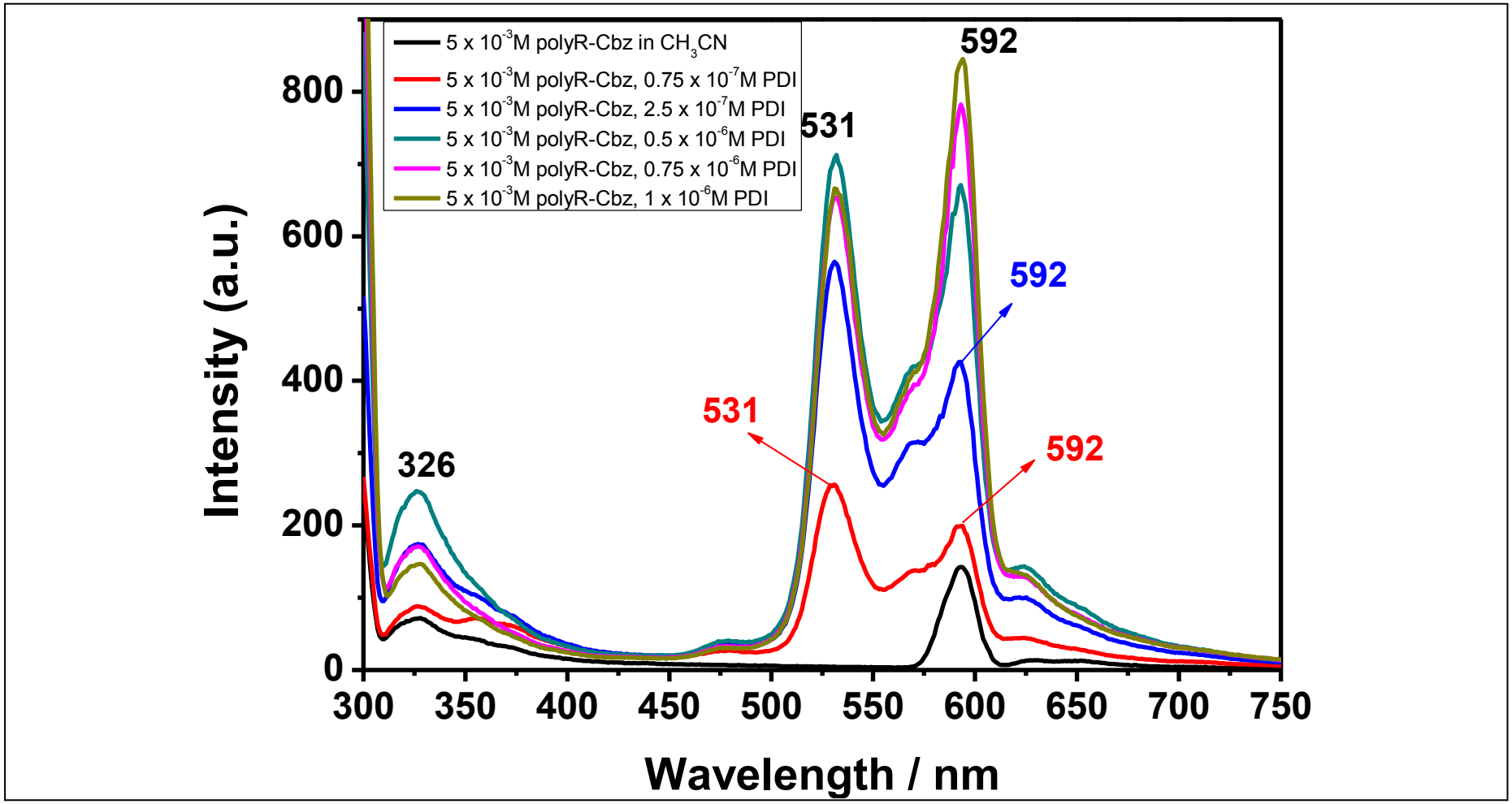

Figure 4.38.Emission (λ_{exc} = 318nm) Spectrum of 10^{-3} M Polycbz with Different Concentrations of PDI in CH_3CN

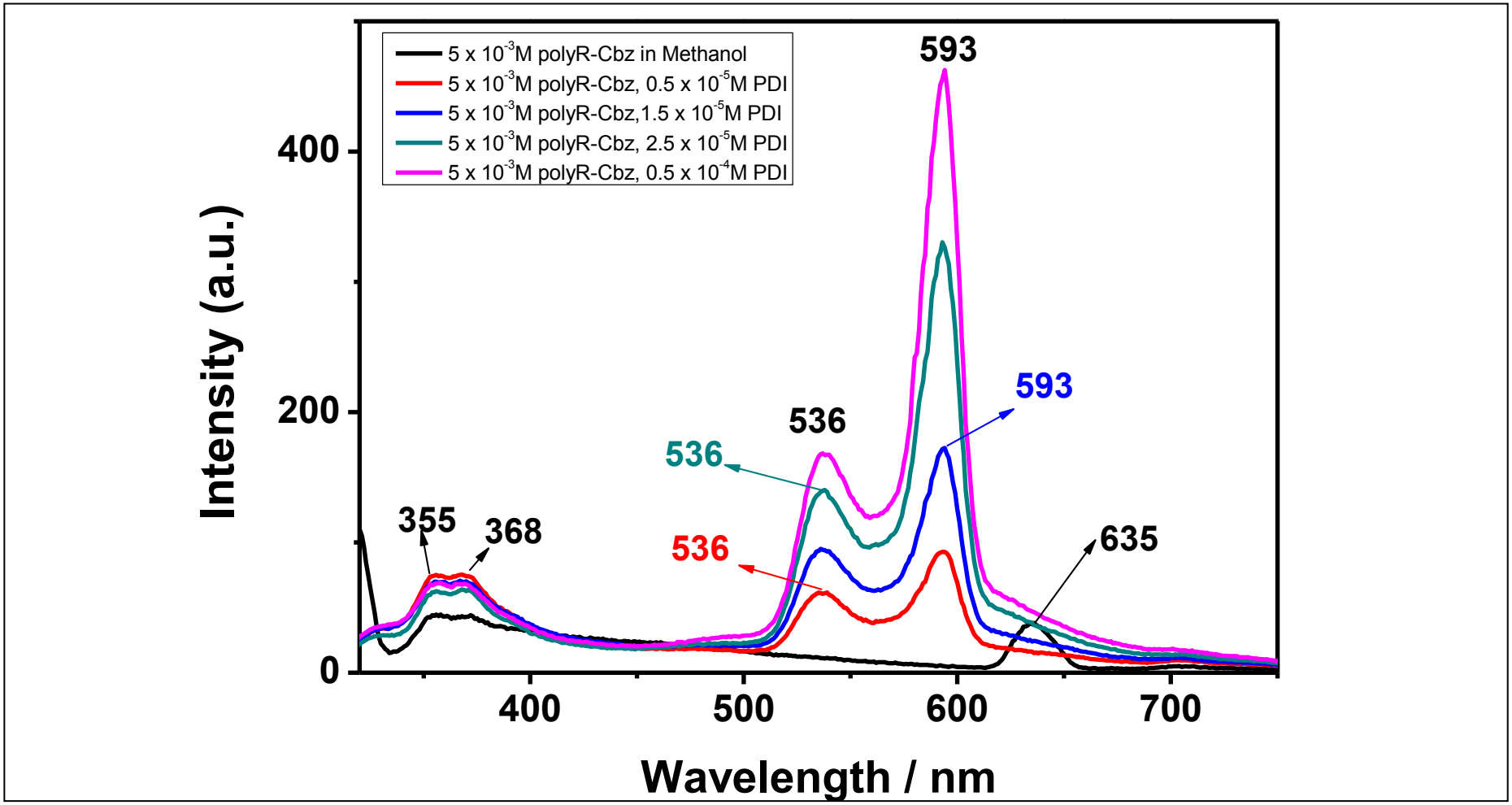

Figure 4.39. Emission (λ_{exc} = 318nm) Spectrum of 5x 10-3M Polycbz with Different Concentrations of PDI in Methanol

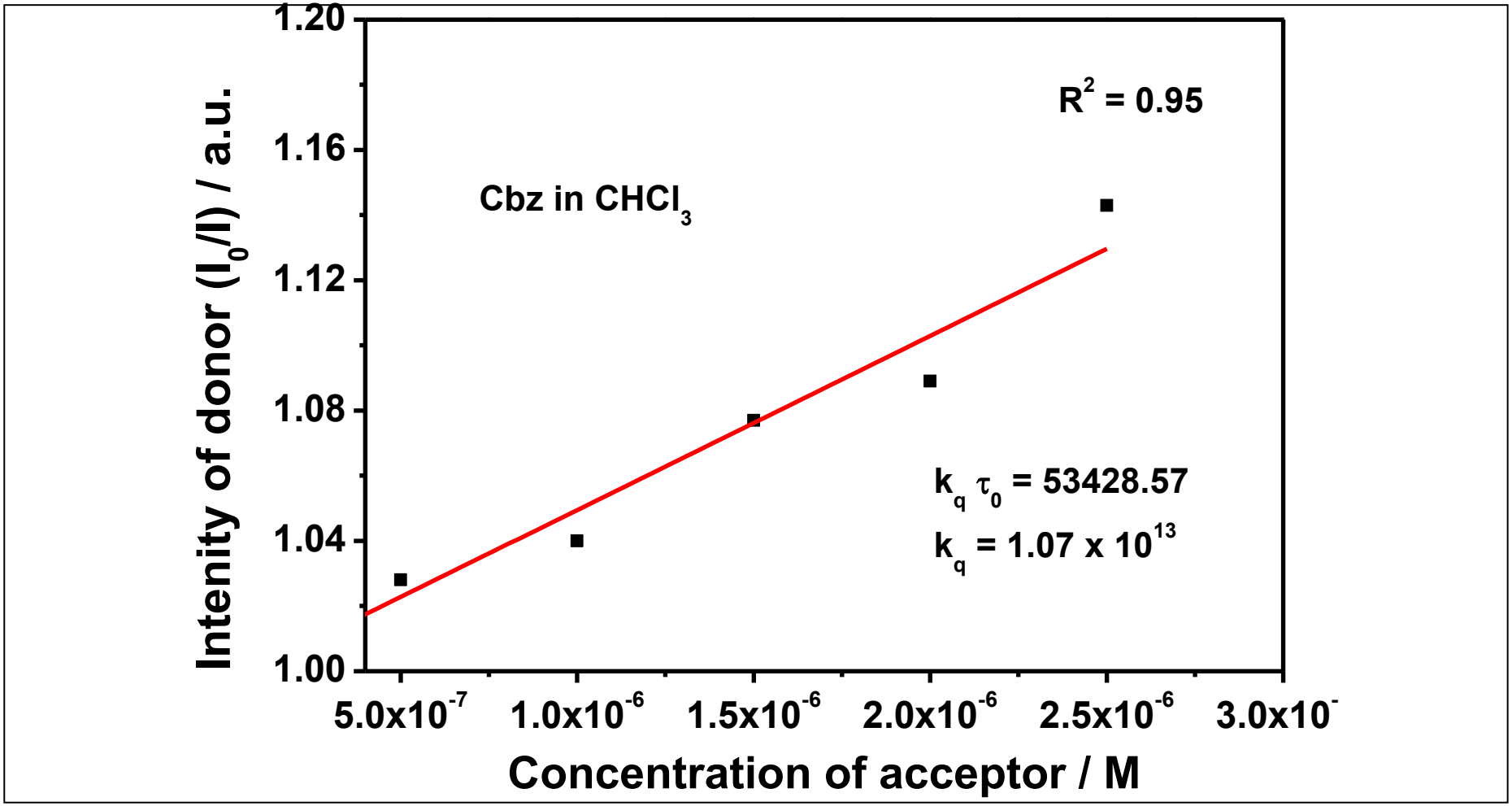

Figure 4.40. Stern-Volmer Plot for the Carbazole and Dehydro-PDI System in Chloroform

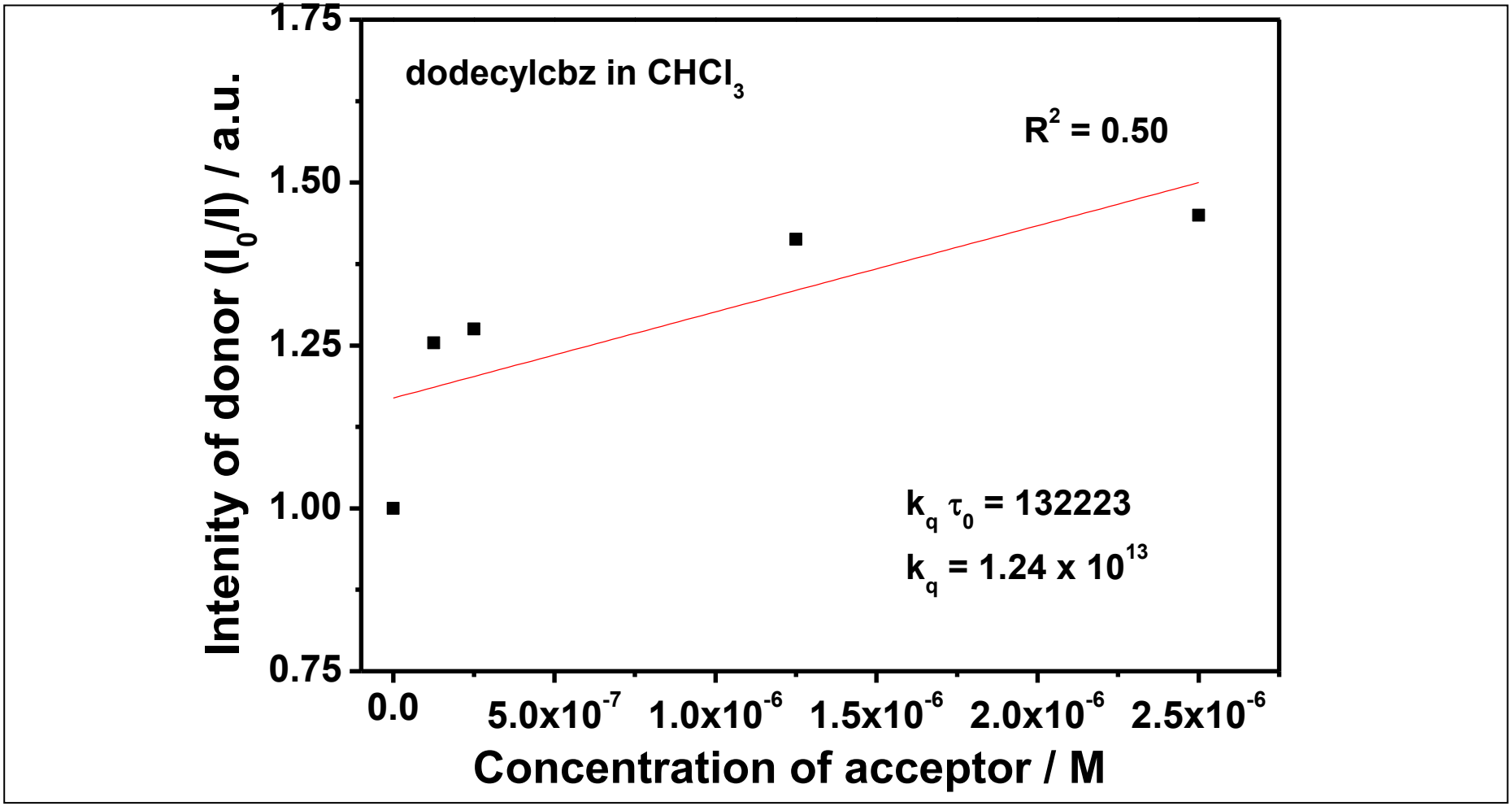

Figure 4.41. Stern-Volmer Plot for the Dodecylcarbazole and Dehydro-PDI System in Chloroform

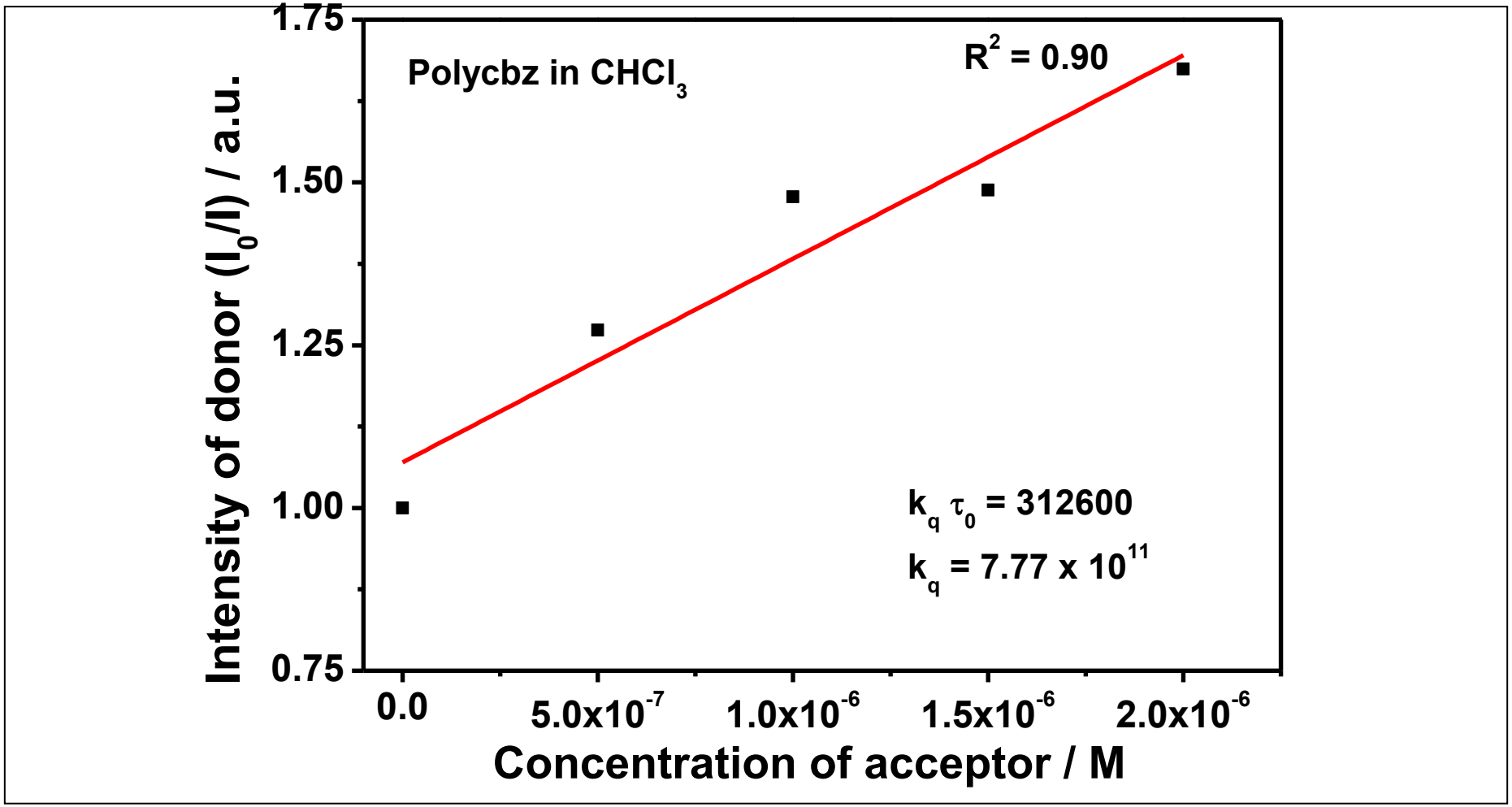

Figure 4.42. Stern-Volmer Plot for the Polycarbazole and Dehydro-PDI System in Chloroform

Chapter 5

RESULTS AND DISCUSSION

The three carbazole compounds and the perylene derivative are synthesized according to the literature procedures.

The carbazole compounds, 2,7-dibromocarbazole (Cbz), 2,7-dibromo-N-dodecylcarbazole (doecylcarbazole), and poly(2,7-N-dodecyl)carbazole (polycbz) are considered as electron donating groups and dehydroabietyl perylene diimide (PDI) is considered as electron accepting group.

The primary aspect concerning energy transfer is that the emission spectrum of the donor should overlap with the absorption spectrum of the acceptor. The three carbazole derivatives are having the excimer emissions up to 450 nm (Figures 4.26 – 4.30) where the absorption of perylene is initializing (Figures 4.5 – 4.7). Although they are not exactly overlapping, they are potential candidates for efficient energy transfer concerning their structures. There is a possibility for electron transfer/charge transfer as the carbazole derivatives are excellent donors and perylene dyes are excellent electron acceptors.

The absorption spectra of carbazole derivatives are shown in Figures 4.8 – 4.16 (4.8–4.10 for dibromocarbazole; 4.11–4.13 for dodecylcarbazole; 4.14–4.16 for polycarbazole). The Figure 4.1 is used to calculate the molar absorptivity of the acceptor, perylene diimide. The molar absorptivities and FWHMs of the three

carbazole derivatives are calculated and tabulated in Tables 4.2 – 4.4 (Figure 4.2). Using this data, theoretical radiative lifetimes are calculated for cbz, dodecylcarbazole and polycarbazole in three different kinds of solvents of varying polarity and are listed in Table 4.5.

Figure 4.3 is the normalized emission spectrum of carbazole and the normalized area is calculated to measure the critical transfer distance between carbazole and perylene dye. Figure 4.4 shown is the absorption of PDI in chloroform from which the molar absorptivity was estimated. All the calculated molar absorptivities, FWHMs, and natural radiative lifetimes and fluorescence lifetimes of the three carbazole derivatives and perylene dye are presented in Tables 4.1 – 4.6.

The critical transfer distances calculated for the systems of carbazole moieties with dehydro-PDI in three different solvents of varying polarity are presented Table 4.7. In all solvents for all the carbazoles and PDI systems, the distances measured represent the long-range energy transfer mechanism. It is notable that the polycarbazole and PDI systems in three different solvents of varying polarity possess very high critical transfer distances (including the huge theroretical radiative lifetimes of polycarbazole, Table 4.5) because of the fact that the calculations were made per molar mass of one unit of monomer.

Importantly, the fluorescence quantum yield for the three carbazole derivatives is considered as 0.5 according to the literature (Table 4.6).

The Figures 4.17–4.25 show the affect of variable perylene concentration on carbazole derivatives' absorption (Figures 4.17–4.19 for carbazole; 4.20–4.22 for

dodecylcarbazole; and 4.23–4.25 for polycarbazole, respectively). For the three carbazole derivatives in chloroform, the absorption intensity is decreased upon increasing the perylene dye concentration gradually. In contrary, the absorption intensities for all the three carbazole derivatives in acetonitrile and methanol were increased upon increasing the concentration of perylene dye.

The forbidden transitions in chloroform are not effective to make ground state complexes. On the other hand, in acetonitrile and methanol, as can be seen the forbidden $S_0 \rightarrow S_2$ transitions are higher in intensity causing strong ground state complexes due to the nitrile electron withdrawing group and hydrogen bonding (and possible protonation) interactions in methanol. These ground state complexes are consequencing the probable charge transfer interactions. Clearly, the solvent molecules and carbazole molecules are under strong intermolecular interactions and forming ground state complexes.

The emission spectra of carbazole derivatives are presented in Figures 4.26 – 4.30. The emission spectra (Figures 4.31–4.39) are in excellent support of their absorption spectra and show the affect of variable perylene concentration on carbazole derivatives' emission (Figure 4.31–4.33 for carbazole emission; 4.34–4.36 for dodecylcarbazole emission; and 4.37–4.39 for polycarbazole emission). For the three carbazole derivatives in chloroform, the excimer emission intensity is decreased upon increasing the perylene dye concentration gradually. In contrary, the excimer emission intensities for all the three carbazole derivatives in acetonitrile and methanol were increased upon increasing the concentration of perylene dye. This is attributed to the high polarity and protic nature (methanol) of the solvents.

It is clear from the emission spectra that in acetonitrile and methanol there were excimer emissions indicating the charge transfers which were also evident in their absorption spectra. The ground state complexes that were evidenced in the absorption spectra and the resultant charge transfer interactions are causing increase in excimer emission intensities of carbazole groups in proportion to the perylene dye emissions. The carbazole group and perylene groups are interacting in conjunction with the solvent molecules giving rise to an interesting charge transfer interactions and thus resulting in an increase in emission intensities. Although there is no efficient nonradiative energy transfer (occurring in chloroform solutions) in acetonitrile and methanol, interesting charge transfer leading to electron transfer are evidenced from carbazole to perylene chromophore (4.26 – 4.39).

The energy transfer studies from Figures 4.31, 4.34 and 4.37 evidence the efficient transfer of energy by long range mechanism (Columbic) from the targeted donor compounds (dibromocarbazole, dodecylcarbazole and polycarbazole) to the acceptor compound (dehydro-PDI) in chloroform. Therefore, the constant of bimolecular quenching is measured for the three carbazole derivatives and PDI systems in chloroform from Stern-Volmer plots (Figures 4.40–4.42). The values are, 1.07×10^{13}, 1.24×10^{13}, and 7.77×10^{11} for carbazole, dodecylcarbazole and polycarbazole, respectively in chloroform.

The critical transfer distances measured (112 $\mathring{A}$ for dibromocarbazole, 120 $\mathring{A}$ for dodecylcarbazole, and 126 $\mathring{A}$ for polycarbazole) are in excellent agreement and in addition Stern-Volmer plots show efficient diffusion-controlled energy transfer in chloroform.

Chapter 6

CONCLUSION

The carbazole compounds, 2,7-dibromocarbazole (Cbz), 2,7-dibromo-N-dodecylcarbazole (doecylcarbazole), and poly(2,7-N-dodecyl)carbazole (polycbz) are considered as electron donating groups and dehydroabietyl perylene diimide (PDI) is considered as electron accepting group.

All the three carbazole derivatives emit excimer light emission and especially for polycarbazole an extended broad excimer emission is obtained in various solvents of different polarities.

For the three carbazole derivatives in chloroform, the absorption intensity is decreased upon increasing the perylene dye concentration gradually. In contrary, the absorption intensities for all the three carbazole derivatives in acetonitrile and methanol were increased upon increasing the concentration of perylene dye. This increase in absorption is due to strong ground state complexes of nitrile electron withdrawing group and hydrogen bonding (and possible protonation) interactions in methanol. These ground state complexes are consequencing the probable charge transfer interactions. It is evidenced that the solvent molecules and carbazole molecules are under strong intermolecular interactions and forming ground state complexes.

For the three carbazole derivatives in chloroform, the excimer emission intensity is decreased upon increasing the perylene dye concentration gradually. In contrary, the excimer emission intensities for all the three carbazole derivatives in acetonitrile and methanol were increased upon increasing the concentration of perylene dye.

The energy transfer studies evidence the efficient transfer of energy by long range Columbic mechanism from the targeted donor compounds (dibromocarbazole, dodecylcarbazole and polycarbazole) to the acceptor compound (dehydro-PDI) in chloroform. The critical transfer distances measured are in good agreement and the values show the long-range mechanism. The stern-Volmer plots are proving the efficiency of energy transfer and hence diffusion-controlled energy transfer.

The ground state complexes that were evidenced in the absorption spectra and the resultant charge transfer interactions are causing increase in excimer emission intensities of carbazole groups in proportion to the perylene dye emissions. The carbazole group and perylene groups are interacting in conjunction with the solvent molecules giving rise to an interesting charge transfer interactions and thus resulting in an increase in emission intensities.

Although there is no efficient nonradiative energy transfer (occurring in chloroform solutions) in acetonitrile and methanol, interesting charge transfer leading to electron transfer are evidenced from carbazole to perylene chromophore.

REFERENCES

Albinsson B. and etal (2007). Electron and energy transfer in donor–acceptor systems with conjugated molecular bridges. Phys. Chem. Chem. Phys. 9. 5847–5864.

Barbara P. and etal (1996). Contemporary issues in electron transfer research
Paul. J. Phys. Chem. 100. 13148-13168.

Cox A. and etal (2011). The transition to microbial photosynthesis in hot spring ecosystems. Chemical Geology. 280. 344–351.

Deperasinska I. and etal (1998). The analysis of excited-state equilibria of weak electron donor-acceptor systems: Tetracyanobenzene-toluene complex. Journal of luminescence. 79. 65-77.

Gao L. and etal (2011). Photochromic and electrochromic performances of new types of donor/acceptor systems based on crosslinked polyviologen film and electron donors. Applied surface science. 257. 3039–3046.

Hoffmann N. (2008). Efficient photochemical electron transfer sensitization of homogeneous organic reactions. Journal of photochemistry and photobiology C: photochemistry reviews. 9. 43–60.

Hurenkamp J. and etal (2008). Tuning energy transfer in switchable donor–acceptor systems. Org. Biomol. Chem. 6. 1268–1277.

Hussner A. and etal (2011). Diurnal courses of net photosynthesis and photosystem II quantum efficiency of submerged lagarosiphon major under natural light conditions. Flora. 206. 904– 909.

Icil H. and etal (1998).Syntheses and properties of a new photostable soluble perylene dye :N,N'-di-(1-dehydroabietyl) perylene-3,4,9,10-bis(dicarboximide). spectroscopy letters. 31(8). 1643-1647.

Jankowska S. and etal (2008). Nonradiative long range energy transfer in donor–acceptor systems with excluded volume. Chemical physics letters. 460. 306–310.

Jeon Y. and etal (2011). Orange phosphorescent organic light-emitting diodes based on spirobenzofluorene type carbazole derivatives as a host material. Dyes and Pigments. 89. 29-36.

Jia C. and etal (2012). Synthesis, physical properties and self-assembly of conjugated donoreacceptor system based on tetrathiafulvalene and functionalized with binding sites. Dyes and Pigments. 94. 403-409.

Koyuncu S. and etal (2009). A new donor–acceptor double-cable carbazole polymer with perylene bisimide pendant group: synthesis, electrochemical, and photovoltaic properties. Journal of polymer science: part A: polymer chemistry.
DOI 10.1002/pola.

Li Z. and etal (2012).Orderly ultrathin films based on perylene/poly(N –vinyl carbazole) assembled with layered double hydroxide nanosheets: 2D fluorescence

resonance energy transfer and reversible fluorescence response for volatile organic compounds. Adv. mater. DOI: 10.1002/adma.201203040.

Malyukin Y. and etal (2005). Nano-scale control of energy transfer in the system ‘‘donor–acceptor’’. Journal of Luminescence. 112. 439–443.

Nome R. and etal (2011). Electronic energy transfer between poly(9,9_dihexylfluorene-2,2-dyil) and MEH-PPV: A photophysical study in solutions and in the solid state. Synthetic Metals. 161. 2154– 2161.

Pan J. and etal (2005). Dendron-functionalized perylene diimides with carrier-transporting ability for red luminescent materials. Polymer. 46. 7658–7669.

Ren H. and etal (2011). Synthesis and luminescent properties of perylene bisimide-cored dendrimers with carbazole surface groups. Polymer. 52. 3639-3646.

Usacheva M. and etal (1991). Electron phototransfer in the initiation of polymerization. Translated from uspekhi khimii. 60. 205-237.

Wen D. and etal (2009). Review of nanofluids for heat transfer applications. Particuology. 7. 141–150.

Wrobel D. and Graja A. (2011). Photoinduced electron transfer processes in fullerene–organic chromophore systems. Coordination chemistry reviews. 255. 2555– 2577.

WU P. and etal (2004). Efficient energy transfer from poly(N-vinyl-carbazole) to tetra-methylester of perylene-3,4,9,10-tetracarboxylicacid. Journal of materials science. 39. 5837 – 5840.

Yasutani Y. And etal (2012). Polycarbazoles: Relationship between intra- and intermolecular charge carrier transports. Synthetic Metals. 162. 1713– 1721.

Zhao J. and etal (2011). One-pot synthesis of 2-bromo-4,5-diazafluoren-9-one via a tandem oxidation-bromination-rearrangement of phenanthroline and itshammer-shaped donor-acceptor organic semiconductors. Tetrahedron. 67. 1977-1982.